UNIVERSITY OF LONDON THESIS

Degree PhD Year 2006 Name of Author KÖCHL Robert

Autophagosome maturation in primary rat hepatocytes

Robert Köchl

A thesis submitted for the degree of Doctor of Philosophy at the University of London

March 2006

Secretory Pathways Laboratory

Cancer Research UK

London Research Institute

ProQuest LLC
789 East Eisenhower Parkway
P.O. Box 1346
Ann Arbor, MI 48106-1346

Abstract

Nutrient deprivation of eukaryotic cells elicits a rapid survival response, including the induction of autophagy. Autophagy, or "self-eating", involves the formation of autophagosomes from an unknown membrane source and the sequestration of cytosolic components, including organelles such as mitochondria, endoplasmic reticulum and small vesicles. Autophagosomes then fuse with protease-containing endosomes and their contents are degraded. This allows the cell to recycle amino acids and to reuse them for the synthesis of new proteins.

To study the formation and fusion of autophagosomes, I have developed in vivo and in vitro assays, based on primary rat hepatocytes cultures. For the in vitro assay, the aim of which is to identify proteins involved in fusion, I have designed specific markers and internalized them into endosomes and autophagosomes. Both vesicle populations have been purified and used to reconstitute fusion in vitro. For the in vivo experiments I expressed the GFP-tagged autophagosomal marker, LC3, in cultured primary rat hepatocytes. By measuring the translocation of GFP-LC3 from a cytosolic pool to newly formed autophagosomes, using a high throughput-imaging system, and by assaying for the lipidation of GFP-LC3, I was able to quantify the rate and magnitude of autophagosome formation and fusion. Starvation led to an increase in the rate of autophagosome formation, and the total number of autophagosomes per cell increased more than two-fold. Autophagosome formation was independent of mTOR, a negative regulator of autophagy in yeast and many cell lines, and could be strongly inhibited by leucine, a regulatory amino acid. I then investigated the role of microtubules in the formation and fusion of

autophagosomes, using the microtubule-depolymerising drugs nocodazole and vinblastine. I found that nocodazole treatment reduced the rate of autophagosome formation and completely inhibited their mobility. In addition, both drugs inhibited fusion with endosomes, showing that an intact microtubule network is also required for fusion. Interestingly, vinblastine also strongly stimulated autophagosome formation, even in nutrient-rich medium. This effect was independent of mTOR activity, but required the autophagy proteins Atg5 and Atg6, suggesting that vinblastine affects a novel signalling pathway upstream of autophagy proteins.

Für Walter und Elda Köchl

Acknowledgements

I would like to thank my supervisor Sharon Tooze for continuous support, for encouragement and discussions, and for giving me the possibility to work in her lab on this exciting project. Furthermore I would like to thank Edmond Chan and Xiao-Wen Hu for their help during my thesis. Many thanks also to all past and present members of the Secretory Pathways lab, especially Franz Wendler, Andrew Young and Harold Jefferies. Thank-you to everyone at the Light Microscopy Unit for their help and to Prof Per Seglen, Monica Fengsrud and Frank Saetre at the Radium Hospital in Oslo for teaching me the rat perfusion technique.

Finally, many thanks to Anett and to my family for always being there when I needed them.

Table of Contents

List of Figures

List of Tables

Abbreviations

ATP	Adenosin triphosphate
AV	Autophagosome
AVi	Immature autophagosome
AVd	Degradative autophagosome
CI-MPR	Cation independent Mannose-6-phosphate receptor
C-terminus	Carboxy terminus
EEA1	Early antigen 1
EM	Electron microscope
ER	Endoplasmic reticulum
ES	Earle's saline (starvation medium)
FM	Full growth medium
GFP	Green fluorescent protein
Hepes	4-(2-hydroxyl)-1-piperazine ethane sulphonic acid
HRP	Horseradish peroxidase
IF	Immuno fluorescence
Lamp	Lysosomal associated membrane protein
LSM	Laser scanning microscope
Mr(k)	Relative molecular weight in kilo Daltons
NSF	N-ethylmaleimide sensitive factor
N-terminus	Amino terminus
PAGE	Polyacrylamide gel electrophoresis
PBS	Phosphate buffered saline
PFA	Paraformaldehyde

PNS	Post nuclear supernatant
RPM	Revolutions per minute
SDS	Sodium dodecyl sulfate
SEM	Standard error of the mean
siRNA	Small inhibitory RNA
SNAP	Soluble NSF attachment protein
SNARE	SNAP-receptor
Stx	Syntaxin
TEMED	N,N,N',N'-tetramethyl-ethylenediamine
Tris	2-amino-2-(hydroxymethyl)-1,3-propanediol
wt	Wild type

Publications

Köchl R, Hu XW, Chan E, Tooze SA. Microtubules facilitate autophagosome formation and are essential for fusion of autophagosomes with endosomes. Traffic. 2006 Feb; 7(2):129-45

Young A, Chan EYW, Hu XW, Köchl R, Hailey D, Lippincott-Schwartz J, Crawshaw S, High S, Hailey DW, Tooze SA. Starvation and UKL1-dependent cycling of mammalian Atg9 between the TGN and endosomes. Submitted to JCS

Chan E, Köchl R, Tooze SA. Book chapter: Cell biology and biochemistry of Autophagy. Autophagy and Immunity. Landes Bioscience. 2006.

1 INTRODUCTION

Eukaryotic cells have two major protein degradation pathways: the proteasome and autophagy. Autophagy, or self-digestion, is a lysosomal protein degradation pathway that was observed first using electron microscopy in the late fifties by Clark et al. (Clark, 1957) in kidneys of newborn mice. It is generally believed to be responsible for the degradation of long-lived cytosolic proteins and organelles, while the proteasome degrades certain short-lived proteins (for review see (Yorimitsu and Klionsky, 2005)). Several different types of autophagy have been described in mammalian cells, including microautophagy, chaperone-mediated autophagy and macroautophagy.

Macroautophagy, also referred to as just autophagy, has been regarded for a long time only as a cellular response to nutrient deprivation and a rescue mechanism for cells to survive periods where nutrients are limiting. Over the last years, however, it has become increasingly clear that autophagy is also involved in processes such as tissue remodelling (Rusten et al., 2004), innate immunity (Deretic, 2005), neurological diseases characterised by protein aggregates and tumorigenesis (Ravikumar et al., 2004; Webb et al., 2003). In addition, autophagy has been suggested to be an important cellular "house-keeping" process, being responsible for the degradation and the turnover of mitochondria and long-lived proteins (Tolkovsky et al., 2002).

Although autophagy was observed for the first time nearly 50 years ago, not much is known about the molecular mechanisms involved. However, a major step forward in understanding autophagy has been made with the

independent identification of over fifteen mutants defective for autophagy in the yeast *S. cerevisiae* by three research groups (Harding et al., 1995; Thumm et al., 1994; Tsukada and Ohsumi, 1993). The nomenclature of the proteins identified in those screens, as well as others, has recently been unified (Klionsky et al., 2003) and all proteins required for autophagy are now called Atg (Autophagy proteins, see also Chapter 1.1). Most of the Atg proteins are required for the formation of autophagosomes, and not much is known about proteins which act at later stages during the maturation of an autophagosome. In recent years homologues for most of the yeast proteins have been found in higher eukaryotes.

In mammalian cells, when autophagy is induced, a phagophore or isolation membrane (Fengsrud et al., 2004) forms in the cytoplasm. The isolation membrane is a flat double membrane structure that grows in size and bends into a cup-shaped structure, thereby sequestering cytosol and organelles, such as mitochondria, endoplasmic reticulum and small vesicles. The isolation membrane then seals at the edge to form an early, immature autophagosome (AVi, immature autophagic vacuole, Figure 3.5).

The sequestration of cytoplasmic constituents is generally believed to be non-selective (Kopitz et al., 1990), although autophagy has been implicated in the specific removal of damaged mitochondria (Tolkovsky et al., 2002). By electron microscopy (EM) AVis appear as double membrane vesicles, which vary between 0.2 to 2 μm in diameter depending on the cell type. The inside of an AVi always looks similar to the surrounding cytoplasm, suggesting no degradation of the content has taken place. In freeze-fracture studies the membrane has been found to be particularly protein-poor (Fengsrud et al.,

2000). AVis then fuse with endosomes or lysosomes giving rise to late, degradative autophagosomes (AVd).

AVds (Figure 3.5) are characterized by their electron dense content and normally only the limiting membrane is visible. AVds contain lysosomal hydrolases and membrane proteins such as Lamp2 and have an acidic lumen (Dunn, 1990a). In AVds the final degradation of the autophagocytosed material occurs. AVds can be further subdivided into amphisomes, which comprise an intermediate stage, and autolysosomes, the final vesicle in the pathway (Figure 1.1).

In the following sections of the Introduction I will summarize the current knowledge on autophagy. I will first describe the genes found in yeast, followed by a chapter about autophagosome formation, in which I will discuss the source of the autophagosome membrane and the machinery required for formation, as well as what is known about signalling pathways involved in autophagosome formation. Finally, I will summarize the current knowledge about autophagosome fusion. In this thesis I define autophagosome maturation as all processes which are necessary to induce autophagosome formation and the subsequent fusion events of a completely formed autophagosome with compartments of the endocytic pathway.

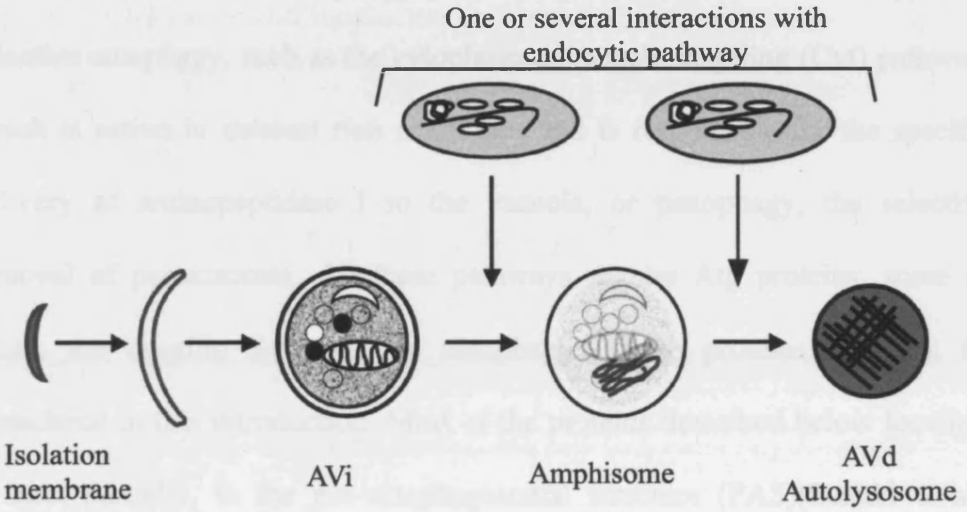

Figure 1.1: Autophagic pathway in mammalian cells. Upon the induction of autophagy, autophagosomes form from an unidentified membrane source, termed the isolation membrane or phagophore. During the formation autophagosomes sequester cytosol and organelles, such as mitochondria, endoplasmic reticulum and vesicles. An AVi then fuses, at least once, possibly several times with different compartments of the endocytic system in order to deliver its contents to a lysosome for degradation. The final compartment is called an autolysosome or AVd

1.1 Molecular components involved in yeast autophagy

Most proteins found in the initial yeast screens (Table 1.1) are involved in the early steps of autophagosome formation (see also Chapter 1.2). Besides the non-selective bulk autophagy pathway, yeast also have several types of selective autophagy, such as the cytoplasm to vacuole targeting (Cvt) pathway, which is active in nutrient rich conditions and is responsible for the specific delivery of aminopeptidase I to the vacuole, or pexophagy, the selective removal of peroxisomes. All these pathways require Atg proteins, some of which are specific for selective autophagy. Those proteins will not be considered in this introduction. Most of the proteins described below localize, at least partially, to the pre-autophagosomal structure (PAS)(Suzuki et al., 2001). The PAS is thought to be the point of origin of newly formed autophagosomes in yeast.

A central role in the induction of autophagy in yeast is played by Atg1, the only kinase so far identified amongst the autophagy proteins. Atg1 is thought to be downstream of the kinase target of rapamycin (TOR), which is generally believed to be the nutrient sensor. In nutrient rich conditions TOR is active and Atg13, which is downstream of TOR, is hyperphosphorylated. When autophagy is induced by starving cells of nutrients TOR is inactivated. Atg13 is partially dephosphorylated and consequently binds to Atg1 together with Vac8, Atg11 and Atg17 (Kabeya et al., 2005; Kamada et al., 2000; Scott et al., 2000).

This activates Atg1 and is necessary for autophagy (Kamada et al., 2000). In yeast there are no known downstream partners of Atg1.

Another complex, thought to be involved in the signalling to autophagy is the Vps34 complex I. Vps34 is a phosphatidylinositol 3-kinase, which forms a complex with Atg6, also called Beclin1 in mammalian cells, and Atg14 and Vps15 (Kihara et al., 2001). Atg18, a PI3P binding protein is recruited to the PAS in a Vps34 complex I dependent manner (Guan et al., 2001).

Besides the two signalling complexes mentioned above there are two ubiquitin-like conjugation processes which play a role in autophagosome biogenesis. The Atg5-Atg12-Atg16 conjugate (Kuma et al., 2002) is thought to be involved in autophagosome formation, but is not present on a completely closed AVi. The Atg8-phophatidylethanolamine conjugate (Ichimura et al., 2004; Kirisako et al., 2000) binds specifically to autophagosomes and stays bound after formation is completed. Both conjugation systems will be described in more detail later on.

Atg9 is the only membrane protein identified so far, which is necessary for autophagy. In yeast Atg9 binds to the PAS, as well as to mitochondria (Reggiori et al., 2005b). Atg9 has been shown to cycle between those two structures in an Atg2 and Atg18 dependent manner (Reggiori et al., 2004a), however, its function remains unknown.

In 2001, Suzuki et al. (Suzuki et al., 2001) grouped the Atg proteins into three classes according to when they act in the pathway (Table 1.2). They used GFP tagged Atg5 and Atg8 and investigated their localization to the punctate PAS in Atg mutants. In mutants where autophagy is inhibited at a late stage, both proteins are recruited to the PAS, while in mutants where autophagy is

inhibited at a very early stage, neither Atg5, nor Atg8 are recruited the PAS. In intermediate mutants, only Atg5 is localized to the PAS. Using this approach Suzuki et al. could classify the Atg proteins into three functional groups which act at distinct time points during autophagosome formation. The autophagy-specific PI3 kinase complex is required early on in autophagosome formation, before the PAS is formed. The two ubiquitin-like conjugation mechanisms are required for PAS formation and the Atg1 kinase complex is required for autophagosome formation. Knocking out any of those genes inhibits autophagy in yeast. See table 1.2 for classification.

Table 1.1: Autophagy proteins in yeast and mammalian cells. Table modified from (Klionsky et al., 2003).

Atg Name	Previous nomenclature	Mammalian homologue	Function
Atg1	Apg1, Aut3, Cvt10	Ulk1	Protein kinase
Atg2	Apg2, Aut8	Not yet identified	Peripheral membrane protein, interacts with Atg9
Atg3	Apg3, Aut1	Atg3	E2-like enzyme, conjugates Atg8 to phosphatidylethanolamine (PE)
Atg4	Apg4, Aut2	Atg4	Cysteine protease, cleaves C-terminal extension or PE from Atg8
Atg5	Apg5	Atg5	Conjugated to Atg12 through internal lysine
Atg6	Apg6	Beclin	Component of the PI3-kinase complex
Atg7	Apg7, Cvt2	Atg7	E1-like enzyme, activates Atg8 and Atg12
Atg8	Apg8, Aut7, Cvt5	MAP1-LC3	Specific autophagosome marker, ubiquitin-like protein conjugated to PE

Atg9	Apg9, Aut9, Cvt7	Atg9	Integral membrane protein
Atg10	Apg10	Atg10	E2-like enzyme, conjugates Atg12 to Atg5
Atg12	Apg12	Atg12	ubiquitin-like protein conjugated to PE, conjugated to Atg5
Atg13	Apg13	Not yet identified	Modifier of Atg1 activity, hyperphosphorylated
Atg14	Apg14, Cvt12	Not yet identified	Component of PI3-kinase complex
Atg16	Apg16, Cvt11	Atg16	Component of Atg12-Atg5 complex
Atg17	Apg17	Not yet identified	Modifier of Atg1 activity
Atg18	Aut10, Cvt18	Wipi49	Peripheral membrane protein, required for localization of Atg2

Table 1.2: Classification of Atg mutants into late acting mutants (Class A), intermediate acting mutants (Class B) and early acting mutants (Class C) (Suzuki et al., 2001), depending on GFP-Atg5 and GFP-Atg8 localizing to the PAS. See text for further details.

	GFP-Atg5 on PAS	GFP-Atg8 on PAS	Mutants
Class A	+	+	Atg1, Atg2, Atg13, Atg17
Class B	+	-	Atg3, Atg4, Atg7, Atg10, Atg12
Class C	-	-	Atg6, Atg9, Atg14, Atg16

1.2 Autophagosome Formation

1.2.1 Two ubiquitin-like protein conjugation processes are required for autophagosome formation.

1.2.1.1 Atg5-Atg12 conjugation and complex

In 1998, Mizushima et al. (Mizushima et al., 1998) showed in a genetic study in yeast that autophagic sequestration of cytosol requires a unique ubiquitin-like protein conjugation system, which leads to the covalent conjugation of Atg5 to Atg12, two proteins essential for autophagy in yeast (Figure 1.2). When Atg5 was mutated at Lys 149, conjugation could not occur anymore and autophagy was blocked. Furthermore, the conjugation between Atg5 and Atg12 is also inhibited in Atg7 and Atg10 mutants, showing that these proteins act as enzymes in the conjugation process (Mizushima et al., 1998). Atg12 is first activated by binding to Atg7, which acts as an E1-like protein. Atg12 is then handed over to Atg10, an E2-like enzyme, before being conjugated with Atg5. In yeast, the Atg5-Atg12 complex has further been shown to interact with Atg16, a small coiled-coiled protein (Kuma et al., 2002). The Atg5-Atg12-Atg16 complex then forms homo-oligomers, which localize to the pre-autophagosomal structure in yeast.

In mouse embryonic stem cells the Atg5-Atg12 conjugate localizes to the isolation membrane (Mizushima et al., 2001). Using GFP tagged Atg5 Mizushima et al. could clearly show that the cup-shaped isolation membrane develops from a smaller crescent-shaped membrane structure. Furthermore,

they demonstrated that the covalent conjugation of Atg5 and Atg12 is essential for the elongation of the isolation membrane.

In addition, Mizushima et al. (Mizushima et al., 2001) could also show that the Atg5-Atg12 conjugate is required for the targeting of Atg8, the only specific autophagosome marker, to the autophagosome membrane. The Atg5-Atg12 conjugate is not present on sealed autophagosomes in yeast (Kim et al., 2002; Suzuki et al., 2001) nor in mammalian cells (Mizushima et al., 2001).

1.2.1.2 Atg8/LC3 conjugation

As mentioned above, Atg8 is the only specific autophagosome marker which binds to newly formed autophagosomes and remains bound after the formation of an autophagosome. In yeast, Atg8 has been shown to be important for the regulation of the size of newly formed autophagosomes. Atg8 mutants were still able to form autophagosomes, however, the autophagosomes were smaller than in wild type controls (Reggiori et al., 2003). Mammalian cells contain several homologues of Atg8; LC3 (Kabeya et al., 2000), GABARAP and GATE16 (Tanida et al., 2003) all of which have been shown to bind to the membrane of autophagosomes. Of these three proteins, LC3, which initially was identified as microtubule associated protein 1 light chain 3 (MAP1-LC3) (Mann and Hammarback, 1994), is the most investigated. Full length LC3 gets cleaved at a highly conserved C-terminal glycine residue by the protease Atg4 (Hemelaar et al., 2003) to give rise to the cytosolic form LC3-I. Upon induction of autophagy LC3-I is modified by a ubiquitin-like process, involving Atg7 and Atg3 as E1-like and E2-like enzymes, and the attachment of a lipid residue,

presumably phosphatidylethanolamine to the glycine residue (Tanida et al., 2004b), in an Atg5-Atg12 dependent manner (Mizushima et al., 2001).

The resulting form LC3-II binds to isolation membranes and autophagosomes and can be used as a specific marker for autophagy (Figure 3.9). In HeLa cells 59 % of AVis and 29 % of AVds labelled positive for LC3 in quantitative immuno-electron microscopy (Eskelinen, 2005). The other Atg8 homologues, GABARAP and GATE16 are less well characterized, but have also been shown to be processed by the same machinery prior to binding to autophagosomes (Kabeya et al., 2004). In human cells there exist at least three distinct LC3 genes with different tissue expression patterns, termed LC3A, LC3B and LC3C (He et al., 2003). In this thesis I used rat GFP-LC3 as a marker for autophagosomes.

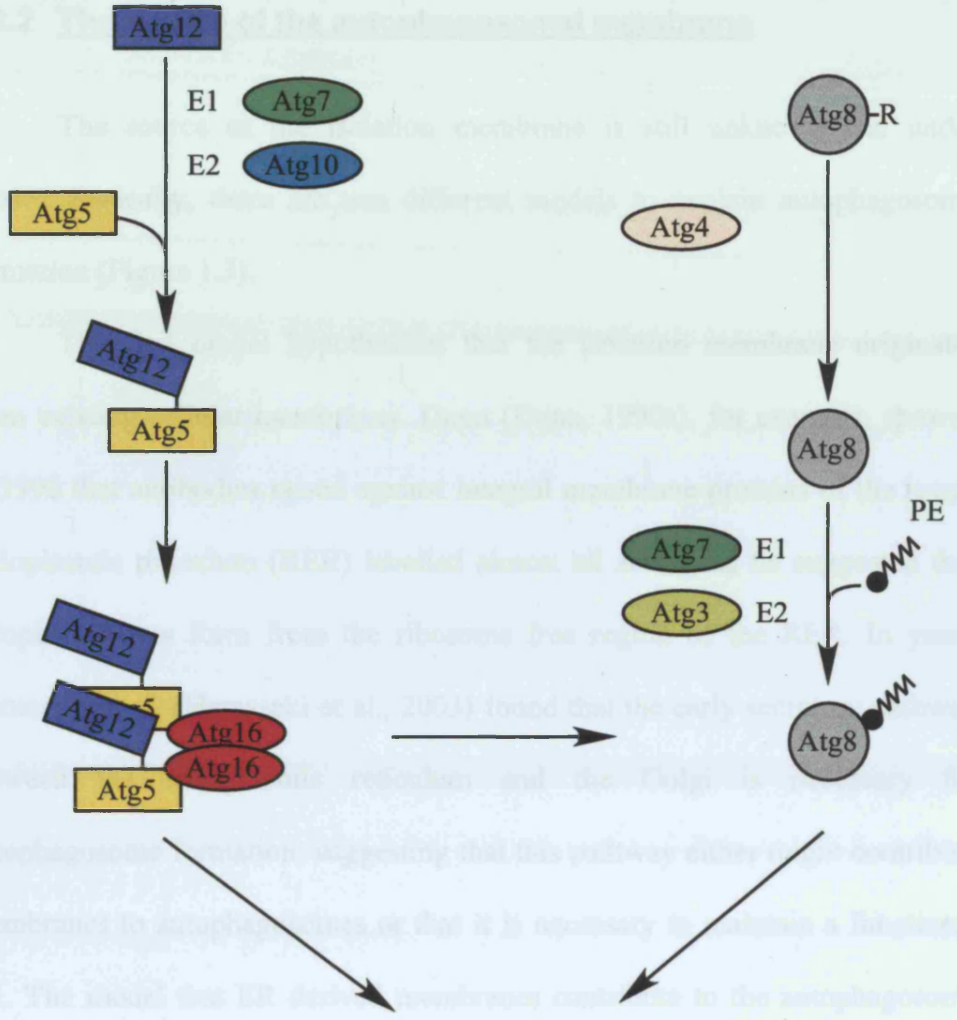

Figure 1.2: Two ubiquitin-like pathways are essential for autophagosome formation. Atg12 is covalently conjugated to Atg5 by Atg7 and Atg10, which act as E1 and E2 enzymes, respectively. The Atg5-Atg12 conjugate can then form hetero-oligomers via Atg16. Formation of this complex is necessary for the elongation of the isolation membrane and for targeting Atg8 to autophagosomes. Full-length Atg8 is cleaved at the C-terminus by Atg4, which exposes a C-terminal glycine residue. Atg8 is then covalently attached to PE and targeted to the autophagosomal membrane.

1.2.2 The source of the autophagosomal membrane

The source of the isolation membrane is still unknown and under debate. Basically, there are two different models to explain autophagosome formation (Figure 1.3).

The first model hypothesises that the isolation membrane originates from existing cellular membranes. Dunn (Dunn, 1990a), for example, showed in 1990 that antibodies raised against integral membrane proteins of the rough endoplasmic reticulum (RER) labelled almost all AVis and he suggested that autophagosomes form from the ribosome free region of the RER. In yeast, Hamasaki et al. (Hamasaki et al., 2003) found that the early secretory pathway between the endoplasmic reticulum and the Golgi is necessary for autophagosome formation, suggesting that this pathway either might contribute membranes to autophagosomes or that it is necessary to maintain a functional ER. The model that ER derived membranes contribute to the autophagosome membrane is further supported by the similar membrane thickness of ER and autophagosomes (Dunn, 1994; Fengsrud et al., 2004). In addition, Reggiori et al. (Reggiori et al., 2004b) suggested that both, ER and Golgi membranes might contribute to autophagosome formation. The involvement of Golgi membranes, was further supported by acid phosphatase staining of phagophores (Frank and Christensen, 1968). Because Golgi also stains for acid phosphatase (Locke and Sykes, 1975) it was suggest that the isolation membrane might come from Golgi membranes. In addition, autophagosome membranes have been shown to contain complex Golgi-derived carbohydrates, suggesting they are derived from post-Golgi compartments (Yamamoto et al., 1990).

The second model hypothesises that the isolation membrane is formed *de novo* through non-vesicular transport or local synthesis of lipids (Juhasz and Neufeld, 2006). In yeast Noda et al. (Noda et al., 2002) suggested that autophagosomes form in three steps, nucleation, assembly and elongation.

In addition, it is feasible that multiple membrane pools play a role in autophagosome formation. It is currently unclear how the isolation membrane grows and bends. In theory, it is possible that it either grows by fusion with other isolation membranes or that it grows because of the incorporation of newly synthesized lipids.

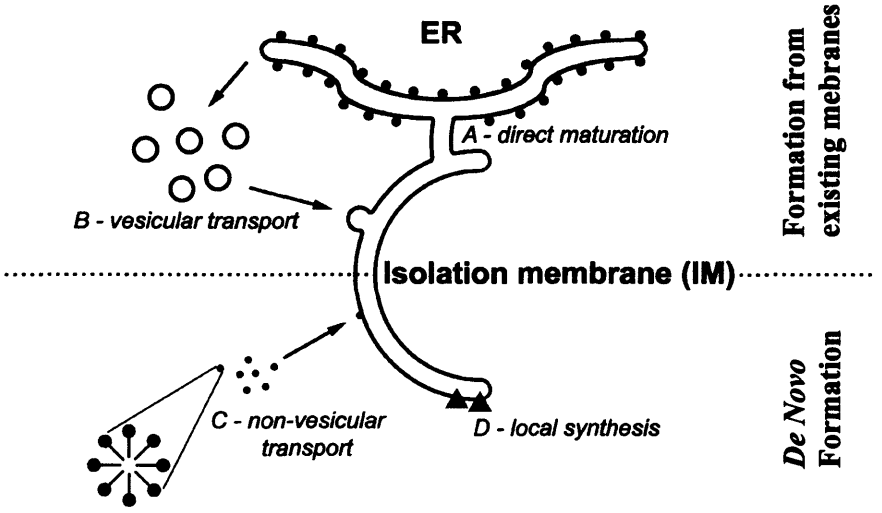

Figure 1.3: The source of the autophagosomal membrane. Two models have been suggested to explain the origin of the isolation membrane. In the first model existing cellular membranes are remodelled to contribute the isolation membrane (A) or membranes might originate from vesicles (B). In the the *de novo* model, membranes are assembled at the site of isolation membrane formation. The lipids might originate from non-vesicular transport (C), or local synthesis (D). Figure taken from Juhasz and Neufeld, 2006.

1.2.3 Induction of autophagy

The primary and conserved role of autophagy is the response to nutrient deprivation. In GFP-LC3-transgenic mice, autophagy was found to be up-regulated in almost all tissues, following starvation (Mizushima et al., 2004), showing its importance during times where nutrients are limited. Kuma et al. (Kuma et al., 2004), for example, showed that mice, lacking Atg5 die within one day after birth. Shortly after birth, when the nutrient supply through the placenta of the mother is cut off, mice undergo a period of starvation until the nutrient supply through the milk is restored. During these first hours, autophagy was up-regulated in control mice and only returned to basal levels after 1 – 2 days. The Atg5 knockout mice, which were not able to undergo autophagy showed reduced amino acid concentrations in plasma and tissues and had signs of energy depletion, underlining the importance of autophagy for survival during (neonatal) starvation.

Despite extensive research, the signalling mechanisms by which nutrients control autophagy are still not very well understood. No "amino acid receptor" has been identified so far, and it was only within the last 5 – 10 years that several proteins and signalling pathways were identified as being involved in autophagy. How they interact and converge to induce autophagy is still unclear. In the following sections, I will summarize the current knowledge about how cells are believed to sense nutrients, especially amino acids, and what implications this has for the induction of autophagy.

1.2.3.1 Amino acids and growth factors

One of the first reports in the literature, showing that autophagy is up-regulated in response to amino acid starvation was published in 1976 by Mitchener et al. (Mitchener et al., 1976). They were able to demonstrate that HeLa cells contained an increased number of autophagosomes, containing sequestered organelles, after the removal of serum and amino acids. Before that, in 1972, Woodside and Mortimore (Woodside and Mortimore, 1972) showed that amino acids, when added to the perfusion buffer, can suppress protein degradation in perfused rat livers, as measured by the release of ^{14}C-labelled valine. Leu, Phe, Tyr, Trp, His and Gln, were found to be especially effective at inhibiting autophagic protein degradation in rat hepatocytes (Poso et al., 1982), with leucine being the strongest inhibitor of all amino acids. These amino acids are therefore called regulatory amino acids. Since then amino acid withdrawal has been shown to induce autophagy in a number of mammalian cell lines and tissues (Gordon et al., 1989; Gutierrez et al., 2004b; Mordier et al., 2000; Tassa et al., 2003), as well as *Drosophila* (Rusten et al., 2004), *C. elegans* (Melendez et al., 2003), *Dictyostelium* (Otto et al., 2004) and plants (Contento et al., 2005).

Besides amino acids, growth factors, such as insulin and glucagon, can also regulate autophagy. Glucagon for example increases autophagy in hepatocytes and mycardiocytes (Kondomerkos et al., 2005), while insulin inhibits autophagy via the PI3K-Akt-Tsc1/2-Rheb pathway upstream of mTOR (Garami et al., 2003; Kanazawa et al., 2004; Pfeifer, 1978; Poli et al., 1981).

1.2.3.2 Amino acid sensing upstream of mTOR

Amino acid signalling is thought to converge at the mammalian target of rapamycin (mTOR) kinase (see also Chapter 1.2.3.3, Figure 1.4)(Beugnet et al., 2003), although, no amino acid receptor has been identified so far.

mTOR receives its upstream input through tuberous sclerosis complex1 and 2 (TSC1/2). TSC1 heterodimerized with TSC2, has GTPase activity towards Rheb, a protein that was shown to bind to the mTOR catalytic domain. TSC1/2 stimulates the conversion of Rheb-GTP to Rheb-GDP, which in turn inactivates mTOR (Long et al., 2005). This pathway has clearly been shown to be involved in the regulation of insulin signalling (Garami et al., 2003), but its involvement in amino acid signalling is still unclear.

$TSC1^{-/-}$ and $TSC2^{-/-}$ rat embryonic fibroblasts were initially found to be resistant to amino acid starvation in contrast to wt cells, as measured by the T^{389}-phosphorylation (see also Chapter 1.2.3.4) of the mTOR substrate p70S6 kinase, implying that the TSC1/2 complex is involved in amino acid sensing upstream of mTOR (Gao et al., 2002).

This model, however, has recently been challenged by Smith et al. (Smith et al., 2005). In $TSC2^{-/-}$ mouse fibroblasts, amino acid withdrawal led to the dephosphorylation of the ribosomal protein S6, as well as p70S6 kinase and other downstream targets of mTOR, such as 4E-BP, clearly demonstrating that mTOR was inactivated, despite TSC2 being knocked out.

Downstream of the TSC1/2 complex is the GTPase Rheb, which has been shown to bind mTOR in an amino acid sensitive manner (Long et al., 2005). Withdrawal of all extracellular amino acids or just leucine alone

reversibly inhibited the binding of Rheb to mTOR. Additionally, over-expression of Rheb activated mTOR and induced p70S6 kinase phosphorylation (Long et al., 2005). Re-addition of amino acids to starved cells increased the amount of GTP-bound Rheb (Roccio et al., 2006), while amino acid starvation followed by insulin stimulation did not increase the GTP loading of Rheb. Taken together, these data clearly show the involvement of Rheb in the amino-acid dependent control of mTOR. The molecular mechanisms by which amino acids regulate Rheb binding are, however, still unclear. Also, it has to be yet formally demonstrated that Rheb function plays a role in the regulation of autophagy.

Besides the TSC1/2-Rheb pathway, the class III PI 3-kinase Vps34, has recently also been implicated in the sensing of amino acids upstream of mTOR (Byfield et al., 2005; Nobukuni et al., 2005). Vps34 forms a complex with Beclin1, the mammalian homologue of yeast Atg6. Byfield et al. (Byfield et al., 2005) immunoprecipitated over-expressed Beclin1 from MCF7 cells and measured the associated Vps34 activity. Amino acid deprivation led to a decrease in Beclin1 associated Vps34 activity, while the amount of Beclin1-associated Vps34 did not change. Additionally, over-expression of Vps34 led to an activation of p70S6 kinase, putting Vps34 upstream of mTOR. Furthermore, inhibition of Vps34, by siRNA knockdown, had no effect on the phosphorylation of TSC2, suggesting that Vps34 is not part of the TSC1/2 pathway towards mTOR. How amino acids modulate this interaction is unclear.

An interesting interaction has also been found for Beclin1 and the anti-apoptotic protein Bcl-2. Beclin1 was found to bind to Bcl-2 in a nutrient-dependent manner (Pattingre et al., 2005). Starvation of HeLa cells led to strong

reduction in the amount of Bcl-2 that could be co-immunoprecipitated with Beclin1. On the other hand, incubation of the cells in nutrient rich medium increased the amount of bound Bcl-2. Pattingre et al. suggested that Bcl-2 binding to Beclin1 might help to regulate the level of autophagy to prevent cells crossing an arbitrary threshold where autophagy becomes a cell death mechanism, instead of a survival mechanism. The relation between the three proteins, Vps34, Beclin1 and Bcl-2 with regards to their ability to regulate the level of autophagy remains to be investigated.

Other amino acid regulated pathways, besides mTOR have also been implicated in the induction of autophagy. In HT-29 cells Ogier-Denis et al. suggested that amino acids act by inhibiting ERK dependent GAIP phosphorylation (Ogier-Denis et al., 2000), while Talloczy et al. (Talloczy et al., 2002) suggested that eIF2alpha kinase is involved in amino-acid starvation induced autophagy in murine embryonic fibroblasts.

Additionally, there is evidence that at least leucine might act via a putative leucine plasma membrane receptor, and it has been suggested that this pathway is mTOR independent (Kanazawa et al., 2004). Although it is clear that amino acids inhibit autophagy, the "amino acid receptor" is still unknown. It is possible and may even be likely that eukaryotic cells might have several amino acid sensing pathways, which potentially converge to regulate autophagy. How these pathways and proteins, e.g. Rheb, the Vps34-Beclin1 and Beclin1-Bcl-2 complexes, and possibly others, interact and how they are coordinated in order to regulate autophagy in response to nutrient-deprivation remains to be determined.

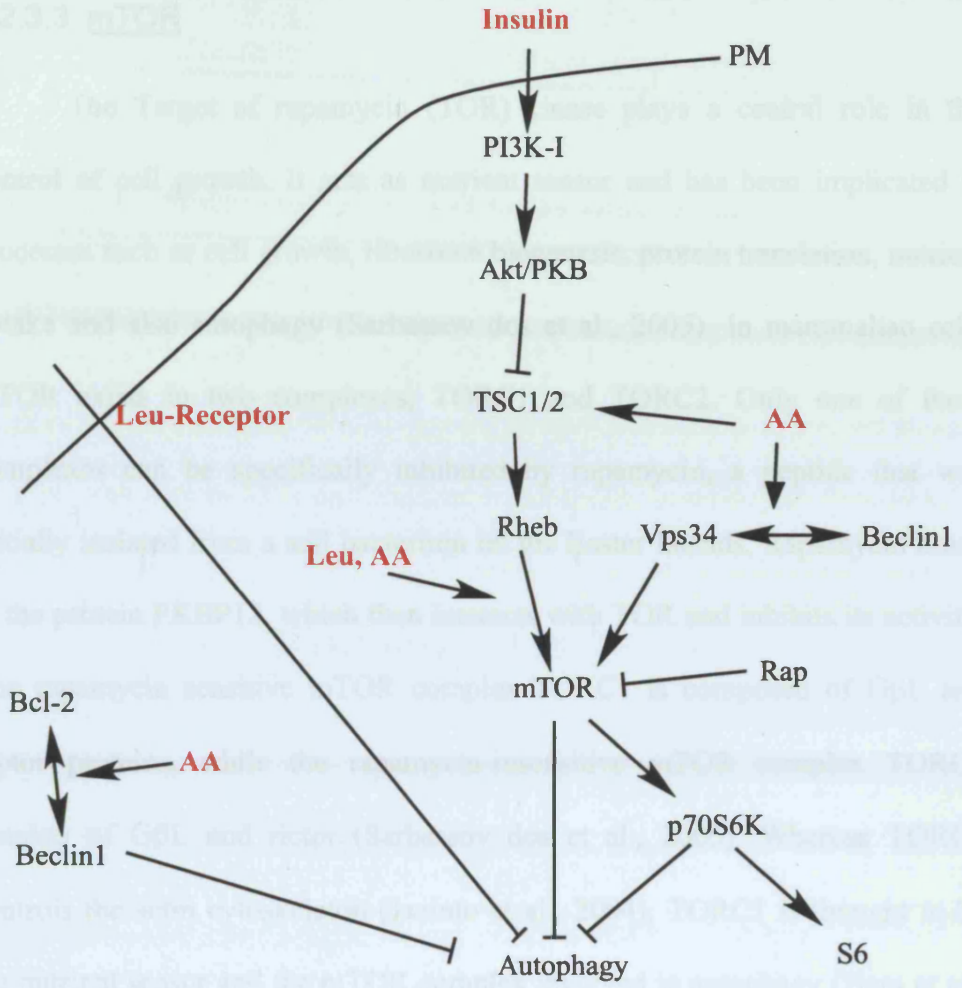

Figure 1.4: Proposed amino acid and insulin signalling pathways regulating autophagy. See also text for further details. Amino acids (AA) are implicated in regulating several protein-protein interactions that are possibly involved in the induction of autophagy. Most affected pathways are potentially upstream of mTOR. AA withdrawal was shown to affect the Bcl-2 - Beclin1, Vps34 - Beclin1 and Rheb - mTOR interactions, leading to the inactivation of mTOR and the induction of autophagy. The TSC1/2 complex has also been implicated in amino acid sensing, although this is controversial. In addition, the existence of a putative leucine receptor, which inhibits autophagy independent of mTOR, has been suggested. Rapamycin (Rap) specifically inhibits mTOR activity. PM, plama membrane. AA and insulin input into the system depicted in red colour.

1.2.3.3 mTOR

The Target of rapamycin (TOR) kinase plays a central role in the control of cell growth. It acts as nutrient sensor and has been implicated in processes such as cell growth, ribosome biogenesis, protein translation, nutrient uptake and also autophagy (Sarbassov dos et al., 2005). In mammalian cells mTOR exists in two complexes, TORC1 and TORC2. Only one of these complexes can be specifically inhibited by rapamycin, a peptide that was initially isolated from a soil bacterium on the Easter Islands. Rapamycin binds to the protein FKBP12, which then interacts with TOR and inhibits its activity. The rapamycin sensitive mTOR complex TORC1 is composed of GβL and raptor proteins, while the rapamycin-insensitive mTOR complex TORC2 consists of GβL and rictor (Sarbassov dos et al., 2005). Whereas TORC2 controls the actin cytoskeleton (Jacinto et al., 2004), TORC1 is thought to be the nutrient sensor and the mTOR complex involved in autophagy (Hara et al., 2002; Tzatsos and Kandror, 2006).

In 1995 Blommaart et al. (Blommaart et al., 1995b) found that rapamycin treatment of hepatocytes partially induced autophagic sequestration of electro-injected cytosolic ^{14}C-sucrose and protein degradation. This was accompanied by an inhibition of phosphorylation of the ribosomal protein S6, indicating the involvement of the p70S6 kinase pathway.

However, the first time, TOR was directly linked to autophagy was in a study conducted by Noda and Ohsumi (Noda and Ohsumi, 1998). Rapamycin induced autophagy, even when the yeast were incubated in full growth medium. Furthermore, rapamycin did not induce autophagy in Atg4, Atg5 and Atg10

mutants, indicating that TOR acts upstream of the Atg proteins as a negative regulator of autophagy.

Since then several studies using different cell types (Amer and Swanson, 2005; Blommaart et al., 1995a; Ravikumar et al., 2004) have shown that TOR or mammalian TOR (mTOR) is clearly involved as a negative regulator in the control of autophagy. Scott et al. (Scott et al., 2004), for instance, could show that the *Drosophila* fat body contains an increased number of autolysosomes in TOR null mutants as compared to wild type flies. In some recent studies including my own, however, certain cell types, such as hepatocytes or C2C12 myotubes, showed some degree of rapamycin-insensitivity (Kanazawa et al., 2004; Kochl et al., 2006; Mordier et al., 2000).

1.2.3.4 Downstream of mTOR

Not much is known about downstream effectors of mTOR with regards to autophagy. In yeast, Atg13 is dephosphorylated when TOR is inhibited by either rapamycin treatment or starvation. This leads to the tighter binding of Atg13 to Atg1, an association which is essential for autophagy, but not the Cvt pathway. It is currently unknown how TOR inactivation leads to dephosphorylation Atg13. A direct phosphorylation and/or the regulation of a phosphatase by mTOR would be possible, but has not been shown yet. In mammalian cells, no Atg13 homologue has been found so far.

In mammalian cells, p70S6 kinase is a potential autophagy regulator downstream of mTOR. p70S6 kinase is specifically phosphorylated by mTOR on threonine-389 during nutrient rich conditions and its activity correlates with the suppression of autophagy (Blommaart et al., 1995a; Moller et al., 2004).

p70S6 kinase phosphorylates the ribosomal protein S6, which leads to increased levels of translation. During periods of starvation or after rapamycin treatment, mTOR is inactivated. This in turn leads to the inactivation of p70S6 kinase and the dephosphorylation of S6, a process which has been linked with the induction of autophagy (Blommaart et al., 1995a).

Controversially, in *Drosophila* Scott et al. (Scott et al., 2004) showed that p70S6 kinase activity is required for starvation induced autophagy. Scott et al. argued that p70S6 kinase either might be involved directly in the induction of autophagy or indirectly by regulating protein synthesis, which would be consistent with data that protein synthesis is required for autophagy (Abeliovich et al., 2000). Furthermore, the authors suggested that down-regulation of p70S6 kinase might limit the extent of autophagy during extended starvation periods, possibly as a protective mechanism against the potentially damaging effects of autophagy.

The reason for this apparent difference remains to be investigated. Besides cell type specific differences it is possible that some residual p70S6 kinase activity remains after autophagy is induced in Blommaart's rat hepatocytes. Alternatively p70S6 kinase might have also other targets than just S6, which might be involved in the induction of autophagy.

Most interesting to me, is the suggestion that the extent of autophagy might be regulated through p70S6 kinase. If this turns out to be true, this would be a another built-in safety net, similar to what Pattingre et al (Pattingre et al., 2005) suggested for the Beclin1-Bcl2 interaction, which might control the balance between autophagy as a rescue or cell death mechanism. However, this remains to be investigated.

1.3 Autophagosome Fusion

In yeast, autophagosomes fuse directly with the vacuole to deliver the cytoplasmic material for degradation. In mammalian cells, on the other hand, autophagosomes fuse with compartments of the endocytic system. It is not clear, however, if there is a preferred endosomal compartment for fusion or if an autophagosome undergoes multiple fusion events with different compartments of the endocytic system. Depending on the cell type there is evidence supporting both a fusion event with early endosomes (Berg et al., 1998) and late endosomes (Berg et al., 1998; Punnonen et al., 1993; Tooze et al., 1990) as well as with lysosomes (Gordon et al., 1992; Lawrence and Brown, 1992). Additionally, autophagosomes have been demonstrated to fuse with small endosome derived vesicles and it has been suggested that it is this way they first acquire enzymes and lysosomal membrane proteins necessary for the acidification and degradation of their content (Punnonen et al., 1993). However, the precise identity of these vesicles is not known. Dunn et al. (Dunn, 1990b) developed a model in which the acidification of an autophagosome starts through the fusion with small vesicles and the delivery of proton pumps and lysosomal membrane proteins, but not lysosomal enzymes. Next, autophagosomes fuse with late endosomes or MVBs, hydrolases are delivered, and an amphisome is produced (Berg et al., 1998). This might then be followed up by another fusion step with lysosomes, which produces an autolysosome (Berg et al., 1998). The pH of an autolysosome was estimated by Tanaka et al. to be approximately 5.5 (Tanaka et al., 2000)(see Figure 1.8 for a model of the different fusion events). Besides the heterotypic fusion with endosomal

compartments also heterotypic fusion between AVis and AVds or amphisomes has been observed (Eskelinen, 2005).

This all indicates that the maturation of an AVi to an AVd is a highly regulated process. It is very likely that some or all of these processes require specific SNARE and Rab proteins to generate the necessary specificity for the following fusion events. In the following chapters I will first give a general overview about membrane fusion, followed by a summary of the current knowledge about the regulation of autophagosome fusion and the role of the cytoskeleton in fusion.

1.3.1 Regulation of membrane fusion by SNARE and Rab proteins

One of the most important distinguishing feature of eukaryotic cells is their compartmentalisation into several different membrane-bound organelles. Secretion of hormones, the uptake of extra-cellular substances, as well as organelle-homeostasis is therefore absolutely dependent on vesicular trafficking events to deliver and retrieve proteins or membrane. These trafficking events have to be tightly regulated to maintain the specificity of the membrane fusion events. Generally there are two types of fusion, heterotypic and homotypic fusion. The latter is less frequent, and can be found, for instance, in immature secretory granule biogenesis (Tooze et al., 2001) or endocytosis (Antonin et al., 2000).

Membrane fusion can be subdivided into three different phases: tethering, docking and fusion. During this process two specific membranes are successfully brought closer and closer together by tethering factors and Rab proteins until specific N-ethylmalemide-sensitive fusion protein (NSF)

attachment receptor (SNARE) proteins on both membranes can form a complex and catalyse the fusion of two membrane bilayers through a conformational change (Figure 1.7A).

Mammalian cells have approximately 35 different SNARE proteins and 60 different Rab proteins (Bock et al., 2001), which are all required for distinct transport steps within the cell and which are highly conserved between organisms.

1.3.1.1 SNARE proteins

SNAREs are small proteins of 100-300 amino acids, consisting of a C-terminal transmembrane domain, a helical SNARE domain and a variable N-terminal domain (see Figure 1.5 for localization of SNAREs). Initially SNAREs were divided into v-SNAREs and t-SNAREs based on their localisation on vesicles or target membranes (Sollner et al., 1993). Because this nomenclature does not work in the case of homotypic fusion events, SNAREs have been reclassified as R-SNAREs and Q-SNAREs according to a highly conserved residue in the SNARE domain (Fasshauer et al., 1997).

The neuronal SNARES Sytaxin-1 (Bennett et al., 1992), SNAP-25 (25 kDa synaptosome-associated protein)(Oyler et al., 1989) and VAMP (vesicle-associated membrane protein)(Trimble et al., 1988) where the first identified. They are archetypical SNAREs and form the basis for the subdivision of SNARE into smaller groups: R-SNAREs (VAMPs), Qa-SNAREs (syntaxins), Qb-SNAREs (SNAP N-terminal) and Qc-SNAREs (SNAP C-terminal) (Figure 1.5).

SNAREs function by binding to cognate SNAREs on the opposing membrane. This involves the parallel pairing of 4 SNAREs via their SNARE domain and leads to the formation of an extremely stable helical SNARE complex (Sutton et al., 1998). The complex is resistant to SDS (Hayashi et al., 1994) and is stable up to 90 °C (Fasshauer et al., 1997). It is generally believed that one SNARE of each of the four groups is required, resulting in a Qa-Qb-Qc-R configuration of the SNARE complex, also called the trans-SNARE complex. . Complex formation then results in a conformational change that brings the membranes close together and overcomes the energy barrier to drive fusion of the lipid bilayers (Figure 1.7B).

After fusion is complete the trans-SNARE complex is disassembled via the AAA ATPase NSF (N-ethylmaleimide-sensitive factor) and its co-factor α-SNAP in an ATP dependent manner, allowing the single SNAREs to participate in the next round of fusion (Sollner et al., 1993)(Figure 1.7B).

Although SNARE function is relatively well understood there are still a number of questions remaining. For example, it is not clear how many SNARE complexes are required for membrane fusion to occur and how these multiple SNAREs would be concentrated in one area to generate, for example a fusion ring. It has also been suggested that SNARE complexes might induce a hemifusion intermediate state, which then requires the action of other proteins to complete the fusion, such as Ca^{2+} dependent synaptotagmin proteins (Jahn and Sudhof, 1999).

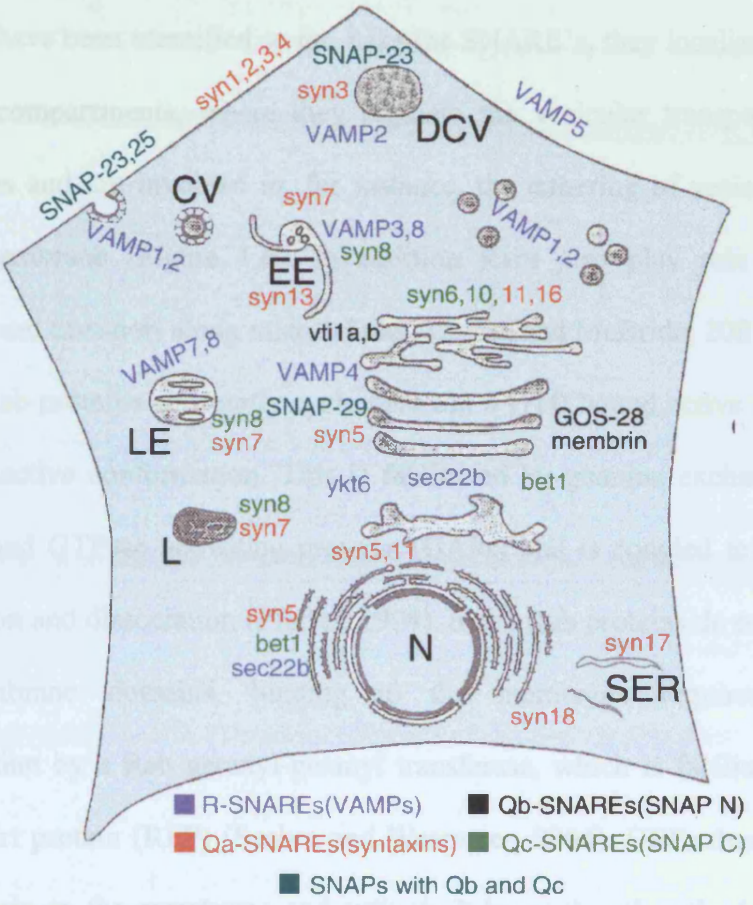

Figure 1.5: Subcellular localization of SNARES. CV, clathrin coated vesicle; DCV, dense core vesicle; EE, early endosome; LE late endosome; L, lysosome; SER, smooth endoplasmic reticulum. Figure taken from Bock, 2001.

1.3.1.2 Rab proteins

Rab proteins are a large family of conserved small monomeric GTPases, playing a role in membrane trafficking events. In humans, more than 60 Rab proteins have been identified so far. Like the SNARE's, they localize to distinct cellular compartments, where they regulate the vesicular transport between organelles and are involved in, for instance, the tethering of vesicles to their target membrane (Figure 1.6). In addition Rabs also play role in vesicle budding and transport along microtubules. (Zerial and McBride, 2001).

Rab proteins constantly cycle between a GTP-bound active and a GDP bound inactive conformation. This is facilitated by guanine exchange factors (GEFs) and GTPase activating proteins (GAPs) and is coupled to membrane association and dissociation (Pfeffer, 1994). Since Rab proteins do not have any transmembrane domains, binding to the membrane requires geranyl-geranylation by a Rab geranyl-geranyl transferase, which is facilitated by the Rab escort protein (REP) (Seabra and Wasmeier, 2004). GEFs then target the Rab protein to the membrane and activate it by exchanging the bound GDP with GTP. Active Rab proteins exert their function by binding to effectors, which then connect the two opposing membranes. After fusion and GTP hydrolysis, GDP dissociation inhibitor (GDI) binds to the Rab and removes it from the membrane. GDI solubilises Rab-GDP in the cytosol by enveloping the geranyl-geranyl groups (Rak et al., 2003)(Figure 1.7A).

Two Rab proteins which are particularly well studied are Rab5 and Ypt7p, the yeast Rab7 homologue. Rab5 regulates the homotypic fusion of early endosomes, as well as transport from the plasma membrane to the early

endosome. One effector of Rab5 is early endosome antigen 1 (EEA1) (Christoforidis et al., 1999). EEA1 is a coiled-coiled protein with a Rab5 binding site on each end, suggesting that it can bridge two endosomes that have membrane bound Rab5, thereby acting as a tethering factor. EEA1 itself interacts with Stx13, which is involved in early endosome fusion (McBride et al., 1999). A similar symmetric binding of a Rab protein has been shown in the case of Ypt7p. Ypt7p binds to the HOPS complex (homotypic fusion and vacuole protein sorting) on two vacuoles, thereby acting as a tether in vacuole fusion (Wang et al., 2002).

Until now a long list of Rab effector proteins have been found, many of them involved in tethering and binding to SNAREs, showing the importance of Rab proteins in the early phases of fusion. It is likely that this complex network of proteins is responsibly for the high specificity and fidelity of fusion events within the cell. It also implies, however, that the recruitment of proteins, required for fusion (and vesicle budding for that matter), must be tightly regulated in a time-wise manner to ensure the integrity of the organelle and the vesicle trafficking pathway.

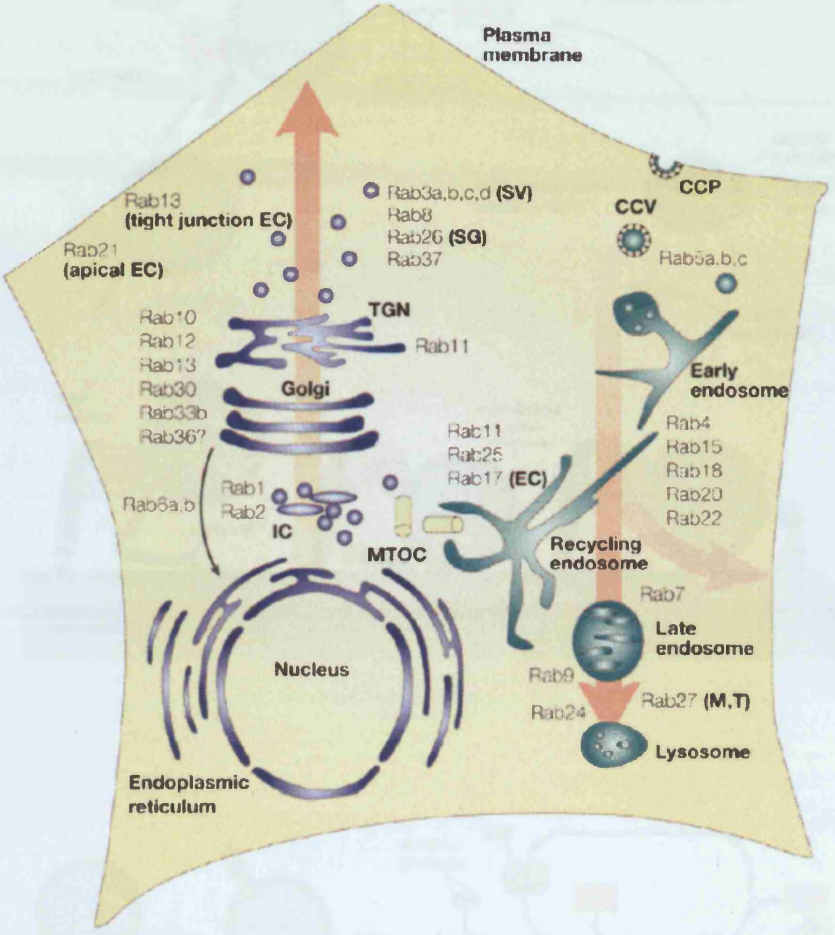

Figure 1.6: Subcellular localization of Rab proteins. CCV, clathrin-coated vesicle; CCP, clathrin-coated pit; EC, epithelial cells; IC, ER–Golgi intermediate compartment; M, melanosomes; MTOC, microtubule-organizing centre; SG, secretory granules; SV, synaptic vesicles; T, T-cell granules; TGN, trans-Golgi nextwork. Figure taken from Zerial, 2001.

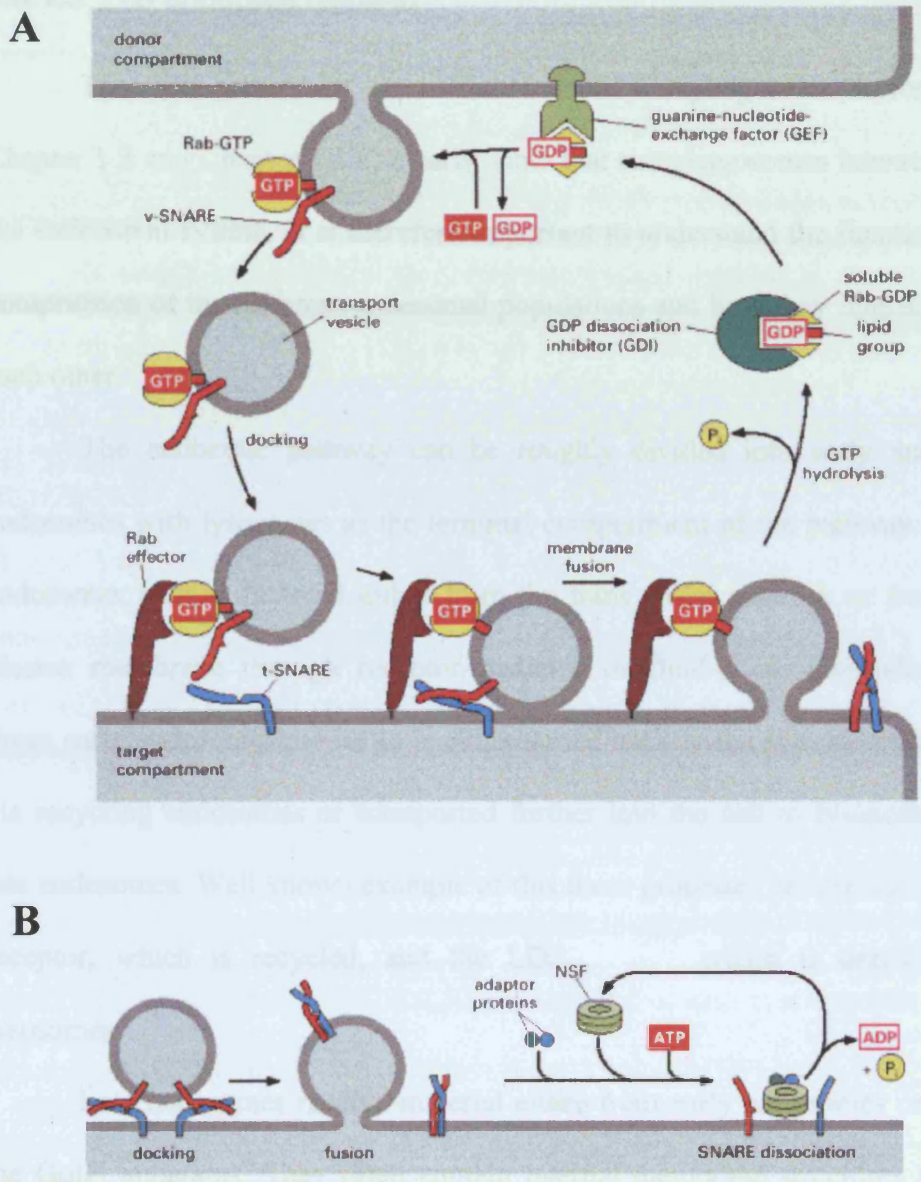

Figure 1.7: Membrane fusion. A) A Rab protein on the donor membrane is activated by a GEF and binds to the newly formed vesicle. The Rab protein and its effectors then tether and dock the vesicle to the target membrane, where SNARE pairing occurs. After the fusion the Rab protein is released from the membrane by GTP hydrolysis. B) SNARE dissociation through NSF and α-SNAP after fusion is complete. Figures taken from Molecular Biology of the Cell, 4th Edition.

1.3.1.3 The endocytic pathway

The data present in the literature about autophagosome fusion (see Chapter 1.3 and Chapter 1.3.2) clearly show that autophagosomes interact with the endosomal system. It is therefore important to understand the function and composition of the different endosomal populations and how they interact with each other.

The endocytic pathway can be roughly divided into early and late endosomes with lysosomes as the terminal compartment of the pathway. Early endosomes receive material either from the trans Golgi network or from the plasma membrane through receptor-mediated or fluid-phase internalization. From early endosomes the cargo is either sorted back to the plasma membrane via recycling endosomes or transported further into the cell to lysosomes via late endosomes. Well known example of this these processes are the transferrin receptor, which is recycled, and the LDL which is degraded in lysosomes.

Late endosomes receive material either from early endosomes or from the Golgi apparatus. They often contain internal membrane structures and/or small vesicles and are referred to as multi-vesicular bodies (MVBs). These structures are formed by the internalization of the endosomal membrane via the ESCRT protein complex (reviewed in (Raiborg et al., 2003)). From late endosomes cargo can then be delivered to lysosomes.

Lysosomes are characterized by an acidic pH of approximately 5.0, the presence of acid hydrolases, and a number of highly glycosylated membrane proteins, such as LAMPs or LIMPs. They receive traffic from the endocytic and

biosynthetic pathway and are responsible for degrading endocytosed material or material delivered from the cytoplasm through autophagy.

Several models exist which explain how material is transported through the endosomal system to lysosomes. The vesicle transport model hypothesizes that early and late endosomes are stable and distinct organelles. Transport to late endosomes in this case occurs through vesicular transport. Late endosomes are then assumed to mature into a lysosome (Mullins and Bonifacino, 2001). In the maturation model, early endosomes form from vesicles originating from the plasma membrane. Material is then retrieved and delivered to the early endosome via vesicular transport. During that process the early endosomes matures to a late endosome and finally lysosome (Rink et al., 2005; Stoorvogel et al., 1991).

Besides those two models, also kiss and run events have been suggested to occur between late endosomes and lysosomes, where the two vesicles briefly touch to exchange material and then separate again, keeping their late endosome/lysosome identity (Bright et al., 2005). Finally, it has been suggested that late endosomes might fuse directly with lysosomes, generating a hybrid organelle (Mullock et al., 1998).

Early endosomes and late endosomes have a distinct protein composition, generating specificity for fusion events. Rab4, Rab5 and Rab11 are associated with early endosomes, while Rab7 and Rab9 can be found on late endosomal structures. The same spatial separation also exists for SNARE proteins. Early endosomes contain VAMP3, 8 and Stx13, late endosomes have VAMP7, 8 and vti1b (Chen and Scheller, 2001; Pryor PR, 2004). Both, early and late endosomes are Stx7 and Stx8 positive(Chen and Scheller, 2001).

Considering, that autophagosomes fuse with compartments of the endocytic pathway, it is likely that they need the same fusion machinery that endosomes or endosomal derived vesicle use to fuse with each other. However, it is currently unclear which particular Rabs or SNAREs are required, especially for the early fusion steps, and how they would be targeted to AVis. The timing of this process is another unknown. To prevent open, unsealed isolation membranes from fusing with endosomes, the fusion machinery would have to be delivered only after the autophagosome has formed or alternatively the activity of the fusion machinery would have to be regulated. This would, however, require the existence of a checkpoint system which would monitor autophagosome formation and closure. So far, there is no data, supporting this idea, possibly with the exception of GATE-16 function during Golgi reassembly after mitosis (Muller et al., 2002). GATE-16, an LC3 homologue, binds the Golgi SNARE GOS28 and thereby prevents it from binding to Stx5. The authors suggest that GATE-16 must be displaced from GOS-28 for trans-SNARE complex formation to occur, which might require a Rab GTPase as with the displacement of Sly1p from Stx5.

1.3.2 Regulation of autophagosome fusion through proteins

Little is currently known in mammalian cells about the regulation of autophagosome fusion and the proteins involved in it. In yeast, the Vam3p t-SNARE is required for the docking and fusion of autophagosomes with the vacuole (Darsow et al., 1997). In addition, Sec18, the yeast NSF homologue, and the t-SNARE vti1 have also been shown to be involved in autophagy in yeast as well as in plants (Ishihara et al., 2001; Surpin et al., 2003)

In CHO cells, Rab24 translocates from a peri-nuclear structure to newly formed LC3-positive autophagosomes when autophagy is induced by starvation (Munafo and Colombo, 2002). Additionally Rab7, a protein required for late endosome fusion(Bottger et al., 1996), has also been implicated in autophagy (Gutierrez et al., 2004b; Jager et al., 2004). Rab 7 localizes mainly to the membrane of AVds, but can also be found in lower quantities on AVis as measured by IF and electron microscopy. SiRNA knockdown of Rab7 led to an increase in AVd numbers, suggesting that a late fusion step is inhibited and that AVds are accumulating under those conditions (Jager et al., 2004). This was further confirmed by labelling early endosomes or lysosomes with rhodamine-dextran. When a dominant negative form of Rab7 was over-expressed, rhodamine-dextran in early endosomes was still transported into autophagosomes, while rhodamine-dextran chased into lysosomes never reached autophagosomes (Gutierrez et al., 2004b). These results suggest that Rab7 is not required for autophagosome fusion with early endosomes but is necessary for the fusion with lysosomes or late endosomes(Eskelinen, 2005).

Besides the above mentioned Rab proteins, the only mammalian SNARE protein which has so far been implicated in autophagosome maturation, is Vti1b, the mammalian homolouge of yeast vti1 (see above) (Atlashkin et al., 2003). Isolated hepatocytes from vti1b$^{-/-}$ mice accumulated multivesicular bodies (MVB) and AVds in their cytoplasm, suggesting that the fusion of AVds with lysosomes and the subsequent complete degradation of the autophagosome contents is impaired.

Both, Vti1b and Rab7 are involved in the fusion of AVds with lysosomes. The AAA ATPase (ATPase associated with a variety of cellular

activities) SKD1, the mammalian homologue of yeast vps4 on the other hand, was shown to be involved in the fusion of autophagosomes with endosomes (Nara et al., 2002). SKD1 plays a role in endosomal transport and MVB biogenesis (Lin et al., 2005). Over-expression of a dominant-negative mutant, SKD1(E235Q) in HeLa cells, impaired autophagy-dependent long-lived protein degradation and led to the accumulation of mainly AVis after starvation. Additionally, the transport of the late-endosome specific lipid lysobisphosphatidic acid to the autophagosomal membrane was inhibited, in HeLa cells over-expressing dominant negative SKD1(E235Q) (Nara et al., 2002).

Finally, mice deficient in cathepsin D or in cathepsin B and L accumulate autophagy-like structures (Koike et al., 2005), as well as the LC3-II form in their brain, showing that the lysosomal function is necessary to execute the last step of autophagy, the degradation of the autophagosome contents.

Together these data indicate that autophagosome fusion is a step-wise process. It is feasible that the sequential fusion is necessary for acquiring the necessary fusion machinery for subsequent fusion events and the maturation of an autophagosome (Eskelinen, 2005).

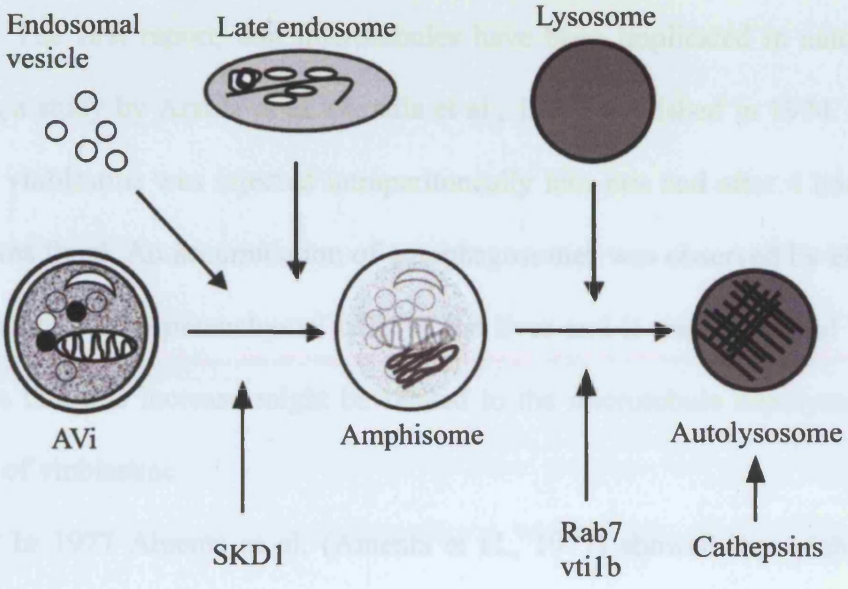

Figure 1.8: Autophagosome maturation model. Possible fusion partners and proteins involved in this fusion reaction are indicated. Figure modified from Eskelinen, 2005.

1.3.3 The role of the cytoskeleton in autophagosome maturation

The role of the microtubule cytoskeleton in autophagosome fusion has been extensively investigated in the past. Most of those studies were based on the use of nocodazole and vinblastine, drugs which bind to tubulin and depolymerise microtubules.

The first report, that microtubules have been implicated in autophagy was in a study by Arstila et al. (Arstila et al., 1974) published in 1974. In this study, vinblastine was injected intraperitoneally into rats and after 4 hours the liver was fixed. An accumulation of autophagosomes was observed by electron microscopy in the parenchymal cells of the liver and it was suggested by the authors that this increase might be related to the microtubule depolymerising action of vinblastine.

In 1977 Amenta et al. (Amenta et al., 1977) showed that vinblastine treatment of rat embryonic fibroblasts, incubated in serum free medium, inhibits the release of ^{14}C-leucine in a protein degradation assay, showing that microtubules are necessary for autophagic protein degradation

Five years later, in 1982 Hirsimaki et al (Hirsimaki and Pilstrom, 1982) suggested that autophagosomes accumulate in hepatocytes after vinblastine injection into mice because their turnover is retarded, but that vinblastine did not prevent the fusion of lysosomes with autophagosomes (Hirsimaki and Reunanen, 1980). In the same year Kovacs et al. (Kovacs et al., 1982) published an EM based study in which they classified autophagosomes into three groups: type I autophagosomes, which are early autophagosomes, type II autophagosomes, which contain highly denatured material at various stages of

degradation, and type III autophagosomes, which contain electron dense remnants of digested material. Vinblastine treatment of isolated rat hepatocytes led to an accumulation of type I autophagosomes, as well as type III autophagosomes. In addition, vinblastine treatment also inhibited protein degradation, suggesting that vinblastine inhibits the fusion of autophagosomes with lysosomes. This study was followed up by Hoyvik et al. (Hoyvik et al., 1986) who could show that vinblastine treatment of isolated hepatocytes inhibited the degradation of ^{14}C-lactose internalized into autophagosomes, strengthening the conclusion that vinblastine inhibits the fusion of autophagosomes.

Similar observations were made by Aplin et al. (Aplin et al., 1992a) in nocodazole treated NRK cells. Starvation of NRK cells in the presence of nocodazole led to an increase in autophagosome numbers and at the same time a decrease in autophagic protein degradation. About 50 % of the accumulated autophagosomes were late autophagosomes, where vesicle acidification had started, however, they were lacking hydrolytic enzymes, suggesting that microtubules are important for the fusion of late autophagosomes with lysosomes. Nocodazole had no effect on autophagosome formation.

More recently two publications (Iwata et al., 2005; Webb et al., 2004) could show that microtubules are necessary for the autophagic degradation of Huntington aggregates.

The data presented above strongly indicates that microtubules are required for efficient autophagosome fusion as several groups could show an accumulation of early autophagosomal structures and impaired trafficking of autophagocytosed material to lysosomes, resulting in the inhibition of

autophagic protein degradation. However, seemingly in contradiction to the data presented above, several studies have been published which showed that autophagosome fusion was independent of microtubule depolymerisation by nocodazole or vinblastine. Vinblastine treatment of Ehrlich ascites tumour cells did not prevent the delivery of lysosomal enzymes into autophagosomes (Punnonen and Reunanen, 1990), suggesting that the accumulation has been caused by the retarded maturation of late autophagosomes. Nocodazole treatment of Ehrlich ascites tumour cells, on the other hand, had no effect at all on autophagosome number in comparison to untreated cells (Reunanen et al., 1988), also suggesting that microtubules are not needed for autophagy. In cultured rat fibroblasts, horse-radish peroxidase (HRP) and cationized ferritin, internalized into endosomes, could reach autophagic vacuoles even if microtubules were disrupted by vinblastine (Punnonen et al., 1993).

Despite extensive investigations about the role of microtubules in autophagosome fusion, the data is still highly controversial. Depending on the cell-type and experimental approach, microtubules have been shown to be required or not for fusion. One possible reason for that might be that the microtubule network was not fully depolymerised at the start of the experiment, as in most studies vinblastine or nocodazole was added to the cells at the beginning of starvation. Depending on the concentration of the drugs and the sensitivity of the cells to the drugs, the microtubule network would only be depolymerised after an initial lag period during which autophagy is unaffected.

Although there is a large amount of data about microtubules and autophagy in the literature, not much is know about other cytoskeleton types in autophagy. In yeast, actin has recently been involved in selective types of

autophagy, such as the cytoplasm to vacuole (Cvt) pathway and pexophagy, the selective degradation of peroxisomes, but not in non-selective bulk autophagy (Reggiori et al., 2005a). In a conditional actin mutant preApe1, the substrate of Cvt vesicles was not targeted to the pre-autophagosomal structure, leading to an early block of the pathway. Depolymerisation of the actin cytoskeleton in mammalian NRK cells with cytochalasin B and D impaired also autophagosome formation (Aplin et al., 1992a). In Ehrlich Ascites tumour cells, on the other hand, actin depolymerisation with cytochalasin B had no effect on vinblastine induced autophagy (Hirsimaki and Hirsimaki, 1984).

Hardly anything is know about the role of the cytoskeleton during autophagosome formation. There is at least one report, showing that the actin cytoskeleton is important for formation, while microtubules were found to be not involved in formation (Aplin et al., 1992a).

1.4 Aim of the thesis

The aim of this thesis was to investigate the molecular requirements for autophagosome formation and fusion. Despite recent advances in the field there is still not much known about those two processes. Neither are the fusion partners of an autophagosome well defined, nor is the order in which AVis interacts with the endosomal system, or the molecular machinery for fusion very well understood. In addition the role of microtubules for autophagosome formation, as well as fusion, is unclear and controversial and most of the findings presented above were published before the Atg genes were found. A more in depth analysis of the role of the cytoskeleton in formation and fusion,

by utilizing the specific autophagosome marker LC3 as well as specific siRNA depletion of Atg proteins, was missing at the beginning of this thesis. I therefore decided to study autophagosome maturation by using a variety of *in vivo* and *in vitro* approaches.

Since most tissue culture cell lines have only a limited capacity to undergo autophagy, I opted to develop a system based on cultured primary rat hepatocytes and adenoviral transduction methods. Rat hepatocytes have been widely used for morphological studies in the autophagy field and were therefore an ideal system for my studies.

Once the rat hepatocyte system was established, I developed a light microscopy based technique to investigate autophagosome formation and fusion independently *in vivo*. Using this assay I investigated the role of mTOR and microtubules in autophagosome formation, as well as the role of microtubules in fusion of autophagosomes.

In parallel I started to develop an *in vitro* autophagosome fusion assay to identify the different fusion partners of autophagosomes and the Rab- and SNARE-proteins required for fusion.

2 MATERIALS AND METHODS

2.1 Reagents

2.1.1 Chemicals and enzymes

Reagents were obtained from Amersham, BDH, BioRad, Calbiochem, Cell Signalling Technologies, Clontech, Fisher Scientific, Gibco, Invitrogen, Merck, Molecular Probes, New England Biolabs, Qiagen, Sigma Aldrich, Stratagene and TAAB. Taq polymerase, distilled H_20, PBS, LB medium, SOC medium, sterile glycerol, Earle's Saline, Dulbecco's Modified Eagle's Medium (DMEM), F12 medium, DMEM:F12 minus valine, DMEM minus antibiotics and glutamine were provided by Cancer Research UK Central Services.

2.1.2 Antibodies

All HRP-conjugated secondary antibodies were from Amersham Pharmacia, and all fluorescently-conjugated antibodies were from Molecular Probes. The following primary antibodies were used:

Table 2.1: Primary antibodies

Antigen	Antibody name	Source	Dilution and application
Atg5	α–Atg5	Eeva Lisa Eskelinen	1:500 WB
Atg6	α–Atg6	BD Transduction Laboratories	1:500 WB

GFP	SG5	Tim Hunt, Cancer Research UK	1:2000 WB 1:50 EM
HA	12CA5	Cancer Research UK Monoclonal Services	1:2000 WB
LC3	STO 227	This study	1:750 WB
LC3	α–LC3	Tomatsu Yoshimori, National Institute of Genetics	1:1000 WB 1:20 EM
p70S6Kinase	α – p70S6K	Cell Signalling Technology	1:1000
p70S6Kinase Thr389	α–phospho-p70S6K	Cell Signalling Technology	1:1000
Tubulin	α–tubulin	Sigma Aldrich	1:200 IF
EEA1	α–EEA1	BD Transduction Labs	1:2500 WB
MP6R	STO52	Sharon Tooze, Cancer Research UK	1:500 WB
Rab7	α–Rab7	Angela Wandinger-Ness, University of New Mexico	1:2000 WB
Lamp2	α–Lamp2	Zymed	1:1000 WB

2.1.3 Constructs and Viruses

Following constructs and viruses were used in this thesis:

Table 2.2: Constructs and viruses used in this study

Construct	Source
GFP-LC3	Tamotsu Yoshimori National Institute of Genetics
Streptavidin (SV)	Peter Stanton, University of Washington
GFP Adenovirus	Philippe Halban, University Hospital Geneva
GFP-LC3 Adenovirus	This study
SV-HA-LC3 Adenovirus	This study, Viraquest

2.1.4 Oligonucleotides

Oligonucleotides were obtained from the Cancer Research UK Oligonucleotide Synthesis Service or Sigma. The following primers were used.

Table 2.3: Primers for cloning of the GFP-LC3 adenoviral construct:

Primer	*Sequence*
GFP-LC3-F	5'-CACCATGGTGAGCAAGGGCGAGGAGCTGTTC-3'
GFP-LC3-R	5'-TCACAAGCATGGCTCTCTTCCTGTTG-3'

Table 2.4: Primers for cloning of the SV-HA-LC3 adenoviral construct

Primer	*Sequence*
HA-F	5'-TCGAGATGGCATACCCATACGACGTCCCAGA CTACGCTAA-3'
HA-R	5'-AGCTTAGCGTAGTCTGGGACGTCGTATGGGT ATGCCATC-3'
LC3-F	5'-CTCAGAACTAGTTCCGTCCGAGAAGACCTTC-3'
LC3-R	5'-GTCGGCGCGGCGGCCGCCAAGCATGGCTCT CTTCCTGTTGC-3'
NSV-stop-F	5'-GTCTGCTGCTTCTATCGCGGGATCCACTAGTTCC-3'
NSV-stop-R	5'-CTGCTGCTTCTATCGCGGGATCCACTAGTTC CGTCC-3'

2.1.5 Peptides

Peptides were obtained from Cancer Research UK's Peptide Synthesis Laboratory.

Peptide:	*Sequence:*
LC3	PSEKTFKQRRSFEQRC
HA	YPYDVPDYA

2.1.6 Bacterial strains

E. coli strain:	*Application:*
DH5α	cloning
XL1-blue	cloning
Top1	pENTR cloning
XL10-Gold	Mutagenesis

2.1.7 Animals

Male Wistar rats were obtained from Charles River (UK) at a weight of approximately 250 g.

2.2 Methods

2.2.1 DNA techniques

2.2.1.1 Preparation of plasmid DNA

Plasmid purifications on a small or large scale were performed with the Qiagen Mini Prep or endotoxin-free Maxi Prep kit, respectively. Bacteria were grown in 5 ml or 200 ml cultures containing the appropriate selection drug for minipreps or maxipreps, respectively. Plasmid concentrations were determined as described in Chapter 2.2.1.2. In the case of cloning experiments, the plasmid insert was sequenced using insert or plasmid specific primers (see Chapter 2.2.1.5).

2.2.1.2 Quantification of DNA

DNA concentrations were quantified in a spectrophotometer at a wavelength of 260 nm after dilution in H_20. An OD_{260} of 1 corresponds to 50 µg DNA/ml double stranded DNA. To assess the purity the absorbance ratio $OD_{260/280}$ was recorded additionally. It was usually between 1.6 and 1.8.

2.2.1.3 Polymerase Chain Reaction (PCR)

PCR reactions were carried out in 100 µl reactions containing 50 ng template DNA, 250 µM dNTPs (Pharmacia), 2 µM forward and reverse primer, and 2.5 units Taq polymerase.

1 cycle	Denaturing	94 °C for 3 min
35 cycles	Denaturing	94 °C for 1 min
	Annealing	55 °C for 30 s
	Extension	72 °C for 1 min/kb
1 cycle	Extension	72 °C for 5 min

2.2.1.4 Restriction digestion

Restriction digests were carried out in 20 µl reactions containing 1 µg DNA, 5 units restriction enzyme (New England Biolabs) and 2 µl 10x restriction buffer supplied with the enzyme. Samples were incubated at 37 °C for 1 – 4 hours before the reaction was stopped by adding 5x sample buffer (Bromphenol blue in 50% glycerine, 1mM EDTA pH 8.0).

2.2.1.5 DNA sequencing

Fluorescent cycle sequencing was performed with the ABI dye terminator kit (Perkin Elmer). 3.2 pmol gene or vector specific primer were mixed with 500 ng double stranded DNA, 8 µl ABI reaction mix and H_20 to a final volume of 20 µl. Cycle sequencing conditions were as follows:

25 cyles	Denaturing	96 °C for 10 s
	Annealing	50 °C for 5 s
	Extension	60 °C for 4 min

To remove primers and dye terminators, samples were purified using the DyeEx 2.0 kit (Qiagen). SDS-Page gel electrophoreses was performed by Cancer Research UK Sequencing Service. Sequences were aligned with Sequence Navigator (ABI) or by performing a translated BLAST search on the NCBI web site.

2.2.1.6 DNA agarose gel electrophoresis

Depending on the size of the DNA, 0.8 – 2% (w/v) agarose was dissolved in TAE buffer (Tris-HCl pH 8.0, 20 mM acetic acid, 1 mM EDTA). Ethidium bromide was added to a final concentration of 0.5 µg/ml. Samples were mixed with 5x sample buffer (Bromphenol blue in 50% glycerine, 1mM EDTA pH 8.0) and separated in TAE at 100 Volts constant.

2.2.1.7 Gel purification of DNA fragments

The desired DNA fragment was cut out from an agarose gel and the DNA was isolated and purified from the gel slice with the QIAquick gel extraction kit (Qiagen).

2.2.1.8 Ligation

Gel purified DNA fragments and vectors were mixed at a molar ratio of approximately 5:1 and ligated with 400 Units of T4 ligase (New England Biolabs) in 20 µl reactions for either 1 hour at room temperature or over night at 16 °C. 5 µl of the ligation was then transformed into *E. coli* (see also Chapter 2.2.1.9).

2.2.1.9 Bacterial transformation

A 50 µl aliquot of competent XL1-Blue cells was mixed with 5 µl ligated DNA or 100 ng plasmid and incubated on ice for 30 minutes before being heat shocked at 42 °C for 45 seconds. 900 µl ice cold SOC medium was added and the reaction was incubated at 37 °C for a further 30 minutes. When ligations were transformed, bacteria were spun down at 6000 rpm for 10 minutes in a micro centrifuge. The bacterial pellet was resuspended in 100 µl LB medium and plated out on agar plates containing kanamycin or ampilicin. In the case of vector transformations 50 µl of the reaction were plated out without prior spinning.

2.2.1.10 Bacterial cryo-preservation

Bacterial cultures were stored as 30 % glycerol stocks at -80 °C.

2.2.1.11 Mutagenesis

Site-directed mutagenesis was carried out with the QuikChange XL kit (Stratagene) according to manufacturers instructions. Primers were designed so

that they had a minimum GC content of 40 %, terminated in either a G or C base and had a melting temperature of at least 78 °C.

1 cycle	Denaturing	95 °C for 1 min
18 cycles	Denaturing	95 °C for 50 s
	Annealing	60 °C for 50 s
	Extension	68 °C for 1 min/kb plasmid
1 cycle	Extension	68 °C for 7 min

Parental DNA was then digested with 10 units DpnI at 37 °C for 1 hour and DpnI-treated DNA was transformed into XL10-Gold Ultracompetent Cells (Stratagene) according to manufacturers instructions.

2.2.2 Tissue culture techniques

2.2.2.1 Maintenance of mammalian cells

HEK293A cells (Invitrogen) were maintained in growth medium (DMEM supplemented with 10 % foetal calf serum and 4.8 mM glutamine). Twice a week cells were split 1:10. For this, HEK293A cells were washed once with PBS (137 mM NaCl, 3.35 mM KCl, 10 mM Na_2HPO_4, 1.84 mM KH_2PO_4, pH 7.2) and then incubated in trypsine/versene (0.05 % trypsin (w/v), 0.02 % EDTA (w/v), 1 % phenol red in PBS) until cells came off the plastic. HEK293 cells were then either split into a new flask or seeded into dishes or plates at the desired concentration.

2.2.2.2 Transient Transfection

Transient transfections in HEK293A cells were carried out with Lipofectamine 2000 (Invitrogen) according to manufactures instruction. Growth medium was changed to growth medium without antibiotics one day before transfection. Cells were then incubated in Optimem in the presence of the reaction mix, containing plasmid DNA and Lipofectamine 2000. The reaction mix was prepared in polypropylene tubes. After 6 hours cells were washed with PBS and normal growth medium (DMEM with 10% fetal calf serum) was added back.

2.2.2.3 Storage and recovery of mammalian cells

For storage in liquid nitrogen HEK293A cells were trypsinised and spun at 1000 rpm for 5 minutes in swing bucket centrifuge (Heraeus). The cell pellet of one confluent T75 flask was resuspended in 3 ml growth medium, containing 20 % foetal calf serum and 10 % sterile DMSO. Cells were frozen at -80 °C in 1 ml aliquots in a Cryo 1 °C Freezing Container (Nalgene) filled with isopropanol to allow slow freezing (1°C/min). After a week, cells were transferred to liquid nitrogen for long term storage.

To recover cells, aliquots were rapidly thawed at 37 °C in a waterbath and added to one T75 flask, containing 25 ml of growth medium. The medium was replaced the following day, after the cells had attached to the plastic.

2.2.3 Protein techniques

2.2.3.1 Protein quantification

Protein concentrations of samples were measured using the BioRad protein assay reagent. IgG standards and samples were diluted in 800 µl H_20 and incubated with 200 µl protein assay reagent for at least 15 minutes. The absorbance at OD_{595} was measured and compared to the standard curve to calculate protein concentrations.

2.2.3.2 Preparation of cell lysates and SDS-polyacrylamide gel electrophoresis

Hepatocytes or HEK293 cells were washed once with ice cold PBS, and then scraped off in PBS. Cells were spun down for 5 min at 1000 g, and lysed in TNTE (20 mM Tris pH 7.5, 150 mM NaCl, 0.3 % Triton X-100, 5 mM EDTA) plus protease inhibitors (250 µM PMSF, 50 µg/ml chymostatin, 0.5 µg/ml leupeptin, 50 µg/ml antipain, 0.5 µg/ml pepstatin A, 0.1 mg/ml pefabloc). Nuclei and insoluble debris was removed from TNTE lysates by spinning in a microcentrifuge (10 min, 13000 rpm, 4 °C). Protein concentrations were determined (see Chapter 2.2.3.1) and samples were mixed with 5x sample buffer (312.5 mM Tris-HCl pH 6.8, 16 % β-mercaptoethanol (v/v), 15 % SDS (w/v), 50 % glycerol (w/v), 0.015 % bromophenol blue (w/v)).

Before loading samples were boiled for 3 minutes. Equal amounts of protein were loaded per lane, and separated on either 12 % SDS-PAGE gels or 10 % SDS-PAGE gels using 90 V constant for 12 minutes, then 120 V until the dye front reached the bottom of the gel. See below for composition of gels. Gel

systems used were either 1.5 mm thick Bio-Rad mini gels (Mini-Proteian II electrophoresis cell) or Cambridge electrophoresis midi gels

Table 2.5: Running gel composition. 4x Lower buffer (6 mM Tris-HCl pH 8.8, 1.6 % SDS). The volumes are sufficient for one mini gel

	10 % Gel	**12 % Gel**
4x Lower buffer	2.25 ml	2.25 ml
30 % Acrylamide **0.8 % Bis**	2.993 ml	3.6 ml
H_2O	3.708 ml	3.1 ml
Temed	4.5 µl	4.5 µl
10 % APS	45 µl	45 µl

Table 2.6: Composition of stacking gel. 4x Upper buffer (2 M Tris-HCl pH 6.8, 1.6 % SDS) The volumes are sufficient for one mini gel

	4.5 % Gel
4x Upper buffer	1 ml
30 % Acrylamide **0.8 % Bis**	0.6 ml
H_2O	2.356 ml
Temed	4 µl
10 % APS	40 µl

2.2.3.3 Western blotting

After SDS polyacrylamide gel electrophoresis, proteins were transferred to nitrocellulose membranes (Schleicher & Schuell) using the Genie blotting system (Idea Scientific Company). Gels and nitrocellulose membranes were embedded in a sandwich of 2 sheets 3MM Whatman paper and several pads on each side. Proteins were blotted at 4°C for 50 minutes at 25 volts constant in blotting buffer (20 mM Tris-OH, 150 mM glycine, 20 % methanol). Transfer and equal protein loading was tested with Ponceau S (Sigma) staining. Blots were blocked by incubating the membrane in blocking buffer (PBS, 5 % skimmed milk powder, 0.02 % Triton X-100) for 1 hour at room temperature or over night at 4 °C. Membranes were then incubated with the primary antibody in blocking buffer for at least 1 hour at room temperature, after which they were washed 3x in blocking buffer and incubated with the secondary HRP-conjugated antibody (Amersham) diluted 1:2000 in blocking buffer. Membranes were then washed 3x 10 minutes in PBS plus 0.02 % Tween-20 and incubated in enhanced chemiluminescence substrate (ECL, Amersham)

2.2.3.4 Immunoprecipitation (IP)

IPs were usually carried out in either TNTE or IP-buffer (50 mM Tris-HCl pH 7.4, 300 mM NaCl, 5 mM EDTA, 1 % Triton X-100). Lysates were first incubated with 5 µg antibody for at least 1 hour at 4 °C on an end over end rotator, before the addition of either 30 µl of a 50 % protein A or protein G-sepharose slurry for an hour. Sepharose beads were washed 3x with PBS before use. In the case of the in vitro fusion assay, based on the internalization of HA antibodies into endosomes (see Chapter 2.2.8.6), protein G-sepharose beads

were added directly, and samples were incubated for 1 hour at 4 °C on an end over end rotator. Beads were then washed 4x in PBS and either used for HRP enzyme assays (see Chapter 2.2.8.2) or for western blotting. In the case of the latter, the 4th wash was removed completely and the beads were boiled for 3 minutes with 30 µl 5x sample buffer in order to elute the bound antigen from the beads and to denature the proteins. To separate the beads from sample, the bottom of the Eppendorf tubes was pierced using a 25 gauge needle, and the tube placed into another empty Eppendorf. The eluent was spun through into the empty Eppendorf and either frozen at -20 °C or subjected immediately to SDS-PAGE and western blotting analysis.

2.2.4 Microscopy

2.2.4.1 Immunocytochemistry and confocal imaging of fixed samples

Hepatocytes were washed once in PBS and fixed in 3 % paraformaldehyde in PBS for 20 minutes at room temperature. Cells were rinsed 3 times with PBS and then incubated in 50 mM NH_4Cl in PBS for 10 minutes before permeabilization with 0.1% Triton X-100 in PBS for 3 minutes. After that, cells were washed in PBS and incubated for 20 minutes in blocking buffer (10% goat serum, 2% BSA, 0.02% Tween 20 in PBS), followed by incubation for 20 minutes in blocking buffer with the primary antibody. Cells were then washed 3 times with blocking buffer, incubated for 20 minutes in blocking buffer with the secondary antibody, washed 3 times with PBS, once with water and mounted on glass slides with Moviol. Secondary antibodies used were either Alexa488 or Alexa555 conjugated. Cells were imaged using a Zeiss LSM 510 confocal microscope equipped with a Zeiss 63x, 1.4NA

Differential Interference Contrast (DIC) Plan-Apochromat or Phase Contrast oil-immersion objective and controlled by Zeiss LSM 510 software. Images were collected using the 493 nm line of an argon laser and the 543 nm and 633 nm lines of a helium-neon laser with 4x or 8x averaging.

2.2.4.2 Confocal time lapse microscopy

Movies showing formation and movement of GFP-LC3-positive vesicles in living hepatocytes were recorded using an Olympus IX70 laser scanning confocal microscope equipped with an ultraview real time spinning disc (Wallac), an Olympus 60X, 1.2W UPlan Fluor oil immersion objective. Hepatocytes were either pre-incubated with 50 μM nocoazole in full growth medium or left untreated, washed 4x with Earle's Saline, containing 20 mM HEPES, with or without nocodazole and then placed into an environmental chamber immediately. Images were captured every 10 or every 23 seconds using Ultraview Imaging Suite Version 5.5 software (Perkin Elmer) and processed with either Metamorph 6.2 (Molecular Devices) or Volocity 3.0 (Improvision) software. Movies were generated by exporting processed images to AVI movies using Microsoft Video1 compression at a 100 % quality setting.

2.2.4.3 High throughput microscopy

Low magnification images of saponin-extracted hepatocytes (see Chapter 2.2.7.1) on coverslips were acquired with an automated high throughput Discovery-1 microscope equipped with a 20X, 0.75 NA, S-Fluor objective using the DAPI and GFP filter set (Chroma). 16 or 9 images (4 x 4 or 3 x 3) per coverslip were captured automatically using Metamorph 6.2

software. (Molecular Devices). The microscope was set up to focus automatically using the built-in image-based focusing algorithm with the following settings: Find 200 nm, Wide 200 nm, Narrow 8 nm. Laser-based focussing was not used.

2.2.4.4 Transmission electron microscopy (TEM)

Hepatocytes were seeded in 6 cm dishes at a density of 1.25 x 10^6 cells, and either mock-infected or infected with an adenovirus encoding GFP or GFP-LC3. After 18-24 h in culture, cells were fixed for 1 hour in 2.5% glutaraldehyde in 0.1 M Sörensen's buffer, pH 7.4, washed 3x in Sörensen's buffer and scraped off the culture dish in 1% gelatin. After the cells were pelleted, and post fixed with 1% OsO_4 for 30 min, they were dehydrated by incubating the pellet in increasing concentrations of ethanol, from 70% to 100%, then incubated over night in 50:50 epon:ethanol and finally embedded in Agar100 resin. Sections were contrasted with 2% uranyl acetate and lead citrate and examined with a JEOL 1200 electron microscope. EM images were acquired with a GATAN Multiscan 600CW camera. EM was performed by Dr. Xiao-Wen Hu (Cancer Research UK)

2.2.4.5 Immuno electron microscopy

Uninfected and GFP-LC3 infected hepatocytes were fixed with 4% paraformaldehyde, 0.2% glutaraldehyde in 0.1 M Sörensen's buffer for 1 h at room temperature and processed as described (Tokuyasu, 1973). Sections were immuno-labelled with rabbit anti-GFP antibody (1:500) or rabbit anti-LC3 antibody (1:60), followed by protein A, conjugated to 10 nm gold particles.

Immuno-electron microscopy was performed by Dr. Xiao-Wen Hu (Cancer Research UK).

2.2.5 Adenovirus techniques

2.2.5.1 Construction of adenoviruses

GFP-LC3 was PCR-amplified using the forward and reverse primers described in Chapter 2.1.4, and cloned into the vector pENTR using the TOPO cloning kit (Invitrogen). GFP-LC3 was then subcloned into pAd/CMV/V5-Dest using the LR Clonase Kit (Invitrogen). To produce viruses HEK293A were seeded at 5 x 10^5 cells per well in a 6-well plate and transfected the following day with the Pac I-digested GFP-LC3 destination vector using Lipofectamine (Invitrogen) (see also Chapter 2.2.2.2). 48 hours post transfection, cells were trypsinised and transferred to 10 cm tissue culture dish containing 10 ml of growth medium. After 10 days, when approximately 80 % of the cells showed cytopathic effects, cells and medium were harvested and subjected to 3 freeze/thaw cycles in dry ice/methanol before spinning down the debris at 5000 g for 15 minutes at room temperature. Supernatants were frozen as 1 ml aliquots at -80 °C to further amplify the virus.

2.2.5.2 Adenovirus amplification

Adenoviruses were amplified in HEK293A cells by adding 600 µl of the initial crude lysates to one 90% confluent T174 flask. 48 hours later 90 – 100 % of cells showed cytopathic effects and were harvested. Adenoviruses were purified using the Adeno-X Virus Purification Kit (BD Biosciences) according to the manufacturers instruction.

2.2.6 Primary rat hepatocyte preparation and cultures

2.2.6.1 Isolation of primary rat hepatocytes

Primary hepatocytes were isolated from approximately 300 g male Wistar rats by a two-step collagenase perfusion method according to Seglen (Seglen, 1993). See Figure 2.1 for a depiction of the perfusion setup. Wistar rats were first anesthetised by an injection of a 0.3 ml/100 g body weight solution of 25 % Hypnorm, 25 % Hypnovel, 50 % H_20 and the abdomen was opened by a transverse incision, while the rat was lying on its back with its snout to the left. The intestines were folded away and 1000 units of heparin were injected into the right iliolumbar vein. Using a crescent-shaped surgical needle, a ligature was placed around the portal vein between the liver and the last tributary vein (see also Figure 2.2). A tube connected to the pump inlet of the perfusion apparatus was put into a bottle with 500 ml perfusion buffer (150 mM NaCl, 6 mM KCl, 10 mM HEPES, 4 mM NaOH), the flow rate was set to 20 ml/min and the pump was switched on. The portal vein was then cut halfway through, approximately 5-10 mm above the ligature, using fine surgical scissors. A cannula was inserted into the vein and secured in place by tightening the ligature. Care was taken not to push the cannula past the first portal branch as this leads to insufficient perfusion of the small lobes of the liver. Once the cannula was in place, the vena cava was cut to release the pressure of the perfusate flow and to sacrifice the animal. At this stage the perfusion buffer flow rate was increased to 50 ml/min and the liver was removed from the carcass and placed on top of a metal mesh on a beaker. After most of the 500 ml perfusion buffer has been consumed, the metal mesh with

the liver and the pump inlet was switched to a beaker containing 50 ml collagenase buffer (12000 units collagenase, 30 mM $CaCl_2$, 80 mM NaCl, 3 mM KCl, 10 mM HEPES, 4 mM NaOH). Collagenase buffer was re-circulated through the liver for 8 minutes before the liver was placed in a 10 x 10 cm dish with 37 °C suspension buffer (55 mM NaCl, 2 mM KCl, 1 mM KH_2PO_4, 1 mM Na_2SO_4, 30 mM HEPES, 30 mM TES, 36 mM Tricine, 50 mM NaOH) and the cells were raked out with a metal tooth dog's comb.

Cells were then filtered through a coarse 250 µm nylon mesh to remove cell clumps and connective tissue debris. After a 30 minutes incubation in a 20 cm glass petri dish at 37 °C with gentle rocking to allow the cells to recover from the pefusion, cells were cooled down to 4 °C, filtered through a 250 µm nylon mesh on top of a 100 µm mesh and transferred to a beaker. Before hepatocytes were seeded into tissue culture dishes they were washed 3x in wash buffer (perfusion buffer, containing 1 mM $CaCl_2$) with brief spins in between (40 g, 2 minutes, 4 °C).

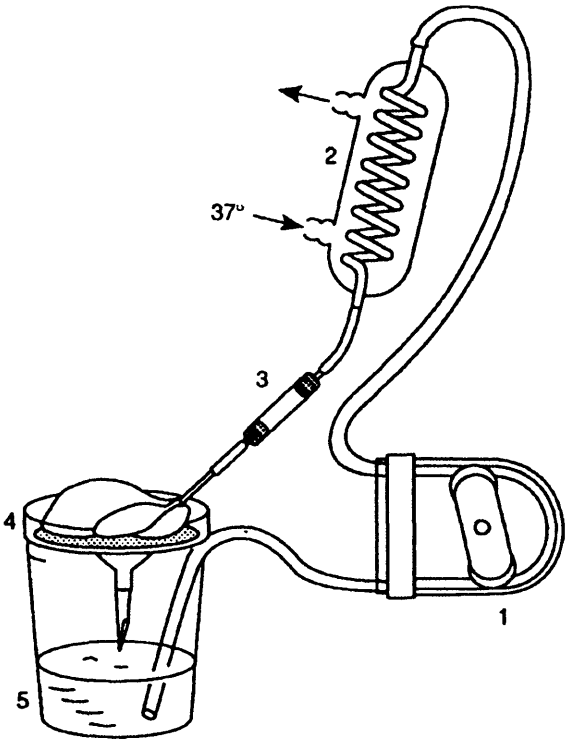

Figure 2.1: Perfusion apparatus. (1) Peristaltic pump; (2) water-jacketed glass coil, connected to a circulating water bath to ensure that perfusion and collagenase buffer are at 37 °C; (3) bubble trap and portal cannula; (4) liver support dish - glass funnel with metal mesh placed inside; (5) buffer reservoir for recirculation of collagenase buffer. Figure taken from Seglen, 1993.

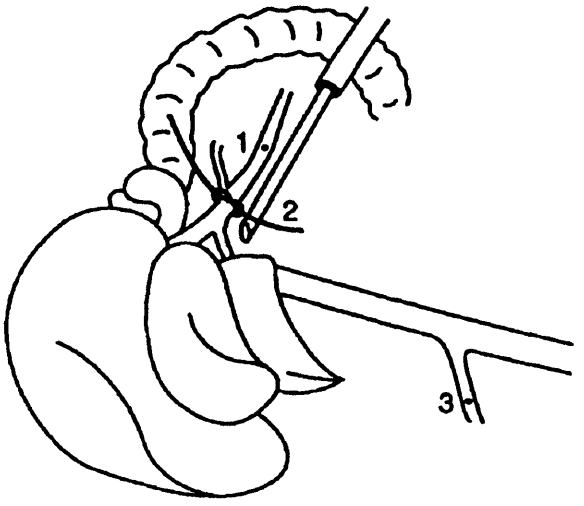

Figure 2.2: Perfusion relevant liver anatomy. (1) Insertion site for portal cannula; (2) cannula aligned to the portal vein before insertion; (3) heparin injection site into iliolumbar vein. Figure taken from Seglen, 1993.

2.2.6.2 Culturing and transduction of primary rat hepatocytes

Isolated hepatocytes were seeded on collagen-coated (10 μg/ml in 30 % EtOH) coverslips or cell culture dishes in full growth medium (1:1 DMEM/F12 containing EGF (30 ng/ml), dexamethasone (10 ng/ml), insulin (400 ng/ml) and collagen (10 μg/ml)). Three hrs after seeding, the hepatocytes were either mock infected or infected with adenovirus encoding various constructs. The adenoviruses were diluted in a small amount of growth medium and added directly to the cell culture dishes. After two hours the growth medium was exchanged, and the cells were incubated overnight. All viruses were titrated to infect 90% to 100% of the isolated hepatocytes after a 2 hr exposure to virus.

2.2.6.3 Induction of autophagy and drug treatments

To induce autophagy, the growth medium was either replenished with fresh growth medium (FM), or cells were washed four times with Earle's saline (ES), and starved for various times in the last wash. Where indicated, the following was added: Vinblastine (50 μM), taxol (5μM), nocodazole (50 μM), wortmannin (100 or 200 nM), LY294002 (10 nM), 3-methyladenine (10 mM), leucine (0.8 mM), rapamycin (25 nM unless otherwise indicated), regulatory amino acids (RegAA (μM): Leu, 204; Tyr, 98; Pro, 437; Met, 60; His, 92; Trp, 93; Ala, 475), Pepstatin A (28 μg/ml) and E64D (10 μg/ml). In the case of vinbastine, taxol and nocodazole, cells were pre-treated for 30 minutes in full growth medium.

2.2.7 Autophagy assays

2.2.7.1 Saponin extraction

For quantitative analysis of GFP-LC3 puncta, cells were saponin-extracted for 5 minutes (0.5% Saponin in 80 mM PIPES pH 6.8, 1mM $CaCl_2$, 5 mM EGTA) before fixation with 3% PFA. Nuclei were stained with Hoechst33342 (5 µg/ml) in PBS for 1 minute. The coverslips were washed twice more with PBS and mounted with Moviol.

2.2.7.2 Quantification of autophagosomes by immuno fluorescence

Low resolution images for the quantification of autophagosomes were acquired from saponin-extracted GFP-LC3-infected hepatocytes cells grown on glass coverslips using an automated Discovery-1 microscope (Molecular Devices) with a 20X, 0.75 NA objective. 16 fields were acquired per condition. Autophagosomes were counted using the Granularity plug-in module of the Metamorph 6.2 software package (Molecular Devices). Granule size and local threshold were chosen so that all vesicles were recognized by the software. Within one experiment settings were kept the same.

2.2.7.3 Quantification of autophagosomes by electron microscopy

Quantification of the number of autophagosomes per μm^2 in epon sections was performed using conventional random sampling techniques using two separate grids for each time point. Between 20 and 30 pictures were taken of each grid. Images with grid bars or other non-relevant material were manually excluded. The samples were assessed in a double-blind fashion. AVis and AVds were distinguished using well-documented criteria, and counted

manually. This was performed by Dr. Xiao-Wen Hu (Cancer Research UK). The area covered by cells in each picture was measured using Metamorph 6.2 software. First, the micrographs acquired were visually inspected to exclude dead cells from the area analysis. Next, a threshold was assigned to the image to distinguish between cells and background. The threshold was then used to create a binary image, where the colour white was assigned to cells and black to the background. After applying an "Open-Close" filter to remove noise, the "Integrated Morphometric Analysis" tool was used to measure the cell area. This tool creates a region around the cells and returns the pixel area of this region, which was then used to calculate square microns.

2.2.7.4 Protein degradation assay

To measure the degradation of long-lived proteins through autophagy hepatocytes were isolated and seeded in 6 well dishes at a density of 0.5 x 10^6 cells. On the same day, after the hepatocytes had attached (usually 5 hours), cells were washed 3x with PBS and the medium was exchanged to fresh growth medium containing reduced concentrations of valine (65 μM) and ^{14}C-valine (0.2 μCi/ml) to label cellular proteins over night. Cells were then chased for 4 hours in fresh growth medium, containing 2 mM valine to allow the degradation of short-lived proteins through the proteasome. For the time course, cells were then either incubated in ES or FM with or without protease inhibitors, containing 2 mM valine. At various time points aliquots of the medium were removed and precipitated with 10 % TCA/1% phosphotungstic acid for at least 30 minutes at 4 °C. Precipitated proteins were pelleted in a microcentrifuge (4 °C, 8000 rpm, 30 min) and the soluble fraction was mixed

with 10 ml of scintillation liquid and counted. For the experiments with the microtubule drugs, cells were pre-treated with vinblastine, nocodazole and taxol as described in Chapter 2.2.6.3. At the end of the experiment, cells were harvested in 1 ml ice cold PBS, containing 1% Trition X-100, and TCA precipitated and pelleted as described above. The TCA insoluble fraction was counted. Percentage degradation was calculated as cpm medium over total cpm in the medium and cells times 100 as described by Gronostajski et al. (Gronostajski and Pardee, 1984).

2.2.7.5 Co-localization of LysoTracker Red with GFP-LC3

Hepatocytes infected with adenoviruses encoding GFP-LC3 were either left untreated or were pre-treated with 50 μM nocodazole or 50 μM vinblastine for 30 minutes in full growth medium, followed by 120 minutes starvation with the respective drug. Hepatocytes infected with adenovirus encoding SV-HA-LC3 were starved for 120 minutes. LysoTracker Red (100 nM) was added to the starvation medium during the last 30 minutes of the experiment, and cells were fixed and mounted as described above in 2.2.4.1. Pictures for the co-localization were acquired with a Zeiss LSM 510 confocal microscope as described by Naslavsky et al (Naslavsky et al., 2003). Co-localization was then measured using the LSM 510 software and was expressed as percentage of the total area of LysoTracker Red, which co-localizes with GFP-LC3 or HA-SV-LC3 structures, respectively. The threshold to distinguish background from signal was set individually for each sample.

2.2.7.6 Inhibition of autophagy with siRNA

Protein knockdown was accomplished by transfecting HEK293A cells, stably expressing GFP-LC3 cells with siRNA (5nM final concentration) using Oligofectamine reagent according to manufacturer's protocols. A siControl2 siRNA (Dharmacon, Lafayette, CO, USA) which engages the RISC complex but produces non-targeting siRNA, a SMART pool siRNA (Dharmacon) towards Atg5 (NM_004849), or a custom designed siRNA duplex towards human Atg6/Beclin1 was used. 72 hours post transfection, cells were then lysed for immunoblotting or treated with 50 μM vinblastine. These experiments were performed by Dr. Edmond Chan (Cancer Research UK).

2.2.8 In vitro fusion assay

2.2.8.1 Biotinylation of horseradish peroxidase (HRP)

HRP was biotinylated as described by Gruenberg et al. (Gruenberg et al., 1989) using the Biotin-X-NHS-Kit (Calbiochem). Briefly, 70 mg HRP was dissolved in 7 ml of 0.1 M $NaHCO_3$ and mixed with 77 mg biotin-X-NHS dissolved in 1.75 ml dimethylformamide. The solution was incubated at room temperature on an end-over-end rotator for at least 1 hour, after which it was dialysed over night against PBS, using Snakeskin dialysis tubing (Pierce) with a molecular weight cut off of 3.5 kDa.

2.2.8.2 HRP enzyme assay

The HRP enzymatic activity of cell lysates, endosomes preparations or fusion assay samples was measured in a spectrophotometer at 455 nm as described by Gruenberg et al. (Gruenberg et al., 1989a). 100 μl sample were

mixed with 900 µl of HRP assay buffer (0.342 mM O-dianisidine and 0.003% H_2O_2 as substrates in 0.5 M Na-phosphate buffer, pH 5 containing 0.1% Triton X-100) and incubated in the dark for up to 1 hour. HRP activity was stopped by adding 0.4 % sodium azide and samples were measured.

2.2.8.3 Endosome purification from rat liver

Early and late endosomes from rat liver were purified according to Ellis et al. (Ellis et al., 1992). The necessary continuous Ficoll gradients were prepared the day before the purification and left over night to smoothen out at 4 °C. 39 ml Beckman Quick-Seal tubes were filled with 5 ml 45 % Nycodenz to serve as a cushion, then a 30 ml 25 % to 1 % (w/v) Ficoll gradient (Ficoll, 250 mM sucrose, 20 mM TES, 1 mM EDTA) was made on top of that. On the day of the experiment, approximately 300 g Wistar rats were anesthetised as described above (Section 2.2.6.1) and perfused with recirculated perfusion buffer, containing either 2 mg/ml biotinylated HRP or 0.2 mg/ml anti-HA antibody for 30 minutes. The temperature of the perfusion buffer was maintained at 37 °C throughout. The liver was then briefly minced with scissors and homogenized in 3x weight (g) with STM buffer (250 mM sucrose, 20 mM TES, 1mM $MgCl_2$) using a potter homogenizer. Homogenates were spun in a JA20 rotor at 2000 g for 10 minutes at 4 °C to generate a PNS. 5 ml PNS was loaded on top of each Ficoll gradient, the tubes sealed and spun at 50000 rpm in a vti50 rotor for 1 hour at 4 °C. Acceleration and deceleration were set to 3. 1 ml fractions were then collected from the bottom and the refractive index was measured. For each gradient, fractions with a refractive index between 1.360

and 1.366, corresponding to late endosomes, and between 1.366 and 1.373, corresponding to lysosomes, were pooled. STM buffer was added to 20.5 ml and the samples were spun at 45000 rpm in a Ti70 rotor for 76 minutes at 4 °C to concentrate the endosomes. The pellets were then resuspended in STM buffer, equal to a quarter of the volume of the original PNS, and samples were snap frozen and stored in liquid nitrogen.

2.2.8.4 Autophagosome purification from cultured hepatocytes

Autophagosomes were isolated from hepatocytes according to Stromhaug et al. (Stromhaug et al., 1998) with the following modifications. Cells were isolated as described above (Chapter 2.2.6.1), seeded on 5 collagen coated 25 x 25 cm square tissue culture dishes and on the same day infected with HA-SV-LC3 encoding adenoviruses (see also Chapter 2.2.6.2). The next day, cells were washed 3x with PBS and autophagy was induced by incubating the hepatocytes in Earle's saline, containing 50 µM vinblastine for 2 hours. Hepatocytes were then scraped off in PBS and the cells from all 5 plates were pooled, pelleted (400 g, 15 minutes, 4 °C) and resuspended in 10 ml of homogenization buffer (HB) (250 mM sucrose, 10 mM HEPES, pH 7.4). Cells were broken with a dounce homogenizer (Wheaton) and the result checked by trypan blue staining. Usually 20 strokes were required for more than 90 % breakage. Lysosomes were removed from the samples by adding 5 ml 1.5 mM gly-phe β-naphthylamide in HB, and the homogenate was incubated for 7 minutes at 37 °C, before centrifuging the samples for 2 minutes at 2000 g and 4°C to generate a PNS. 14 ml PNS were loaded on a Nycodenz step gradient (7 ml 13.5 % and 16 ml 9.1 % Nycodenz in HB in SW28 Beckman tubes) and

spun for 1 hour with 28000 rpm at 4 °C; acceleration and deceleration set to 1. Finally, the autophagosome band between the two Nycodenz steps was collected and used immediately for fusion assays or frozen at -20 °C for western blotting.

2.2.8.5 Generation of rat liver cytosol

Livers of starved rats were minced with scissors and homogenized in STM buffer (see Chapter 2.2.8.3), equal to 3x the weight of the livers (g). The homogenate was centrifuged in a JA20 rotor for 10 minutes at 2000 g at 4 °C and then spun further in a Ti70 rotor at 100000 g for 1 hour at 4 °C. The supernatant was collected and desalted on PD10 columns (Pharmacia). 1 ml aliquots were snap frozen and stored in liquid nitrogen. Typical cytosol concentrations were about 20 mg/ml.

2.2.8.6 *In vitro* reconstitution of fusion between autophagosomes and endosomes, containing anti-HA antibodies

Autophagosomes were always prepared fresh. Aliquots of endosomes were thawed rapidly at 37 °C and centrifuged as 100 µl aliquots in 1.5 ml Eppendorf tubes at 35000 rpm for 37 minutes at 4 °C in a Ti50.2 rotor. Pellets were resuspended in either 100 µl rat liver cytosol (approximately 20 mg/ml) or STM buffer and mixed with 100 µl autophagosomes, 25 µl HA-peptide (1 mg/ml in STM buffer) and 10 µl ATP-regenerating system (100 mM ATP, pH7; 800 mM creatine phosphate, 3200 U/ml creatine phosphokinase and 30 mM GTP). Samples were incubated at either 37 °C or 4 °C for 45 minutes. As controls single components of the fusion reaction were omitted and replaced

with the buffer they were made in. After 45 minutes samples were placed on ice for 4 minutes before TNTE was added. Samples were vortexed and incubated on ice for 20 minutes before being centrifuged at 12000 rpm at 4 °C for 10 minutes in a microcentrifuge. The supernatant was then transferred to a new tube and incubated for at least one hour on a end over end rotator. Beads were then spun down for 2 minutes at 2000 rpm at 4 °C and washed 3x with PBS. Samples were then prepared for SDS-PAGE as described in Chapter 2.2.3.4.

2.3 Supplemental Material on CD

2.3.1 Description of movies

Movie M1. Infected cultured hepatocytes expressing GFP-LC3 were imaged with an Ultraview spinning disk microscope. Frames were acquired every 23 seconds for 2 hours, and all frames are shown. The frame rate of the movie is 15 per second.

Movie M2. As described in M1.

Movie M3. As described in M1, but frames were acquired every 10 seconds for 15 minutes, starting 7 minutes after the beginning of starvation. All frames are shown The frame rate of the movie is 10 per second.

Movie M4. As in M1, but cells where pre-treated with 50 μM nocodazole in FM for 30 minutes. Frames were acquired every 10 seconds for 15 minutes, starting 5 minutes after the beginning of starvation. All frames are shown The frame rate of the movie is 10 per second.

3 AUTOPHAGOSOME FORMATION IN PRIMARY RAT HEPATOCYTES

3.1 Aim

Tissue culture cell lines have only a low capacity to undergo autophagy. In NRK cells, for instance, up to 0.8% of the cytoplasmic volume is occupied by autophagosomes after a 2 hour starvation period in amino acid free medium (personal communication from Eeva-Liisa Eskelinen, University of Helsinki). In tissues and primary cells in culture on the other hand autophagy is induced to a much greater extent upon starvation. In cultured mouse hepatocytes, for example, up to 3% of the cytoplasmic volume was occupied by autophagosomes even under full growth medium conditions (Tanaka et al., 2000). As shown in GFP-LC3 transgenic mice, tissues with particularly high numbers of autophagosomes after starvation are liver, kidney and heart (Mizushima et al., 2004). We therefore decided to use primary rat hepatocytes as our model system to investigate autophagosome maturation, as they have been extensively used in the past to study autophagy. Most of these studies however were based on morphological methods only. For that reason I decided to develop a primary rat hepatocyte model which is amenable to genetic modification, using adenoviruses to specifically express a GFP-tagged version of the autophagosome marker MAP1-LC3 (GFP-LC3). Using a variety of microscopic and biochemical techniques I confirmed that GFP-LC3 is localized correctly to autophagosomes and over-expression itself has no effect on the

induction of autophagy. Furthermore I determined the rate of autophagosome formation using time course experiments with fixed or live cells.

3.2 Generation of LC3 specific antibodies

I developed rabbit polyclonal antibodies against the N-terminal domain of rat LC3. For this purpose, a peptide comprising amino acids 2–18 (see Chapter 2.1.5 for sequence) was synthesized and coupled to keyhole limpet hemocyanin. The conjugated peptide was sent to Harlan (England) for immunization of rabbits. The antibodies STO227 and STO228 recognized the endogenous protein by western blotting of liver lysates and this interaction could be competed by pre-incubation of the antibody with excess peptide (Figure 3.1). However, these antibodies did not give a specific signal in immuno-fluorescence experiments. These findings indicate that these antibodies are valid probes for the detection of endogenous and over expressed LC3 (see also Figure 3.9).

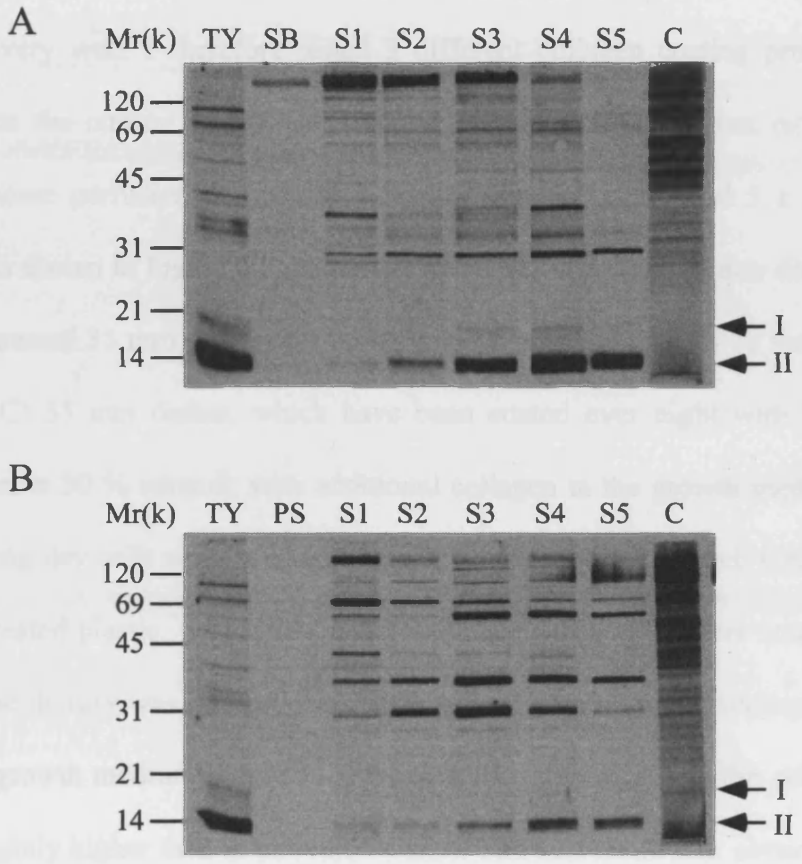

Figure 3.1: Both antibodies, STO227 and STO228, recognize LC3. 1.5 mg hepatocyte lysate from starved Wistar rats was separated on a 12 % mini gel, with a comb with 2 wells only (marker and sample) and blotted to nitrocellulose. The nitrocellulose membrane was cut into thin strips and probed with an anti-LC3 antibody provided by Tamotsu Yoshimori (TY), pre-immune serum (PS), sera from test bleeds and final bleed (S1-S5) or serum from the final bleed, pre-incubated with 0.1 mg/ml antigen-peptide for 1 hour (C). Serum concentration was 1:1000. A) STO227 antibody. B) STO228 antibody. Arrows indicate the two LC3 forms LC3-I (I) and LC3-II (II), running at approximately 17 kD and 14 kD, respectively.

3.3 Culturing of hepatocytes

Hepatocytes, when seeded on tissue culture plastic or coverslips, do not attach very well. I therefore tested 3 different collagen coating protocols to optimize the culture conditions. Hepatocytes were isolated from rat liver by collagenase perfusion according to Seglen (Seglen, 1993) and 5 x 10^5 cells were, as shown in Figure 3.2, either seeded in (A) untreated 35 mm dishes or in (B) untreated 35 mm dishes, but with 10 ng/ml collagen type IV in the medium or in (C) 35 mm dishes, which have been coated over night with 10 ng/ml collagen in 30 % ethanol, with additional collagen in the growth medium. The following day cells were washed, visually inspected and counted. Cells seeded on untreated plastic, were often round and only about 50 % were attached and flat. The density was generally low, indicating a loss of cells. Adding collagen to the growth medium reduced the number of round cells and the cell density was slightly higher than in untreated dishes. The best result was obtained when dishes were coated with collagen over night and collagen was additionally present in the medium. Most cells were flat and the cell density was the highest of all 3 treatments, indicating that cells had attached firmly. However, even in this case there were approximately 5 % dead cells. For the following experiments in this thesis, collagen was added to the medium and additionally dishes were coated with collagen over night.

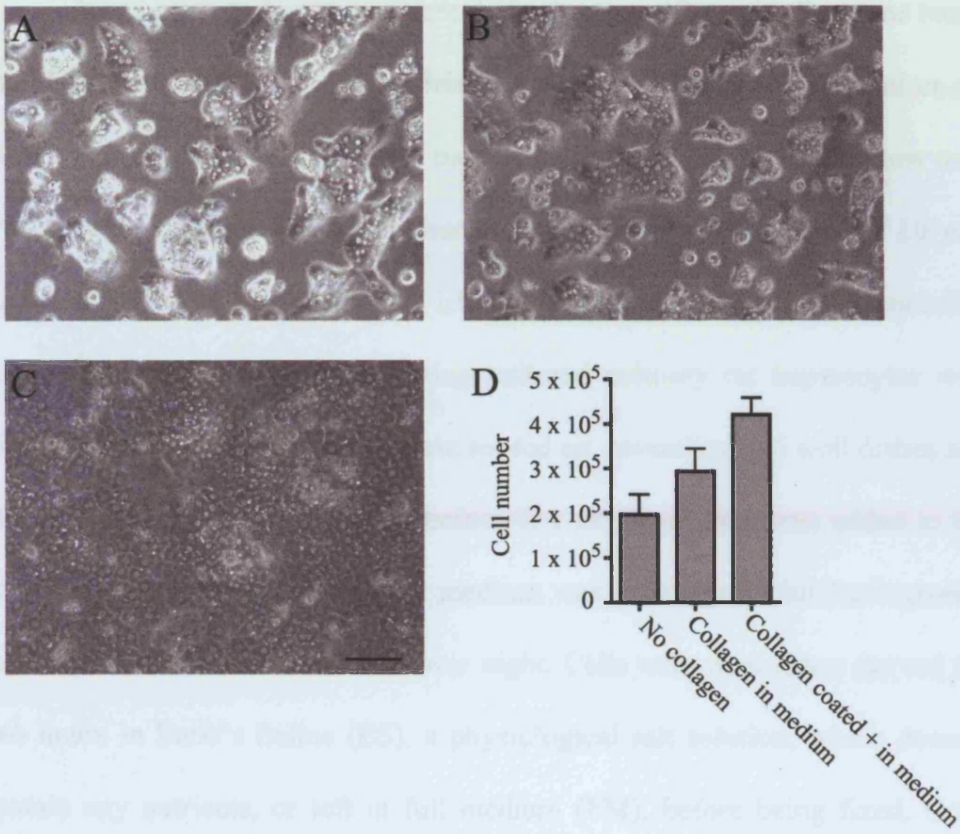

Figure 3.2: Optimization of collagen coating. 5 x 10^5 hepatocytes were seeded either on untreated plastic (A), or on untreated plastic, but with 10 µg/ml collagen in the growth medium (B), or on plastic, coated over night with 10 µg/ml collagen, and with collagen in the medium (C). The following day, cells were visually inspected (A-C) or trypsinized and counted (D). Data in D is the mean of 3 replicates +/- SEM. Bar equals 100 µm.

3.4 Infection of hepatocytes with GFP-LC3 encoding adenoviruses

Since primary hepatocytes are difficult to transfect with liposome based methods, I decided to use adenoviruses instead. Tsutsui et al. (Tsutsui et al., 2003), for instance, showed that a multiplicity of infection (MOI) as low as 1 was enough to infect 80 % of cultured hepatocytes, while a MOI of 10 was sufficient to infect 100 % of cells. I therefore generated a GFP-LC3 encoding adenovirus and tested it by infecting cultured primary rat hepatocytes with different amounts of virus. Cells were seeded on coverslips in 6 well dishes and allowed to attach for three hours, before 0, 1 or 10 µl virus was added to the growth medium. After 2 hours the medium was exchanged with fresh growth medium and cells were incubated over night. Cells were then either starved for two hours in Earle's Saline (ES), a physiological salt solution, which doesn't contain any nutrients, or left in full medium (FM), before being fixed. Cells were visualized using epifluorescence and confocal microscopy. In initial experiments, I incubated the cells over night with the virus, a treatment resulting in cell death. After a 2 hour incubation, hepatocytes were healthy and their morphology didn't change in comparison to uninfected cells. 1 µl virus was sufficient to infect more than 95 % of cells. In hepatocytes incubated with full medium, cytoplasmic GFP-LC3 was largely diffuse, and was also detected in the nucleus. After 2 hrs of starvation in Earle's saline, there was a dramatic increase of punctate vesicular structures labelled with GFP-LC3 (Figure 3.3). Uninfected hepatocytes had a high level of autofluorescence.

Analysis of these cells with confocal microscopy showed that many of the punctate structures are "doughnut" shaped, with GFP-LC3 staining the rim of a vesicular structure (Figure 3.4). To verify that the GFP-LC3 positive vesicles formed in starved hepatocytes are autophagosomes I incubated cells for 2 hours with various PI3-kinase inhibitors, which have been shown to inhibit the formation of autophagosomes (Codogno and Meijer, 2004). As shown in Figure 3.4, the formation of GFP-LC3-positive vesicular structures during starvation was inhibited by treating starved cells with LY294002 (LY), 3 methyladenine (3MA) or wortmannin (WM). Addition of those drugs had no visually apparent effect on the health of the hepatocytes. These results suggest that cultured and infected hepatocytes respond to starvation by inducing autophagy and that GFP-LC3 is targeted to newly formed autophagosomes.

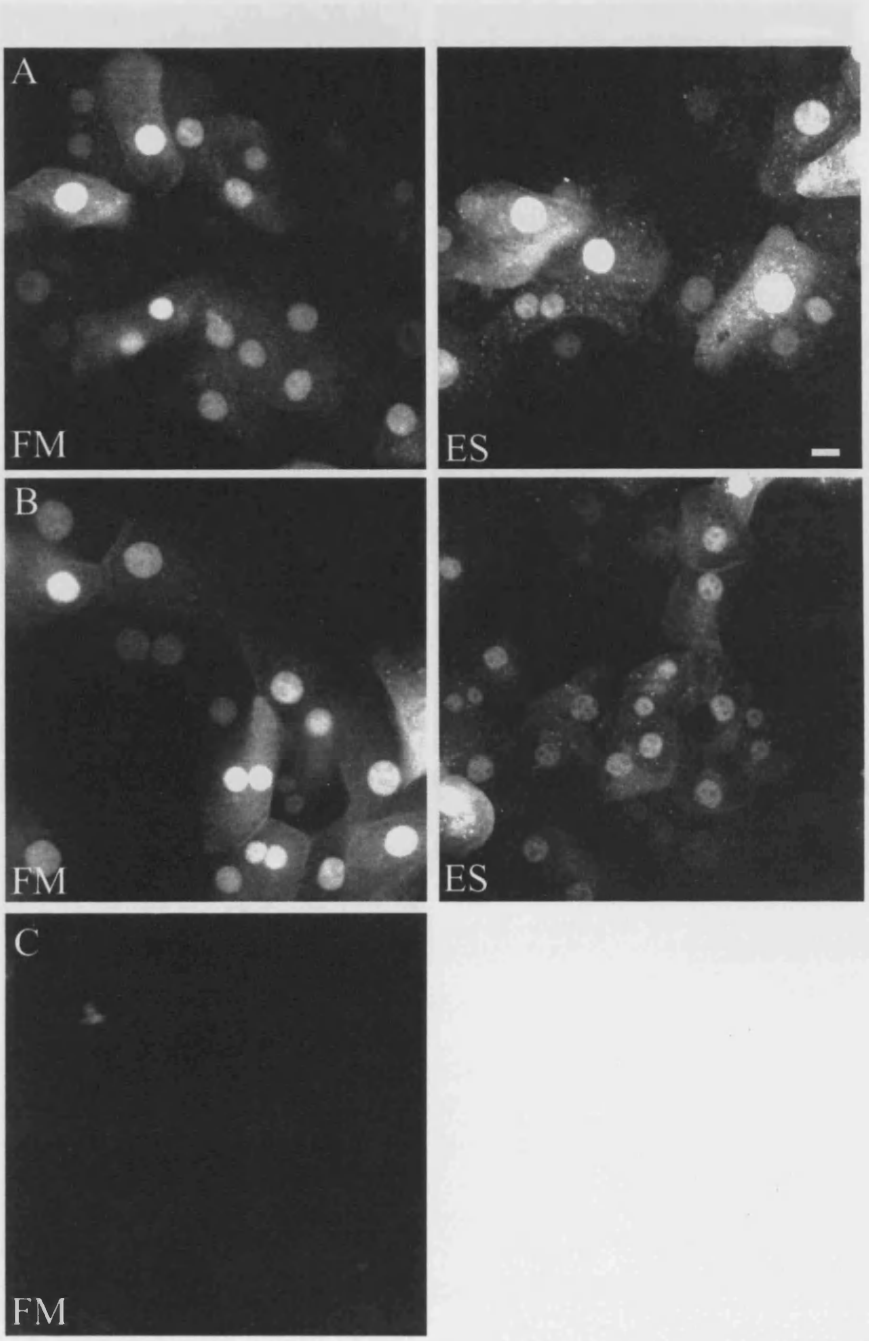

Figure 3.3: Epifluorescence microscopy of hepatocytes infected with GFP-LC3. Hepatocytes were seeded in 35 mm tissue culture dishes, infected with 1 µl (A), 10 µl (B) or 0 µl (C) GFP-LC3 encoding adenovirus. The following day, cells were either incubated in full medium (FM) or starved in Earle's Saline (ES) for 2 hours, before being fixed and analysed using an epifluorescence microscope with a 40 x objective. Images were recorded with the same settings. Bar equals 10 µm

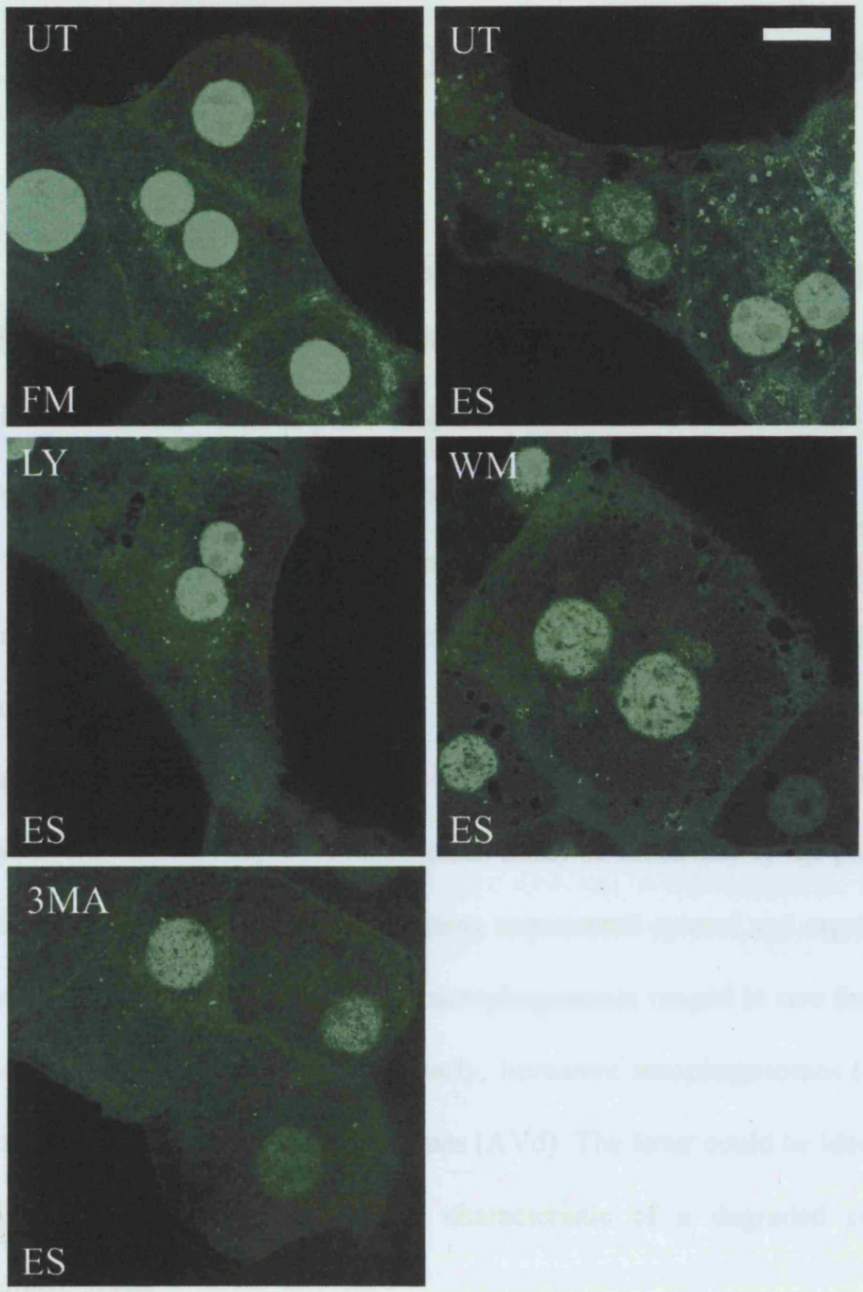

Figure 3.4: Confocal microscopy of rat hepatocytes infected with GFP-LC3. Hepatocytes were isolated, seeded and infected with adenoviruses encoding GFP-LC3, and incubated overnight in full medium (FM). The following day, cells were either left untreated (UT) in FM, or were starved in ES for 2 hours, with no drugs (UT) or in the presence of 10 nM LY294002 (LY), 200 nM wortmannin (WM) or 10 mM 3-methyladenine (3MA) and then visualized for GFP with a LSM 510 laser scanning microscope. Bar equals 10 μm.

3.5 Characterization of the starvation response by electron microscopy

To further confirm that infection itself has no effect on autophagy and that the GFP-LC3 labelled structures are autophagosomes and not an artefact of viral infection, Xiao-Wen Hu performed both conventional thin section electron microscopy and immunogold labelling of cryosections.

Hepatocytes were isolated and infected with GFP-LC3 encoding adenoviruses. The following day the cultured hepatocytes were starved for 10, 45 or 90 minutes in Earle's Saline, before being fixed and processed for conventional electron microscopy. Within 10 minutes, autophagosome formation was induced and autophagosomes could be identified by the presence of a double membrane structure, containing sequestered cytosol and organelles, such as mitochondria (Figure 3.5). The autophagosomes ranged in size from 0.8 – 2 μm, and could be classified into early, immature autophagosomes (AVis) and into late, degradative autophagosomes (AVd). The latter could be identified based on their electron dense core, characteristic of a degraded content (Eskelinen, 2004).

Additionally, to confirm that GFP-LC3 gets targeted to these newly formed autophagosomes, cryoimmunogold labelling experiments of infected hepatocytes expressing GFP-LC3 were performed by Xiao-Wen Hu. Hepatocytes were isolated, infected with GFP-LC3 encoding adenovirus or not, and starved for 2 hours in ES. Using both an anti-GFP antibody and an anti-LC3 antibody, Xiao-Wen Hu could identify vesicles with gold-particle

decorated membranes, which had the morphology of autophagosomes and contained sequestered cytosol and sometimes also mitochondria (Figure 3.6).

To characterize the starvation response in more detail and to make sure that viral infection alone does not induce autophagy, I performed a time course experiment with cultured hepatocytes to analyse the morphology and number of AVis and AVds over a 120 minutes starvation period. Cultured hepatocytes were either mock infected or infected with GFP or GFP-LC3 encoding adenoviruses. The following day, cells were starved in ES for 0, 30 and 120 minutes, fixed and processed for conventional electron microscopy (Figure 3.7A). Comparison of Avi and Avd numbers at 0, 30 and 120 mins in non-infected cells, GFP, or GFP-LC3-infected cells showed that there was no clear effect of either adenovirus on the type or number of AVs present.

To analyse the distribution of early and late autophagosomes during starvation in more detail a more extensive time course was performed using GFP-LC3-expressing hepatocytes. Cells were starved for 0, 15, 30, 60 and 120 minutes, fixed and processed for electron microscopy (Figure 3.7B). Quantification of autophagosomes from random sampled pictures, showed that the AVi number increased immediately upon shifting cells to starvation medium, and continued to rise until about 30-60 minutes, after which a plateau was reached. The number of AVds increased over the whole time course of the experiment.

In summary, these experiments show that cultured and infected primary hepatocytes are still able to respond to starvation and that GFP-LC3 is targeted correctly to newly formed autophagosomes. In addition, infection with GFP-LC3 encoding adenoviruses did not affect the normal starvation response. After

an initial burst, AVi numbers stayed constant, while the number of AVds was continuously increasing.

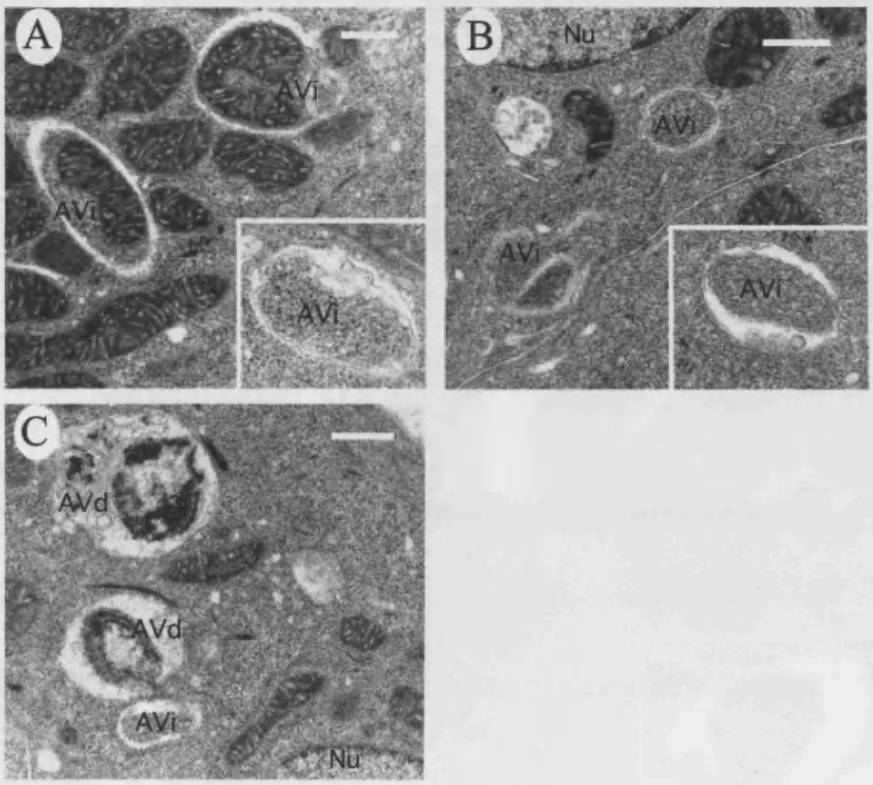

Figure 3.5: Conventional thin section electron microscopy of infected hepatocytes. (A-C) Hepatocytes were infected with adenovirus expressing GFP-LC3 and cultured over night. Cells were starved for 10 mins (A), 45 mins (B) or 90 mins (C), fixed and thin section electron microscopy was performed by Xiao-Wen Hu. Immature, early autophagosome (AVi), degradative late autophagosome (AVd), Nucleus (Nu). Bar equals 500 nm.

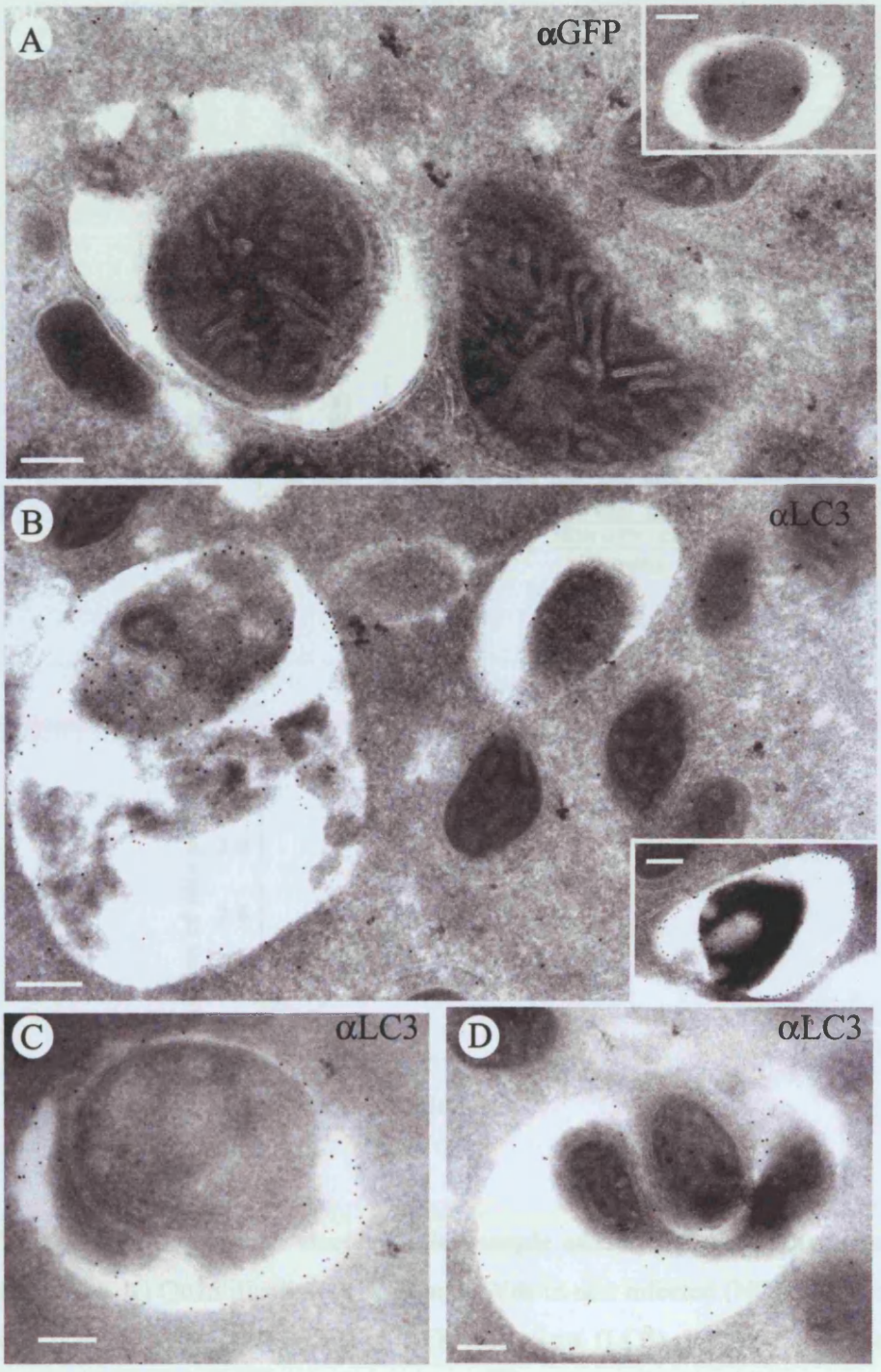

Figure 3.6: Immunogold electron microscopic analysis of LC3 in starved rat hepatocytes. Hepatocytes were either infected with adenovirus expressing GFP-LC3 (A and B), or uninfected (C and D) and fixed 2 hours after starvation in ES. Cryosections were labelled with anti-GFP (A) or anti-LC3 (B-D) followed by 10 nm protein A gold. Bars equal 100 nm.

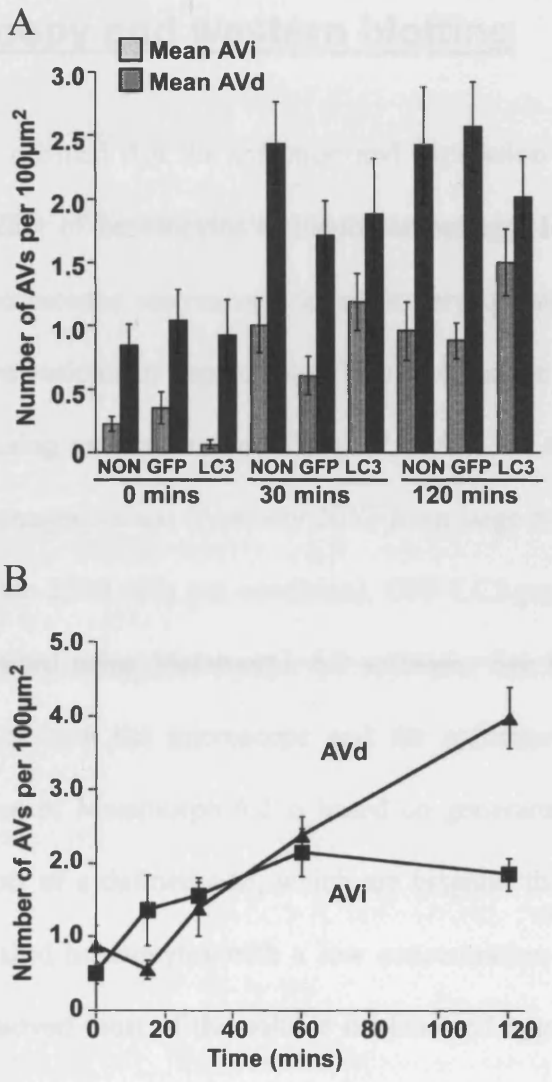

Figure 3.7: Quantitative electron microscopic analysis of autophagosome formation. A) Quantification of AVis and AVds in non infected (NON) cells or cells infected with GFP (GFP) or GFP-LC3 virus (LC3). B) AV number in GFP-LC3 infected hepatocytes. A minimum of 40 images were captured from 2 grids. Error bars indicate SEM.

3.6 Quantification of autophagy by fluorescence microscopy and western blotting

Having confirmed that the infection and expression of GFP-LC3 does not affect the ability of hepatocytes to induce autophagy, I decided to use an automated epifluorescence microscope to accurately quantify the number of GFP-LC3 positive vesicles in hepatocytes. This microscope system has a built in automatic focusing mechanism and allows therefore the unbiased collection of images at low magnification (typically 20X) from large numbers of cells (on average greater than 2500 cells per condition). GFP-LC3-positve structures per nucleus were counted using Metamorph 6.2 software. See Figure 3.8A and B for an example of how the microscope and the software works. Since the counting algorithm of Metamorph 6.2 is based on generating local thresholds and detecting spots of a defined size, which are brighter than the surrounding area, I permeabilized hepatocytes with a low concentration of saponin before fixation. This removed most of the soluble nuclear and cytosolic fluorescence and made it easier for the software to count the autophagosomes. Cells in FM (Figure 3.8A and C) had only a few (approximately 5 per cell) punctate GFP-LC3-positive structures. In ES-starved cells on the other hand, there was a clear increase in the amounts of punctate vesicular staining (Figure 3.8B and D), which could be measured using this system (Figure 3.8E).

In addition to the autophagosome number, I examined the processing and modification of both GFP-LC3 and endogenous LC3 after starvation by western blotting. During starvation soluble LC3 (LC3-I) is cleaved by Atg4

(Tanida et al., 2004a) and modified by the addition of a lipid, most likely phosphatidylethanolamine (Kabeya et al., 2004), to form LC3-II. On western blots the LC3-II form has a lower mobility and can be clearly distinguished from the unconjugated LC3-I form. Therefore I infected cultured hepatocytes with GFP-LC3 encoding adenoviruses, or alternatively used non infected hepatocytes, and starved them for 2 hours in ES, before solubilization. In a parallel set of samples, hepatocytes were saponin extracted before solubilization. In uninfected and unextracted cells in FM, both LC3-I and LC3-II were detected using an antibody against endogenous LC3, however, the band corresponding to LC3-I was predominant (Figure 3.9A). Using an antibody to GFP, GFP-LC3-I and GFP-LC3-II were detected in lysates from unextracted cells in both FM and ES. After 120 min in ES, the amount of the faster migrating LC3-II increased, as did the GFP-LC3-II (Figure 3.9B). Western blotting of saponin extracted cells (SAP in Figure 3.9) more clearly revealed increased levels of LC3-II and GFP-LC3-II, both of which selectively remained on the membranes after saponin extraction, indicating that the higher molecular weight form is the cytosolic form and the lower molecular weight form the membrane bound, lipid conjugated LC3 form.

Together these results indicate that spot counting and analysis of LC3 processing are suitable methods to investigate starvation induced autophagosome formation.

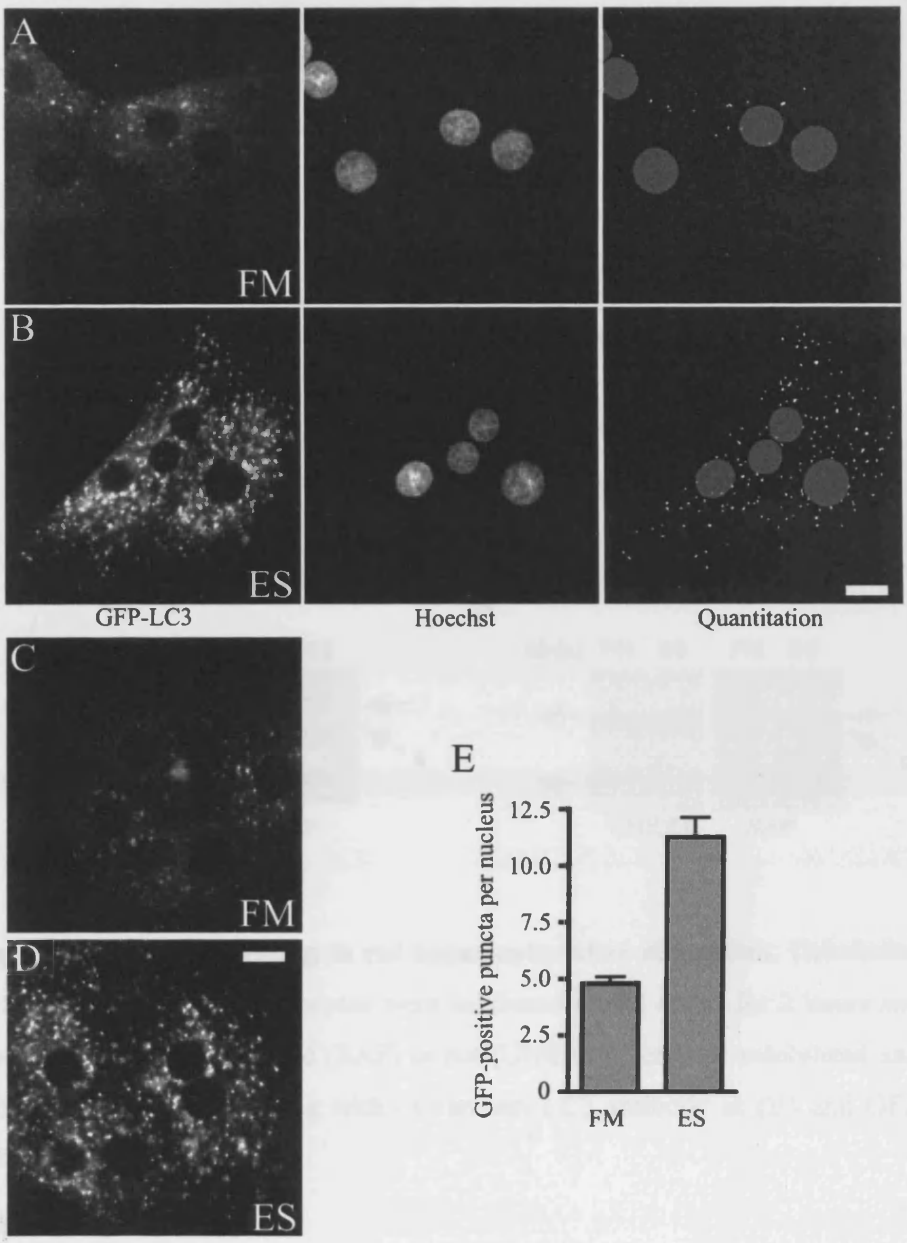

Figure 3.8: Quantification of autophagosomes in GFP-LC3 expressing hepatocytes. Hepatocytes expressing GFP-LC3 were incubated for 120 minutes in either FM (A, C) or ES (B, D) and processed as described in Materials and Methods. GFP-LC3-positive puncta were counted using Metamorph 6.2. Panel A) and B) shows the principle of the counting algorithm. Metamorph creates a computer generated image by detecting Hoechst stained nuclei and GFP-LC3 spots based on an intensity and size threshold. Total GFP-LC3 spot number is then divided by the number of nuclei. Data in (E) was obtained from data similar to that shown in C) and D) and is the mean +/- SEM of 16 pictures, containing approximately 2500 cells. Bar equals 10 μm.

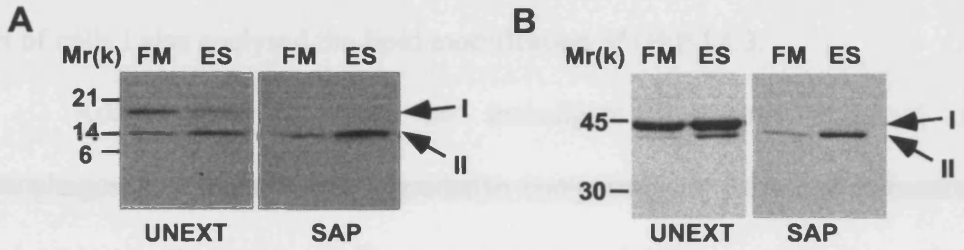

Figure 3.9: LC3 processing in rat hepatocytes after starvation. Uninfected or GFP-LC3 infected hepatocytes were incubated in FM or ES for 2 hours and then either saponin extracted (SAP) or not (UNEXT), scraped, solubilized and subjected to western blotting with (A) an anti LC3 antibody or (B) anti GFP antibody.

3.7 Time course of autophagosome formation in fixed cells

Having developed and established the light microscopy based counting technique, I decided to study the kinetics of autophagosome formation in cultured primary hepatocytes. I therefore infected cells with GFP-LC3 encoding adenoviruses and performed a series of time courses over 120 minutes, after which I analysed the appearance of fluorescent GFP-LC3 puncta. In a parallel set of cells I also analysed the lipid modification of GFP-LC3.

Additionally, in order to investigate the time required for autophagosomes to fuse with degradative compartments, I decided to incubate hepatocytes in the presence of lysosomal protease inhibitors and to compare the degree of degradation of GFP-LC3 between treated and untreated cells by looking at both, the vesicle number and GFP-LC3 processing by western blotting.

To test which protease inhibitors work best in cultured hepatocytes I carried out an initial pilot experiment where I incubated cells in the presence of E64, leupeptin or pepstatin A (Figure 3.10). E64d is specific for cysteine proteases, but does not inhibit serine proteases. Leupeptin is a dual specificity serine/cysteine protease inhibitor, which inhibits enzymes such as papain and cathepsin B, while pepstatin A is an aspartic proteinase inhibitor and inhibits for instance cathepsin D and pepsin. Maximal inhibition of lysosomal proteases and maximal GFP-LC3-I/II protection was obtained with the protease inhibitors

(PI) E64D and pepstatin A; in the following experiments E64D and pepstatin A were always added together.

For the time course experiments, GFP-LC3 expressing cells were incubated in FM or ES for various times, without or with the lysosomal protease inhibitors, and then extracted with saponin, fixed, and analysed for GFP-LC3 positive autophagosomes (Figure 3.11A and B). In ES, the number of AVs increased until 30 to 60 minutes and then reached a plateau. When protease inhibitors were added to ES, the number of autophagosomes continued to increased over the time course of the experiment. On the other hand, cells, which were incubated in FM had a constant low number of autophagosomes over 120 minutes. Addition of protease inhibitors substantially increased this low number. After 120 minutes in FM with PI, hepatocytes had a similar number of autophagosomes than cells starved in ES.

In parallel experiments I analysed the appearance and accumulation of GFP-LC3-II by western blotting (Figure 3.11C). The results largely reflected the data obtained using the vesicle count assay. In FM without PI, GFP-LC3-II was only present in very low amounts; however, could be clearly detected after 90 minutes if protease inhibitors were added (Figure 3.11C top panel). In ES, GFP-LC3-II started to increase after 15 minutes; addition of protease inhibitors enhanced this effect even more (Figure 3.11C bottom panel).

The fact that autophagosomes could be accumulated in FM when protease inhibitors where added, suggests that hepatocytes have a basal rate of AV formation. Starvation of the cells quickly stimulates AV formation within 15 minutes (see also Chapter 3.5). The addition of protease inhibitors increases

the number of AVs, and the amount of GFP-LC3-II detected in both FM and ES, reflecting an inhibition of degradation.

To confirm that the time course of AVd appearance parallels autophagosomal degradation, and that this is inhibited by E64D and pepstatin A, I measured the degradation of ^{14}C-valine labelled proteins in GFP-LC3-expressing hepatocytes during a 2 hour incubation in FM or ES, with or without protease inhibitors (Figure 3.11D). Degradation of long-lived proteins has been used to quantify autophagy in many cell types (Mizushima, 2004). I found that incubation of cells in ES resulted in the highest rate of degradation of ^{14}C-labelled proteins, and this degradation was fully inhibited by protease inhibitors to a level comparable to cells incubated in FM, or FM plus protease inhibitors.

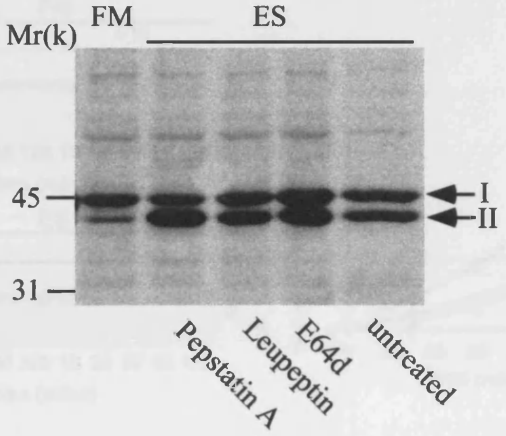

Figure 3.10: Lysosomal protease inhibitors protect GFP-LC3 degradation. GFP-LC3 expressing hepatocytes were either incubated in FM or in ES for 2 hours, or in ES with 28 μg/ml pepstatin A or 0.25 mg/ml leupeptin or 10 μg/ml E64d.

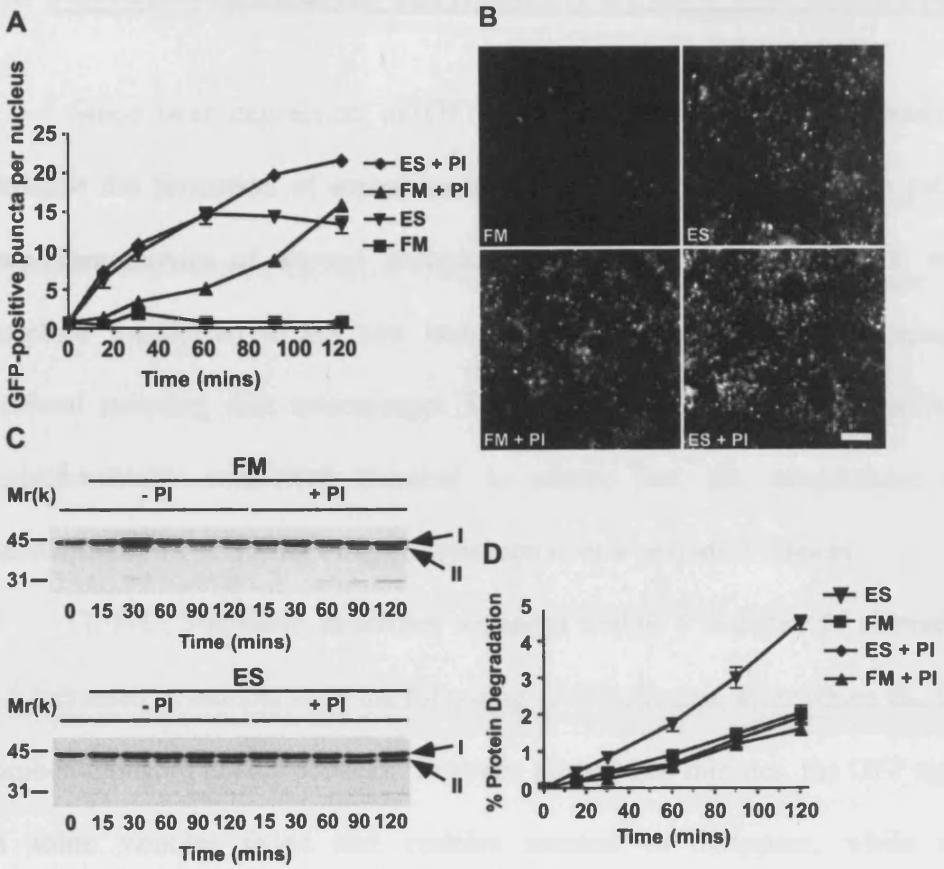

Figure 3.11: Quantification of autophagosome formation and protein degradation in cultured hepatocytes. Hepatocytes expressing GFP-LC3 were incubated in FM or ES, without or with the protease inhibitors E64D and pepstatin A (PI) for 0, 15, 30, 60, 90 and 120 mins. A) Time course of autophagosome formation. Automated quantification was performed on approximately 2800 cells per time point on images acquired with a 20X objective. B) Representative images of the hepatocytes acquired for quantification from the 120 min time points. C) Immunoblotting with anti-GFP antibody was performed on samples taken from the same time points. D) ^{14}C-valine labelled protein degradation in hepatocytes incubated in FM and ES with or without PI. Samples were taken from the medium at 0, 15, 30, 60, 90 and 120 mins. Bar in B) equals 10 microns. Data in A (means +/- SEM of 16 acquired fields), B and C are representative of 3 independent experiments. Data in D (mean +/- SEM of triplicates) are representative of 2 independent experiments.

3.8 Autophagosome formation in live hepatocytes

Since over expression of GFP-LC3 also provides the possibility to visualize the formation of autophagosomes in live cells, I decided to record time-lapse movies of starved hepatocytes. GFP-LC3 expressing cells were therefore transferred to ES and imaging was immediately started using a confocal spinning disk microscope. The microscope was equipped with an environmentally controlled chamber to ensure that the temperature was maintained at 37°C during image acquisition over a period of 2 hours.

GFP-LC3-positive structures appeared within 5 minutes of starvation, and increased in number over the following 45-60 minutes, after which the total number appeared to stay constant. Between 60 and 120 minutes, the GFP signal on some vesicles faded and vesicles seemed to disappear, while new autophagosomes appeared, suggesting the turn over of vesicles (see also Figure 3.11). A panel of images extracted from one movie (see supplementary movie Fig. M1) is shown in Figure 3.12. Most autophagosomes moved over short distances only, in a stop-start random fashion and only a few more motile autophagosomes were seen, which moved in a random direction, occasionally reversing (Figure 3.13A, arrowhead; see also supplementary movie Figure M1 and M2). There was no indication of a directional movement, and there was no detectable clustering in a juxtanuclear area. Frequently, autophagosomes appeared to interact or fuse, and then to move apart again (Figure 3.13B). Sporadically, tubular structures extended from the autophagosomal membranes,

which were relatively stable over 1 minute, before retracting (Figure 3.13C) and occasionally autophagosomes could be seen to move along these structures.

To compare the appearance of autophagosomes during starvation in live cells with fixed cells, I analysed the number of GFP-positive structures in the movies using Metamorph 6.2 software and found that the shape of the curve (Figure 3.12B) correlated well with the time course shown in Figure 3.11A.

In the electron microscopy analysis in Figure 3.7B, I could show that after 60 minutes of starvation most autophagosomes are AVds. This suggests firstly, that most GFP-positive structures in the movies have matured to late autophagosomes through fusion with endosomes or lysosomes and secondly, that fusion does not change the mobility of autophagosomes

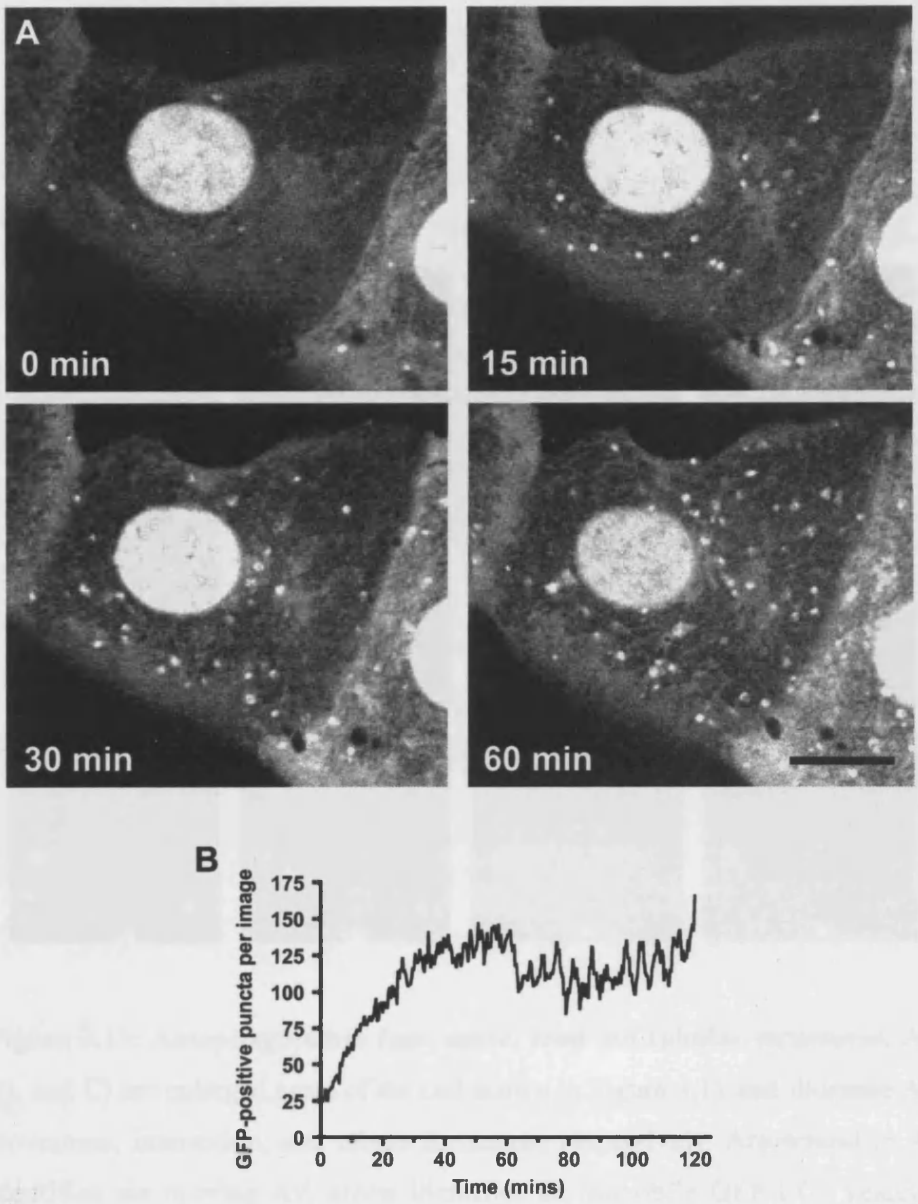

Figure 3.12: Dynamics of autophagosome formation in live cells during starvation. Live-cell confocal imaging was performed on hepatocytes expressing GFP-LC3 after transfer to ES at 37°C. Confocal sections were acquired using an Ultraview microscope over 120 min at 23 sec intervals. A) Representative images from the supplementary movie (see M1 and M2) at 0, 15, 30 and 60 min. B) Quantification of total number of autophagosomes formed in each frame of the movie (whole field, 6 cells). Data is representative of 2 movies. Bar in A) equals 10 μm.

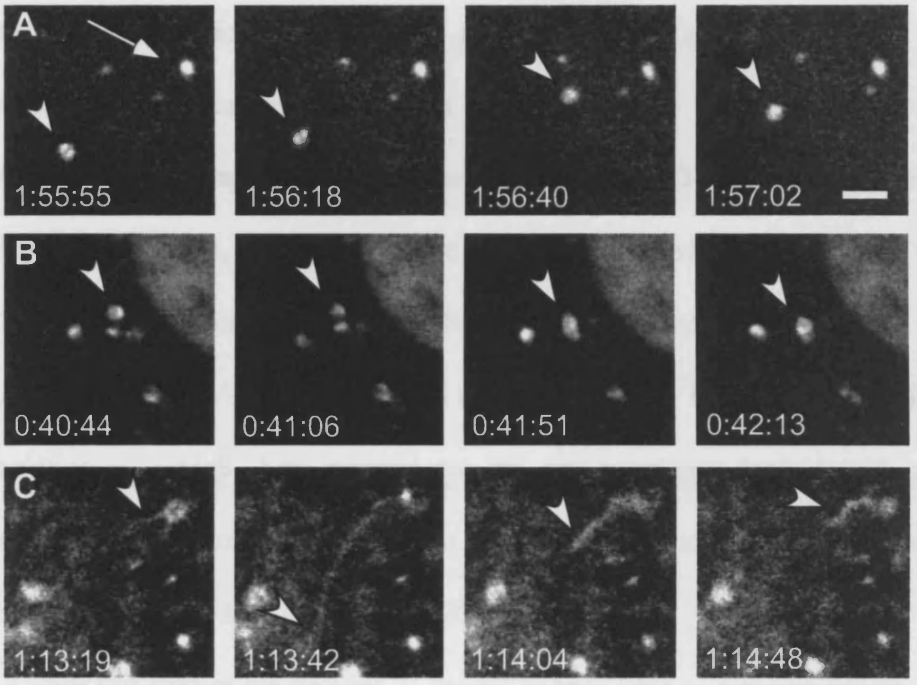

Figure 3.13: Autophagosomes fuse, move, send out tubular structures. A), B), and C) are enlarged areas of the cell shown in Figure 3.12 and illustrate AV movement, interaction, and tubule formation, respectively. Arrowhead in A) identifies the moving AV, arrow identifies an immobile GFP-LC3 vesicle. Arrowhead in B) identifies interacting AVs, in C) the growing, and retracting, end of the tubule. Time on panels show in hr:min:sec when the frames were captured. Bar is 2 μm.

3.9 Discussion

When autophagy was described first in the late fifties (Clark, 1957), the only way to identify autophagosomes was by electron microscopy. In the mid 90ies, a huge step forward has been made in the autophagy field with the independent identification of the yeast autophagy genes by several groups at approximately the same time (Harding et al., 1995; Thumm et al., 1994; Tsukada and Ohsumi, 1993). One of the proteins identified in those screens was Atg8, which is the only protein identified so far that binds specifically to and remains associated with newly formed autophagosomes. LC3, the mammalian homolouge of Atg8 has proven to be an excellent tool to identify autophagosomes in mammalian cells at both the light and ultrastructural level when tagged with GFP (Kabeya et al., 2000).

For our studies we decided to use rat hepatocytes as a model for several reasons. First, hepatocytes have been used extensively in the past to study autophagy and autophagosomes are therefore morphologically very well defined and characterised in this cell type, and secondly hepatocytes have a high capacity to undergo autophagy. A big disadvantage, however, is that primary hepatocytes are difficult to transfect and most studies were therefore restrained to using morphological or biochemical assays only.

I therefore decided on using an adenoviral system to express GFP-LC3 in order to investigate the molecular mechanisms involved in the formation of autophagosomes and the regulation of this pathway in mammalian cells.

In this thesis I can show that cultured primary rat hepatocytes are amenable to genetic manipulation and that over-expression of GFP-LC3 does not induce autophagy on its own, contrary to what has been reported for other tissue culture model systems. This might be because hepatocytes have a larger capacity to buffer increased quantities of exogenous protein and are therefore less "stressed" or because the induction of autophagy is more tightly controlled than in other cell lines. In addition, adenoviral infection per se has no effect on the morphology or the life span of hepatocytes in culture. Using the adenovirus system I was able to infect up to 100% of cells thereby allowing quantitative analysis to be carried out.

I found that hepatocytes have a low basal level of autophagy in full growth medium, which can be made visible by the addition of lysosomal protease inhibitors. At steady state I found between 1 to 5 autophagosomes per nucleus.

After the cells were shifted to starvation medium autophagosomes formed rapidly and an increase in GFP-LC3 labelled vesicles could be seen as soon as after 15 minutes, which is similar to what Kabeya et al. (Kabeya et al., 2000) reported previously. As expected this increase could be inhibited by the addition of PI3K inhibitors. Interestingly after approximately 60 minutes I always saw that the number of autophagosomes reached a plateau of 11-15 autophagosomes per nucleus. I speculated that this could either mean that the new synthesis of autophagosomes is down regulated after 30 to 60 minutes or alternatively, that the GFP-LC3 in autophagosomes formed during the first 30 to 60 minutes gets degraded when it reaches the lysosome. A possible reason for the downregulation could be a feedback mechanism, whereby the cell stops

the production of new autophagosomes because it has generated enough new amino acids to allow the replenishment of the cellular amino acids pool, thereby alleviating the requirement for ongoing or additional autophagy. Alternatively, the machinery to form autophagosomes is limiting. To address this question I incubated starved cells in the presence of protease inhibitors. In this case the number of GFP-LC3 positive autophagosomes continued to increase in a linear fashion, showing that autophagosomes are continuously formed during the short term starvation experiments. This was also confirmed by the quantitative electron microscopy time course where the number of AVds continued to increase, while the number of AVis reached a plateau at 60 minutes. This suggests that after 60 minutes many of the GFP-LC3 positive structures are AVds, as expected also from previous studies (Dunn, 1994).

In addition, by using live-cell imaging and by following autophagosomes labelled with GFP-LC3, I could confirm the time course data obtained with fixed cells. I detected GFP-LC3-positive autophagosomes within 5 minutes after transferring the cells to ES. Most autophagosomes moved in a seemingly random start-stop manner over relatively short distances, while only a few vesicles travelled over longer distances. Frequently I saw GFP-LC3-positive structures interacting, possibly fusing with each other. Judging from the movies, however, it is unclear if these potential fusion reactions would be homotypic fusions between different AVis or AVds or if they are heterotypic fusions between an AVi and AVd. In addition, I regularly observed GFP-LC3-positive tubules extending from the autophagosomes and retracting, and in some cases it appeared as if the autophagosomes followed the tubular structure. The exact nature and function of these GFP-LC3 positive tubules is currently

unclear. It is, however, conceivable that these structures might be related to microtubules, since LC3 has initially been described to be a subunit of Microtubule-associated protein 1A and B (MAP1-LC3) (Mann and Hammarback, 1994). Further research will be required to determine the exact nature and function of these tubules. There was no discernable change in the movement or localization of the autophagosomes over the 120 minutes incubation.

Being able to infect 95% to 100% of the hepatocytes with the GFP-LC3 encoding adenovirus I could for the first time, evaluate the kinetics of autophagosome formation using an automated imaging system and Metamorph 6.2 software. I found that AVis form with $t_{1/2}$ of approximately 15 minutes in ES. The rapid induction I observed in the cultured hepatocytes is clearly faster than what Mizushima et al. (Mizushima et al., 2004) have observed in the liver of GFP-LC3 transgenic mice, where GFP-LC3-labelled autophagosomes could only be detected after 24 hours starvation of the animal, suggesting that cultured hepatocytes are more sensitive to nutrient deprivation. I hypothesize that this could be either because they are derived from rats starved for 20 hours or as a result of the ex-vivo culturing conditions, or both.

In conclusion, I have developed a system based on the adenoviral expression of GFP-LC3 in cultured primary hepatocytes. I was able to show that hepatocytes are amenable to genetic manipulation and that GFP-LC3 can be used to study autophagosome formation in fixed cells as well as in real time after amino acid withdrawal or drug treatments. Furthermore, I was able to show that hepatocytes undergo basal autophagy, even in full medium. Basal

autophagy might full-fill house keeping functions, such as the degradation of old and damaged mitochondria or the degradation of long-lived proteins.

4 AMINO ACID SIGNALLING

4.1 Aim

Amino acid deprivation of cells is one of the strongest inducers of autophagy. It is generally believed that the Target of Rapamycin (TOR) plays an essential role in sensing the level of amino acids (Feng et al., 2005; Tokunaga et al., 2004) and it has been shown that amino acid withdrawal leads to the inactivation of TOR (Hara et al., 1998). In yeast (Noda and Ohsumi, 1998) and in many cell lines inhibition of TOR or mammalian TOR (mTOR), respectively, by rapamycin results in the induction of autophagy independent of nutrient levels, as measured by an increase in protein degradation, LDH sequestration and the number of AVis and AVds by EM (Blommaart et al., 1995a; Eskelinen et al., 2002; Mordier et al., 2000; Shigemitsu et al., 1999). Recently, however, there have been some conflicting reports showing that amino acids can inhibit autophagy also via TOR-independent pathways (Kanazawa et al., 2004; Mordier et al., 2000). Based on a serendipitous result I obtained with rapamycin, we therefore decided to study the role of mTOR in autophagosome formation using our primary rat hepatocyte system and the quantification assay I developed.

4.2 Autophagosome formation is independent of mTOR

During the initial characterization of the virally infected hepatocytes expressing GFP-LC3, I also incubated them in FM containing 25 nM rapamycin. Intriguingly after a visual inspection I found that rapamycin, when added to FM, did not induce autophagosome formation (Figure 4.1A). To ensure that the rapamycin I added was active, and that the concentration was high enough to inhibit mTOR, I incubated cells with or without 25 nM rapamycin for 120 minutes in FM or ES. The cells were then harvested in the presence of phosphatase inhibitors and blotted with a phospho-specific antibody against threonine 389 of p70S6K, a residue specifically phosphorylated by active mTOR (Feng et al., 2005). In FM, rapamycin treatment of hepatocytes inhibited p70S6k phosphorylation within 120 minutes, demonstrating that a concentration of 25 nM rapamycin is sufficient to inactivate mTOR (Figure 4.1B). ES incubation, on the other hand, was also sufficient to inhibit mTOR activity in the cultured hepatocytes, regardless of the rapamycin addition. As a control I checked the total p70S6K levels to ensure that starvation or rapamycin treatment has no effect on the total amount of p70S6K (Figure 4.1B).

To quantify the above observed effect of rapamycin on autophagosome numbers, I incubated cells in FM or ES with or without 25 nM rapamycin for 120 minutes and then analysed the saponin-extracted and fixed cells using the automated epifluorescence microscope (Figure 4.2A). As expected, hepatocytes expressing GFP-LC3 had only a low number of autophagosomes when

incubated in FM, while incubation in ES for 120 minutes caused a significant increase in the number of GFP-labelled autophagosomes. Addition of rapamycin to full medium did not significantly increase the number of autophagosomes formed during the 2 hour incubation period ($p<0.01$), showing that inactivation of mTOR had no effect on the total autophagosome number per cell (Figure 4.2B).

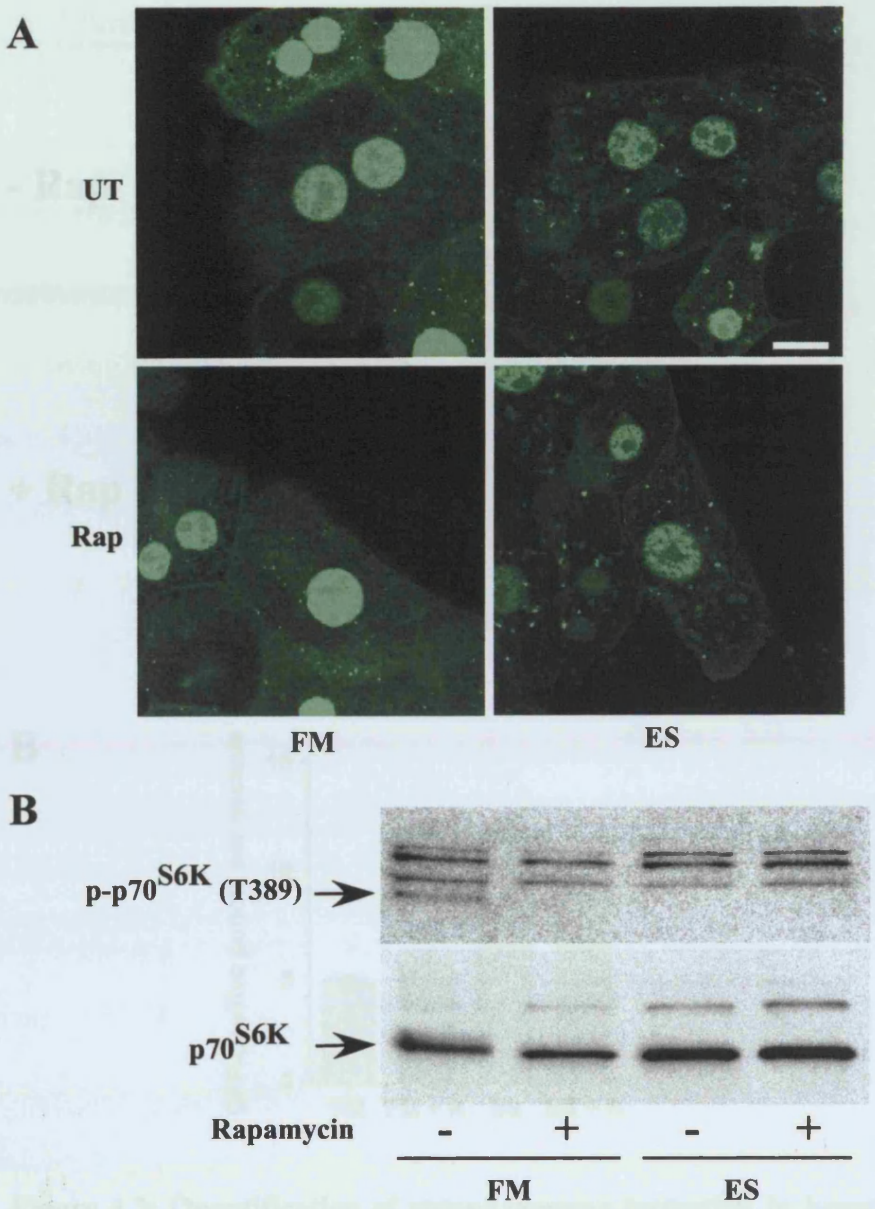

Figure 4.1: Inhibition of mTOR does not induce autophagosome formation in hepatocytes. Cultured hepatocytes expressing GFP-LC3 were incubated in either FM or ES in the absence (UT) or presence of 25 nM rapamycin (Rap) for 2 hrs. After incubation cells were A) fixed and visualized with a confocal LSM 510 microscope, or B) extracted in TNTE buffer, plus phosphatase inhibitors. Anti-p70S6K or anti-phospho-p70S6K antibodies were used to detect p70S6K in FM or ES with or without rapamycin. Bar in A equals 10 microns. Data shown in A and B is representative of 3 independent experiments.

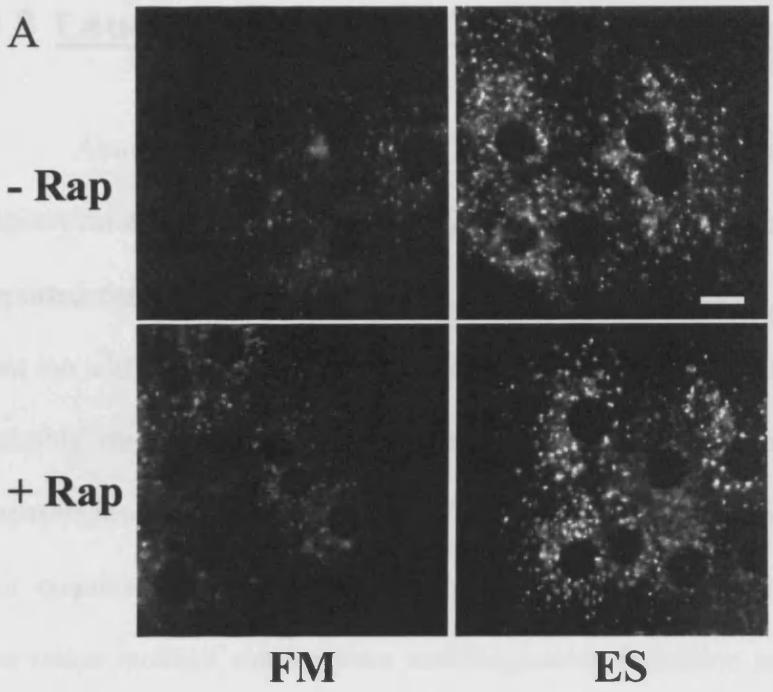

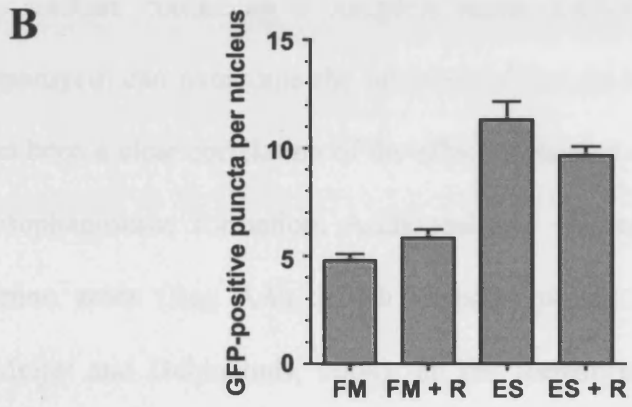

Figure 4.2: Quantification of autophagosome formation in hepatocytes treated with rapamycin. Cultured hepatocytes expressing GFP-LC3 were incubated in either FM or ES in the presence or absence of 25 nM rapamycin (Rap or R) for 2 hours. After incubation cells were A) and B) saponin permeabilized and fixed and B) quantified with the Discovery-1 microscope. 3300 cells were quantified per condition in B. Bar in A) equals 10 microns. Data shown in A and B is representative of 3 independent experiments

4.3 Leucine is a strong inhibitor of autophagy

About the same time when I found that inactivation of mTOR with rapamycin did not activate autophagy, Kanazawa et al. (Kanazawa et al., 2004) reported data using proteolysis as a read-out for autophagy, which suggested that the addition of leucine may rescue autophagy independently of mTOR and possibly through an unidentified recepTOR in the plasma membrane of rat hepatocytes. Therefore, using the GFP-LC3 expressing hepatocyte cultures and our quantitative assay, I decided to investigate whether leucine addition to starvation medium can suppress autophagosome formation to the same extent as medium containing a complete amino acid mixture, and if addition of rapamycin can overcome the inhibitory effect of leucine. So far there has not yet been a clear correlation of the effect of leucine or leucine and rapamycin on autophagosome formation. Additionally, I studied the effects of regulatory amino acids (Reg AA), which suppress protein degradation by autophagy (Meijer and Dubbelhuis, 2004), on the formation of the GFP-LC3 positive vesicles. Reg AA are a selection of 8 amino acids which have been found to be particularly effective in inhibiting autophagy (Leu, Tyr, Pro, Met, His, Trp, Ala). Most Reg AA are essential amino acids.

I incubated hepatocytes expressing GFP-LC3 for 120 minutes in ES, containing Reg AAs, 0.8 mM leucine, 0.8 mM leucine plus 25 nM rapamycin or isoleucine. As a control I used cells incubated in FM or ES without additions (Figure 4.3). In accordance with earlier experiments, ES starvation for 120 minutes increased the number of autophagosomes approximately threefold.

Addition of 4X the plasma serum level of leucine to ES during the starvation period suppressed the formation of autophagosomes to a level comparable to FM or regulatory amino acids in ES, while the addition of isoleucine had no effect, showing that the effect is specific for leucine. In addition, the inhibitory effect of 4X leucine on autophagosome formation was not changed by simultaneous addition of rapamycin (Figure 4.3), suggesting that leucine inhibits autophagy in a largely mTOR independent manner.

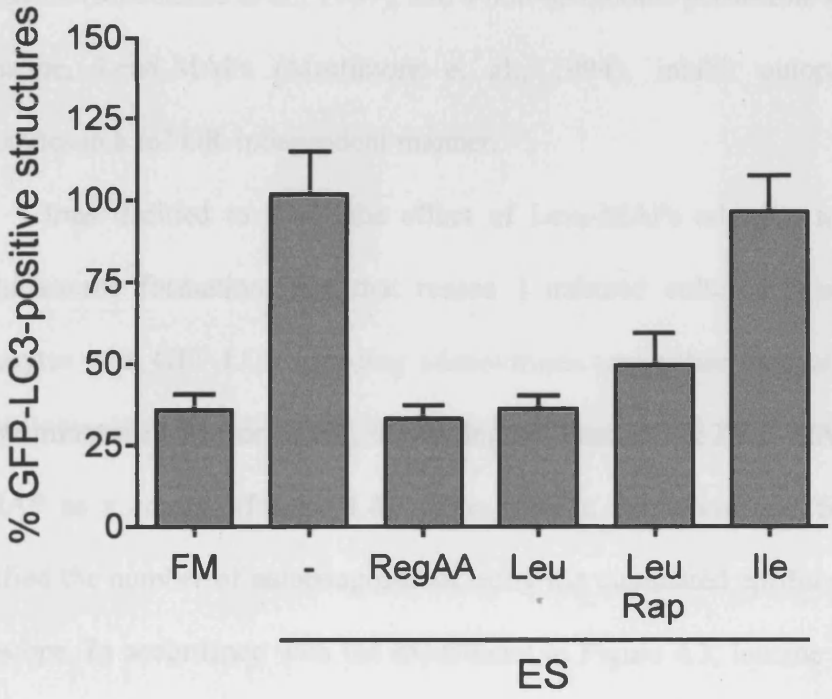

Figure 4.3: Leucine inhibits autophagosome formation largely independent of mTOR. Infected cultured hepatocytes expressing GFP-LC3 were incubated for 2 hours in either FM, or ES containing regulatory amino acids (RegAA (μM): Leu, 204; Tyr, 98; Pro, 437; Met, 60; His, 92; Trp, 93; Ala, 475), 0.8 mM (4x plasma level) leucine (Leu), 0.8 mM leucine plus 25 nM Rapamycin (Leu, Rap) or 0.8 mM (4 x plasma level) isoleucine (Ile). 100% the maximum number of puncta obtained after incubation in ES. Data shown is representative of 4 independent experiments.

4.4 Leucine signals through a novel pathway largely independent of mTOR

Using protein degradation assays, it has previously been demonstrated that leucine (Mortimore et al., 1987), and a non-membrane permeable analogue of leucine, Leu8-MAPs (Mortimore et al., 1994), inhibit autophagy in hepatocytes in a mTOR-independent manner.

I thus decided to study the effect of Leu_8-MAPs addition to ES on autophagosome formation. For that reason I infected cultured primary rat hepatocytes with GFP-LC3 encoding adenoviruses and either incubated them for 120 minutes in FM or in ES, containing 4x leucine, 4x Leu_8-MAP or 4x Ile_8-MAP as a control (Figure 4.4). After saponin extraction and fixation I quantified the number of autophagosomes using the automated epifluorescence microscope. In accordance with the experiment in Figure 4.3, leucine addition inhibited autophagy to a level similar than in hepatocytes in FM. Interestingly Leu_8-MAP addition also significantly inhibited autophagosome formation, however, not to the same level as leucine. Ile_8-MAP treatment, on the other hand, had no statistically significant effect on the number of autophagosomes when compared to ES alone. In summary these results suggest that leucine inhibits autophagy partially through a putative receptor from the plasma membrane in agreement to the data presented by Kanazawa et al. (Kanazawa et al., 2004).

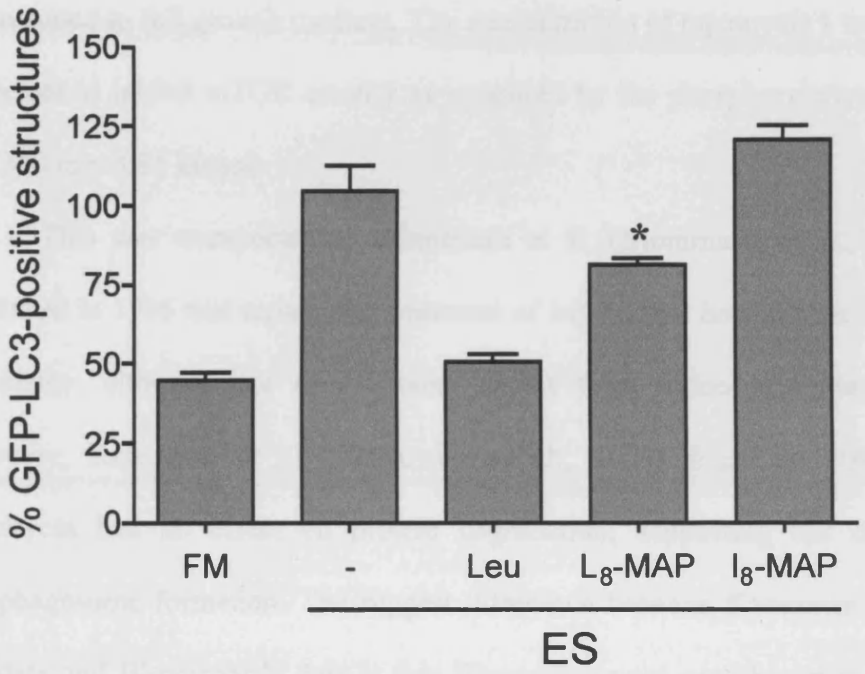

Figure 4.4: Leucine inhibits autophagosome formation via a novel pathway originating from the plasma membrane. Infected cultured hepatocytes expressing GFP-LC3 were incubated for 2 hours in either FM, or ES containing 0.8 mM (equals 4X plasma concentration) leucine (Leu), or either 0.8 mM L8-MAP or 0.8 mM I8-MAPs. 100% the maximum number of puncta obtained after incubation in ES. * for L8-MAPs $p<0.01$ versus ES, Leu, I8-MAPs. Data shown is representative of 2 independent experiments.

4.5 Discussion

When I developed our rat hepatocyte model I found that rapamycin treatment did not induce the formation of GFP-LC3-positive autophagosomes when added to full growth medium. The concentration of rapamycin I used was sufficient to inhibit mTOR activity as measured by the phosphorylation status of T389 in p70S6 kinase.

This was unexpected as Blommaart et al. (Blommaart et al., 1995a) published in 1995 that rapamycin treatment of isolated rat hepatocytes induces autophagy, although not to the same extent than amino acid starvation. However, Kanazawa et al. (Kanazawa et al., 2004) found in 2004 that rapamycin had no effect on protein degradation, supporting our data on autophagosome formation. The biggest difference between Kanazawa's data, my data and Blommaart's data is that Blommaart used cycloheximide in his protein degradation assays to inhibit the reincorporation of amino acids into new proteins during the time course of the assay. Cycloheximide treatment on its own has been shown to suppress autophagy (Khairallah and Mortimore, 1976) and to induce p70S6 kinase phosphorylation (Price et al., 1989). Rapamycin treatment, on the other hand, reduces p70S6 kinase phosphorylation by inhibiting mTOR activity. In yeast, the combined treatment of cells with rapamycin and cycloheximide, led to a reduction of autophagosome size. It is therefore conceivable that the additional cycloheximide treatment might have influenced Blommaart's results. In our own preliminary experiments using cycloheximide I observed that rapamycin treatment can partially induce

autophagy in hepatocytes, incubated in ES with 4x leucine and cycloheximide, thereby repeating Blommaart's data, while rapamycin treatment alone did not induce autophagosome formation, although I could clearly show that mTOR was inhibited.

The fact that rapamycin addition to full medium or starvation medium, containing 4x leucine, did not stimulate autophagosome formation supports the idea that amino acids, and especially leucine, may inhibit autophagy in cultured primary hepatocytes through a mTOR-independent mechanism. This hypothesis was further strengthened by the partial suppression of autophagosome formation by the membrane impermeable leucine analogue Leu_8-MAP, supporting the data for a putative plasma membrane leucine receptor which is not upstream of mTOR or signals independently of mTOR (Kanazawa et al., 2004; Mordier et al., 2000). Additionally, since Ile_8-MAP treatment could not inhibit autophagy, this also suggests that amino acid sensing might be a highly specific process, possibly involving several specific "amino acid receptors" located in the cytoplasm or on the plasma membrane.

mTOR seems to be clearly involved in the regulation of autophagy by insulin (Kanazawa et al., 2004) and could still be involved in later events in autophagy, but does not appear to be part of the sensory mechanism for starvation in the primary rat hepatocyte, as well as in C2C12 myotubes (Mordier et al., 2000).

Using our high throughput counting assay, I was able to correlate the results obtained using protein degradation assays with our results relating to the formation of autophagosomes. Protein degradation assays measure the flux of proteins through the system, which relies on a formed autophagosome fusing

with an endocytic compartment, acidification, degradation, and finally, transport of the free amino acids out of the autolysosome and into the cytosol and medium. However, protein degradation assays do not measure the extent of autophagosome formation directly as any block or disturbance at any stage in this pathway may give the impression of autophagy being inhibited. Visualization by electron or light microscopy and quantification of autophagosome formation, under the conditions investigated above, however, should allow a definitive conclusion to be made about the mTOR-independent effect of leucine, and can also provide a system amenable to the identification of the putative plasma membrane leucine receptor and its downstream signalling molecules.

5 THE ROLE OF MICROTUBULES IN FORMATION AND FUSION

5.1 Aim

As discussed in chapter 1, microtubules have been shown to be required in a number of different membrane trafficking steps. The role of microtubules in autophagosome formation and fusion, however, is not completely clear and there are several conflicting reports in the literature. Depolymerising microtubules with nocodazole, for instance, had no effect on the fusion of autophagosomes with lysosomes in Erlich ascites tumour cells (Reunanen et al., 1988), while Aplin et al. (Aplin et al., 1992b) showed that autophagosome fusion was inhibited in NRK cells. Similar conflicting reports have been described when microtubules were disrupted with vinblastine. Fengsrud et al. (Fengsrud et al., 1995) showed that fusion was inhibited in isolated hepatocytes, while Punnonen et al. (Punnonen et al., 1993) demonstrated that in cultured rat fibroblasts fusion with prelysosomal compartments was not affected.

I therefore decided to study the role of microtubules in fusion and maturation, using the quantitative high throughput system, developed in chapter 3.6, and the microtubule perturbing drugs taxol, vinblastine, and nocodazole. Taxol is a microtubule stabilizer (Schiff and Horwitz, 1980), which inhibits microtubule dynamics. Vinblastine and nocodazole (Panda et al., 1996; Samson et al., 1979), on the other hand, both prevent tubulin polymerization by binding

to tubulin subunits, and therefore ultimately lead to the depolymerization of the microtubule network. In order to investigate formation and fusion independently, the drugs were used in conjunction with lysosomal protease inhibitors.

5.2 Effect of microtubule drugs on cultured primary rat hepatocytes

To assess the effect of nocodazole, taxol and vinblastine on the microtubule network in cultured primary rat hepatocytes I isolated cells and infected them with adenoviruses, encoding GFP-LC3. The following day, hepatocytes were either left untreated or were pre-incubated with 50 μM nocodazole, 5 μM taxol or 50 μM vinblastine in full growth medium, before transferring them to starvation medium, containing the respective drug. Cells were then either fixed directly after the pre-treatment (t = 0) or after 15 or 120 minutes starvation and stained with an anti-tubulin antibody (Figure 5.1).

After the 30 minute pre-incubation with either nocodazole or vinblastine, the microtubules were largely depolymerised, with single, long microtubules remaining in nocodazole treated cells. In cells treated with taxol, the microtubule network stayed intact, and no obvious difference to untreated cells could be observed. After a further 15 or 120 minutes incubation in ES in the presence of nocodazole or vinblastine the microtubule network was completely depolymerised. In the vinblastine treated samples large aggregates could be observed, which became more numerous over the time course of the experiment. On the other hand, in the taxol treated and untreated cells the

microtubule network was unchanged, also indicating that starvation alone does not affect the structure of the microtubule network. In summary, these results suggest that the 30 minut pre-incubation and the drug concentrations used, were sufficient to largely depolymerize the microtubule network. Importantly, the cells didn't change shape during the course of the experiment and generally looked healthy.

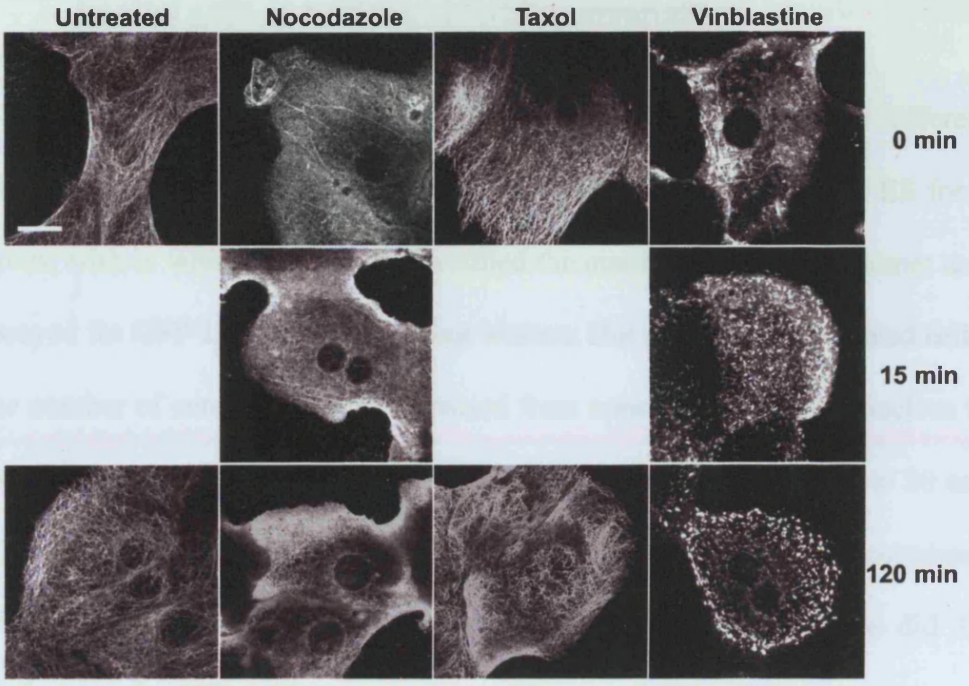

Figure 5.1: Effects of nocodazole, taxol and vinblastine on the microtubule structure. Hepatocytes were pre-treated with 50 μM nocodazole, 5 μM taxol or 50 μM vinblastine in FM for 30 mins, and then either fixed and stained for tubulin immediately (0 min), or incubated for a further 15 or 120 minutes in ES with the drug. Projections of z-stacks acquired on a LSM 510 confocal microscope are shown. Bar equals 10 μM.

5.3 Microtubules are required for autophagosome fusion with degradative compartments

5.3.1 Autophagosome number in vinblastine and nocodazole treated cells is protease inhibitor insensitive

Hepatocytes expressing GFP-LC3 were pre-treated with the different microtubule drugs as described above and either incubated in FM or ES for 2 hours, with or without PI. I then quantified the number of autophagosomes and assayed for GFP-LC3 lipidation, using western blot analysis. In untreated cells, the number of autophagosomes increased from approximately 3 per nucleus to 14 after starvation. Addition of PI to ES or FM increased the number to 20 and 15 autophagosomes per nucleus, respectively (Figure 5.2B), which correlated well with the results from the time course shown in Figure 3.11, as did the analysis of GFP-LC3 processing (Figure 5.2C). The number of autophagosomes and the amount of GFP-LC3-II in cells treated with taxol largely mirrored untreated cells, both in the absence and presence of protease inhibitors.

Incubation of hepatocytes with nocodazole, however, resulted in a number of differences. Firstly, the number of autophagosomes after starvation in ES with nocodazole, approximately 10, was not increased by the addition of protease inhibitors, as it was in untreated cells. Secondly, the number of autophagosomes in cells incubated in FM with nocodazole was elevated after a 2 hour incubation and this number was insensitive to the addition of protease inhibitors. GFP-LC3-II formation in nocodazole treated cells reflected these

results (Figure 5.2C), as there was a constant elevated level of GFP-LC3-II in both FM and ES, which was not sensitive to protease inhibitors.

Incubation with vinblastine had similar effects as nocodazole treatment on the number of autophagosomes with regard to the insensitivity of the autophagosome number to protease inhibitors in FM as well as in ES. Interestingly however, the number of autophagosomes was highly elevated in the pre-treated sample, and this did not significantly change after 120 min (Figure 5.2B). Accordingly, the amount of GFP-LC3-II was also strongly increased by vinblastine (Figure 5.2C).

I used the sensitivity of GFP-LC3 fluorescence and GFP-LC3-II amounts to protease inhibitors as an indirect measure of fusion of autophagosomes with a degradative compartment. In nocodazole and vinblastine treated hepatocytes addition of protease inhibitors had no protective effect on the number of GFP-LC3 positive vesicles and the amount of GFP-LC3-II, suggesting that fusion was inhibited. Additionally, the number of autophagosomes and the amount of GFP-LC3-II was increased after 2 hours incubation in FM with nocodazole or vinblastine, indicating the accumulation of autophagosome due to a lack in fusion and degradation.

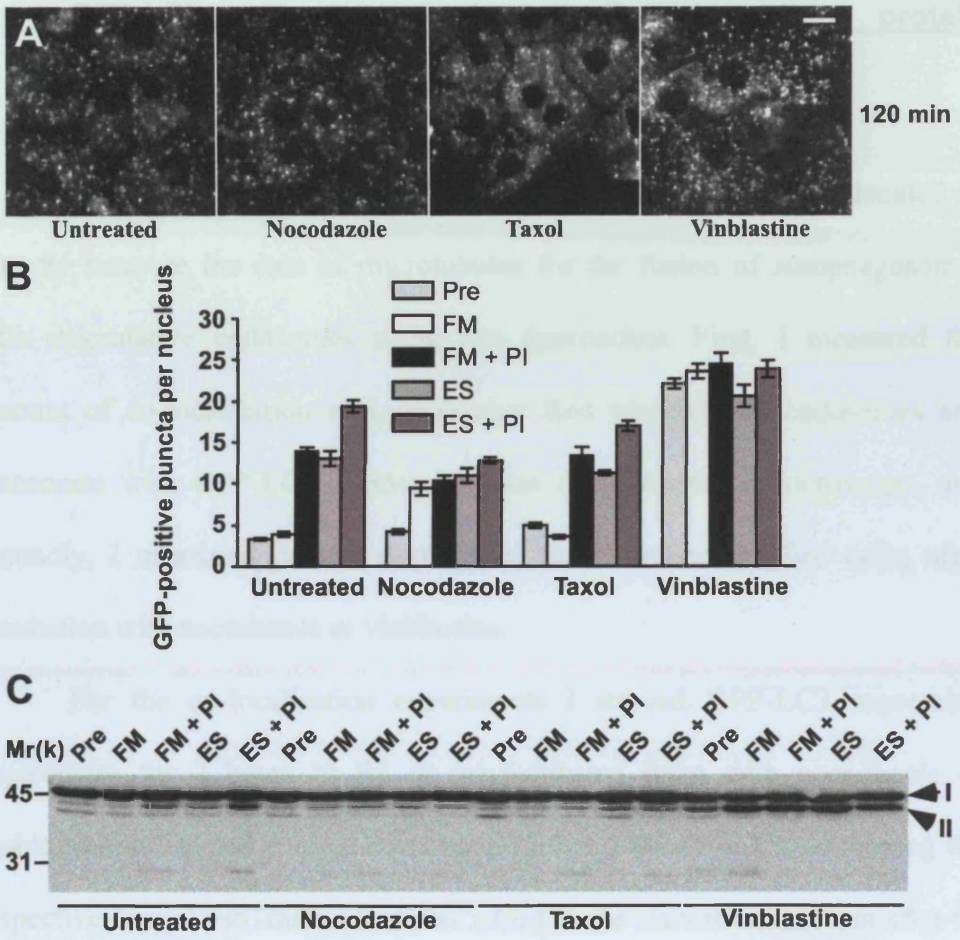

Figure 5.2. Effect of microtubule drugs on fusion. Hepatocytes were pre-treated with 50 μM nocodazole, 5 μM taxol or 50 μM vinblastine in FM for 30 mins, and then either fixed immediately, or incubated for a further 120 minutes in FM or ES, with or without the drug. A) Representative images of GFP-LC3 distribution at 120 min in ES, without or with drug, after saponin extraction acquired with a Discovery-1 microscope. B) Quantification of autophagosomes after treatment with drugs. Images of the cells were analysed as described in Materials and Methods. C) Samples from the time course were analysed by immunoblotting with anti-GFP antibody. Bars in A) equals 10 microns. Data in B (mean +/- SEM of 16 acquired fields) is representative of 3 independent experiments.

5.3.2 Vinblastine and nocodazole treatment reduces the overlap of GFP-LC3 with LysoTracker Red and inhibits protein degradation

Since the data presented above is an indirect measure, I decided to directly measure the role of microtubules for the fusion of autophagosomes with degradative endosomes using two approaches. First, I measured the amount of co-localization of LysoTracker Red labelled late endosomes and lysosomes with GFP-LC3-positive vesicles using confocal microscopy, and secondly, I measured protein degradation in ^{14}C-valine labelled cells, after incubation with nocodazole or vinblastine.

For the co-localization experiments I starved GFP-LC3 expressing hepatocytes for 2 hours in ES or pre-incubated them with nocodazole or vinblastine in FM and starved them for a further 2 hours in ES, containing the respective drug. LysoTracker Red was added to the starvation medium after 90 minutes in ES. Cells were then fixed and the extent of co-localization was quantified using confocal imaging and the LSM software (Figure 5.3A and B). I found that in untreated cells, approximately 20% of the LysoTracker Red signals co-localized with GFP-LC3, while in nocodazole or vinblastine treated cells there was less than 10% co-localization between LysoTracker Red and GFP-LC3 vesicles. To ensure that treatment with nocodazole or vinblastine did not affect the total number of LysoTracker Red positive vesicles or the distribution of these vesicles, I quantified the number of LysoTracker Red-positive puncta using Metamorph 6.2 software and visually compared their distribution in the cell (Figure 5.4). I could find no statistically significant

difference between samples. Additionally the distribution of LysoTracker Red positive vesicles seemed to be unaffected by the drug treatment.

For the protein degradation assay, GFP-LC3 expressing hepatocytes were either left untreated or were pre-treated with nocodazole or vinblastine in FM. Cells were then further incubated in FM or ES with or without protease inhibitors for an additional 2 hours (Figure 5.5). In untreated cells, ES incubation resulted in an increase in protein degradation that was reduced by the addition of protease inhibitors, confirming the results obtained in Figure 3.11. Nocodazole or vinblastine pre-treatment of cells followed by 2 hours in ES led to a clear reduction in the amount of protein degradation. Some residual protein degradation remained which was sensitive to protease inhibitors, suggesting that a very low amount of fusion still occurs, despite the vinblastine and nocodazole treatment. Taxol on the other hand had no effect on protein degradation, and was similar to untreated cells.

In summary, nocodazole and vinblastine treatment of hepatocytes led to a strong reduction in the co-localization of LysoTracker Red-positive endosomes and lysosomes, and GFP-LC3-positive autophagosomes, as well as a clear reduction in the amount of protein degradation. These results demonstrate that fusion of autophagosomes with endosomes or lysosomes, requires an intact microtubule network.

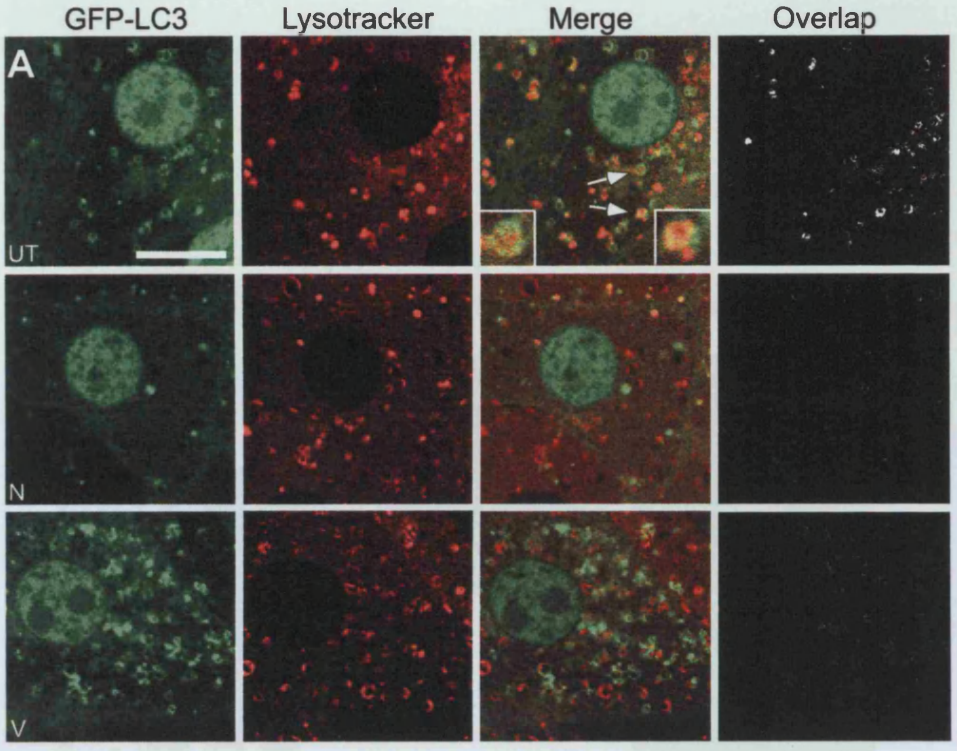

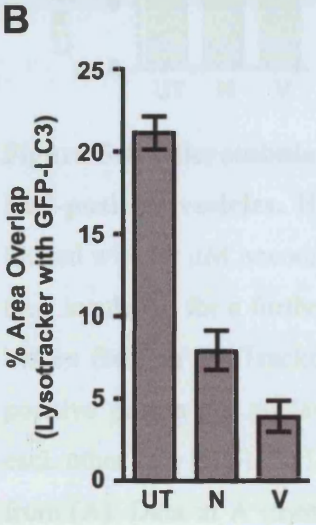

Figure 5.3: Nocodazole and vinblastine inhibit fusion of autophagosomes with endosomal compartments. A) Co-localization of LysoTracker Red with GFP-LC3. Hepatocytes were either untreated (UT), or pre-treated with 50 μM nocodazole (N) or 50 μM vinblastine (V) and then starved in ES for 120 mins in the absence or presence of the respective drug. LysoTracker Red was added 30 mins before fixation. The Overlap panel shows the co-localization detected by the LSM 510 software. Insets show two examples of autophagosomes co-localizing with LysoTracker Red-positive organelles. Top arrow indicates the position of autophagosome shown in the left inset, bottom arrow shows the autophagosome in the right inset. B) Quantification of co-localization. Data in A and B (mean +/- SEM of 10 and 9 fields, respectively) is representative of 2 independent experiments. Bar in A is 10 μm.

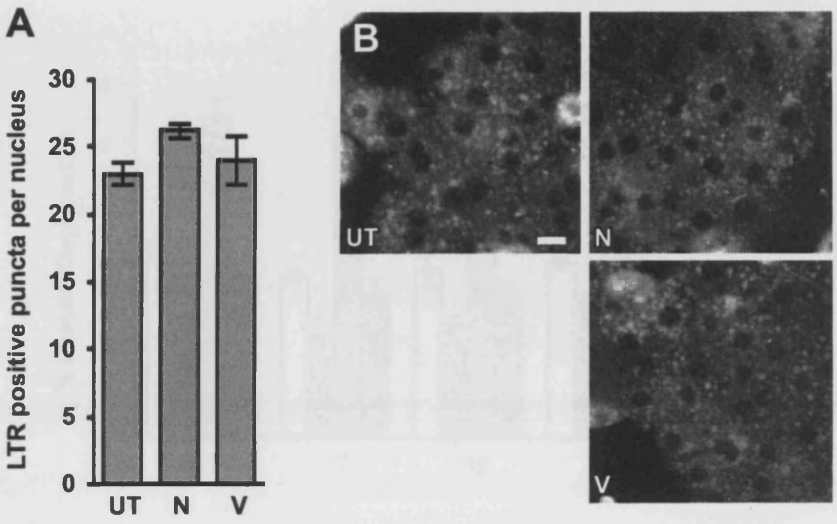

Figure 5.4: Microtubule drugs do not affect the number of LysoTracker Red-positive vesicles. Hepatocytes were either left untreated or were pre-treated with 50 μM nocodazole or 50 μM vinblastine in FM for 30 minutes, and then incubated for a further 2 hours in ES with the respective drug. 30 minutes before fixation LyoTracker Red was added. A) number of LysoTracker Red-positive puncta per nucleus. All columns are not significantly different from each other ($p > 0.05$). B) Low magnification epi-fluoresence images of samples from (A). Data in A (mean +/- SEM of 9 fields, approximately 1000 cells) is representative of 2 experiments. Bar in B equals 10 μM

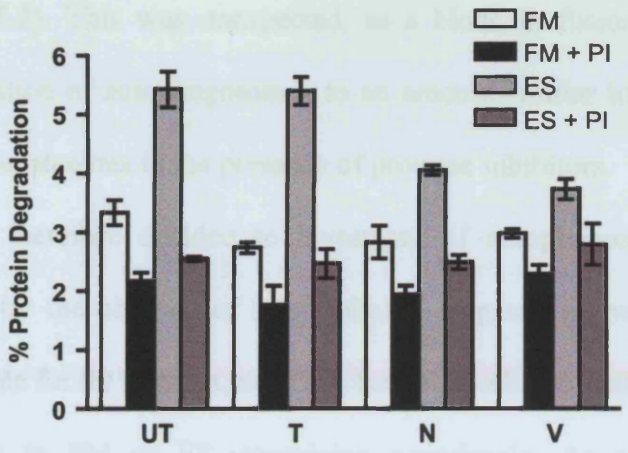

Figure 5.5: Vinblastine and nocodazole inhibit autophagosomal protein degradation. ^{14}C-valine protein degradation assay. Hepatocytes were either untreated, or pretreated with 5 μM taxol or 50 μM nocodazole or 50 μM vinblastine and then incubated for a further 2 hours in FM or ES with or without PI and the respective drug. Data (mean +/- SEM of triplicates) is representative of 2 independent experiments.

5.4 Microtubules facilitate autophagosome formation

Interestingly, after 120 minutes starvation in ES the number of autophagosomes in nocodazole treated samples was less than in untreated cells (Figure 5.2). This was unexpected, as a block in fusion should lead to the accumulation of autophagosomes to an amount similar to what I measured in starved hepatocytes in the presence of protease inhibitors.

I therefore decided to investigate if autophagosome formation was affected by the absence of microtubules. Hepatocytes were pre-treated with nocodazole for 30 minutes, and then further incubated with or without protease inhibitors in FM or ES, containing nocodazole. As a control I included hepatocytes starved in ES with protease inhibitors. The presence of protease inhibitors should ensure that I measure formation only and that the degradation of GFP-LC3 during the time course of the experiment does not influence the result.

In agreement with the data shown in Figure 5.2 I found that at 120 minutes the amount of autophagosomes in FM with nocodazole was elevated to a level similar to cells starved in ES with nocodazole (Figure 5.6A). Addition of protease inhibitors to both, FM and ES, containing nocodazole, had no effect and did not further increase the number of GFP-LC3 positive puncta. Interestingly, in ES and nocodazole treated samples, at early time points the rate of autophagosome formation was reduced in comparison to cells starved in

ES in the presence of protease inhibitors, showing that formation was affected by nocodazole.

I next investigated the effect of nocodazole on autophagosome movement using live cell imaging. For this reason I pre-treated hepatocytes for 30 minutes with nocodazole in FM, before transferring them to ES, also containing nocodazole. As a control I used hepatocytes starved in ES. Approximately 5 minutes after switching the cells to ES I started imaging for 15 minutes. Images were acquired every 10 seconds to increase our ability to detect moving vesicles. In ES the majority of the GFP-LC3 positive structures moved rapidly over short distances (see supplementary movie Fig. M3), while the autophagosomes in the nocodazole treated cells (see supplementary movie Fig. M4) showed very little or no movement. Figure 5.6C shows frames extracted from the movies M3 and M4. Together, these results suggest that an intact microtubule network facilitates the formation of autophagosomes in ES, and that newly formed autophagosomes move on microtubules.

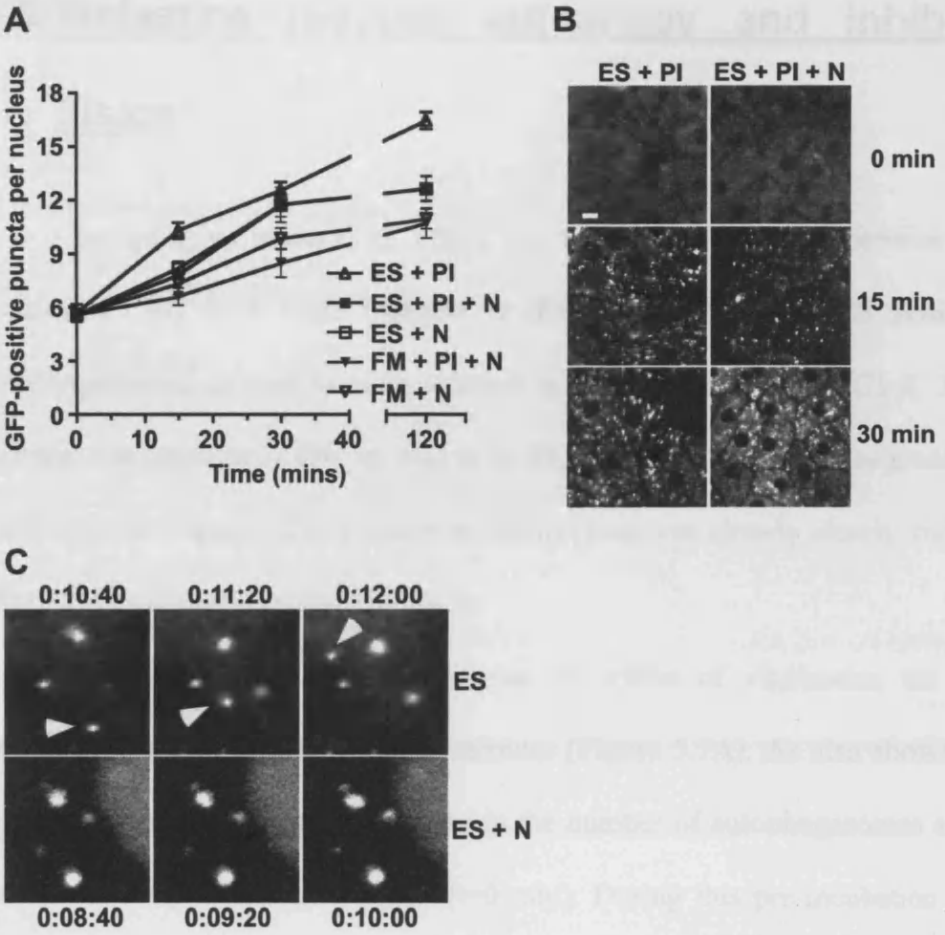

Figure 5.6: Nocodazole inhibits fusion and reduces the rate of autophagosome formation. A) Time course of autophagosome formation. Hepatocytes were pre-treated without or with 50 μM nocodazole (N) for 30 minutes, saponin extracted and fixed immediately, or incubated for a further 15, 30 or 120 mins in ES with PI, and without or with nocodazole. At 15 minutes the nocodazole-treated sample is statistically different to ES + PI ($p < 0.05$). B) Representative images from the time course in A. C) Representative enlarged areas from the supplementary movies (see S3 and S4). Cells were incubated in ES (upper panel) or were pre-treated with nocodazole in FM and then shifted to ES plus nocodazole (lower panel). Time is shown in hr:min:sec. Arrowhead indicates a moving autophagosome. Data in A (mean +/- SEM of 16 acquired fields) is representative of 2 independent experiments. Bar in B) equals 10 microns, bar in C) equals 2 microns.

5.5 Vinlastine induces autophagy and inhibits fusion

Intriguingly, besides its effect on fusion, vinblastine treatment of hepatocytes led to a large increase in the number of GFP-LC3 positive autophagosomes, as well as to an increase in the amount of GFP-LC3-II. This increase was apparent in FM, as well as in ES, and was not sensitive to protease inhibitors (see Figure 5.2). In addition, the increase was already clearly visible after 30 minutes pre-treatment in FM.

I therefore decided to investigate the effect of vinblastine on the formation in a time course over 120 minutes (Figure 5.7A). As also shown in Figure 5.2, there was a strong increase in the number of autophagosomes after the 30 minute pre-treatment in FM (t=0 min). During this pre-incubation the number of vesicles increased more than threefold. This correlated well with the increase in the amount of GFP-LC3-II at t=0 (Figure 5.7B). During the following 120 minute incubation FM or ES with or without PI in the presence of vinblastine the number of vesicles increased further. This increase was independent of the treatment. As a control hepatocytes were incubated in FM plus PI or in ES with or without PI. When vinblastine was added at the beginning of the experiment (Figure 5.7C) the number of autophagosomes started to increase within 15 minutes incubation in FM or ES. Interestingly, after 15 minutes starvation in the presence of vinblastine the number of autophagosomes was consistently higher than in hepatocytes incubated in FM

with vinblastine. However, this increase was no longer apparent after 30 minutes (Figure 5.7C).

The effect of vinblastine on autophagosome formation in FM and ES, however, seems to be unrelated to its depolymerising effect on microtubules, as the full extent of the depolymerisation of the microtubules occurred only after 30 minutes of pre-treatment (Figure 5.1). At 30 minutes there were still single microtubules left in the cell. Additionally, depolymerising the microtubule network with nocodazole did not correlate with the accelerated autophagosome formation observed after treatment with the vinblastine.

Based on those results I wanted to investigate if the vinblastine-induced increase in autophagosomes depends on known Atg proteins using siRNA interference techniques. All siRNA experiments were carried out by Edmond Chan, a post-doc in our laboratory.

Since primary hepatocytes are difficult to transfect and can not be cultured for more than 3 days before they start to dedifferentiate they are not ideal for these experiments. We therefore decided to use HEK293A cells stably expressing GFP-LC3 (HEK293/GFP-LC3). HEK293/GFP-LC3 cells responded to vinblastine like primary rat hepatocytes. Incubation with vinblastine in FM for 60 minutes led to an increase in the number of autophagosomes as detected by the appearance of GFP-positive vesicles (Figure 5.8A).

Atg5 and Atg6/Beclin have both been shown previously to be required for mammalian autophagy (Kuma et al., 2004; Liang et al., 1999; Qu et al., 2003). Thus we transfected HEK293A cells with siRNAs to deplete these proteins and asked if vinblastine treatment still resulted in an increase of GFP-LC3-II by western blotting. 72 hours after the siRNA treatment of the

HEK293/GFP-LC3 cells both Atg5 and Atg6 protein levels were depleted by more than 90% (Figure 5.8B). In those Atg5- or Atg6-deficient cells GFP-LC3 conversion from GFP-LC3-I to GFP-LC3-II was strongly reduced after vinblastine treatment (Figure 5.8C). As a control we used siRNAs against firefly luciferase, which engages the RISC complex but produces non-targeting siRNA. The increase in GFP-LC3-II upon vinblastine treatment was also sensitive to wortmannin (Figure 5.8C). Together these data suggest that the stimulation of autophagosome formation by vinblastine occurs through the normal pathway, dependent on Atg proteins and PI3-kinases.

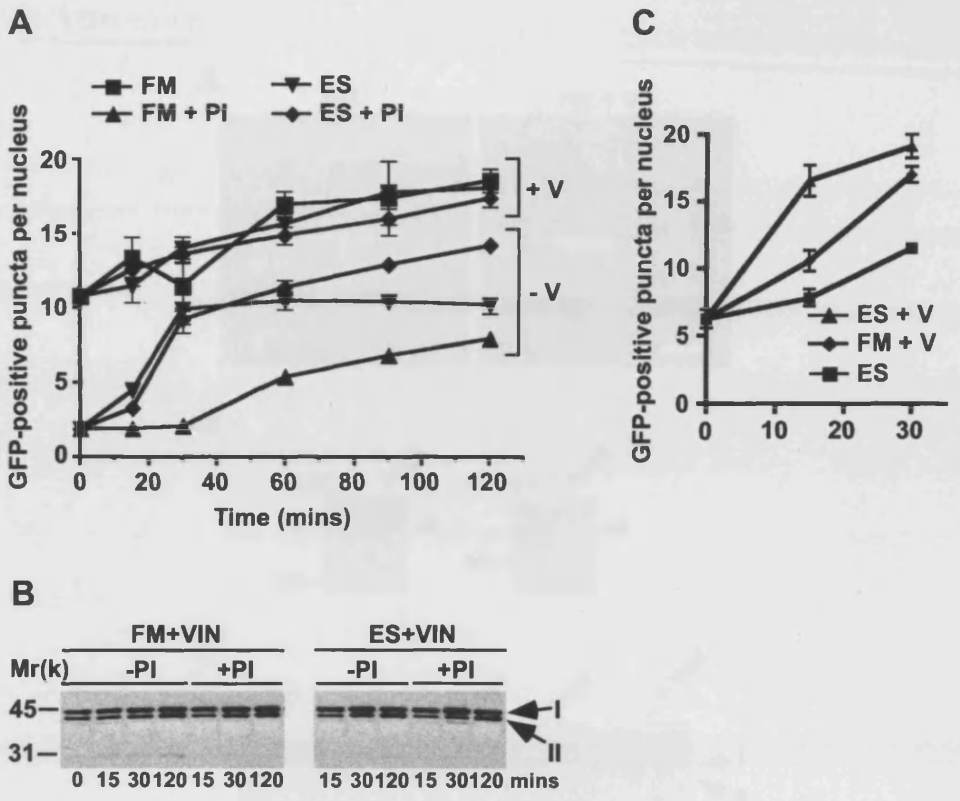

Figure 5.7: Vinblastine inhibits fusion and induces autophagy in hepatocytes. A) Time course of autophagosome formation after vinblastine treatment. Hepatocytes were pre-treated with 50 μM vinblastine for 30 mins in FM, and either saponin extracted and fixed immediately, or incubated for a further 15, 30, 60, 90 and 120 mins under various conditions. Samples with vinblastine treatment: FM, ES and ES+PI; samples without vinblastine treatment: FM+PI, ES and ES+PI. B) Hepatocytes were pre-treated with 50 μM vinblastine and then incubated for a further 0, 15, 30 or 120 mins in FM or ES, without or with PI in the presence of vinblastine. At the given time points cells were harvested and analysed. C) Time course of autophagosome formation after vinblastine treatment. Hepatocytes were incubated in FM or ES with vinblastine or in ES alone for 15 or 30 minutes and then saponin-extracted and fixed. Data in A and C (mean +/- SEM of 16 acquired fields) is representative of 2 independent experiments Data in B and C is representative of 3 and 2 independent experiments, respectively.

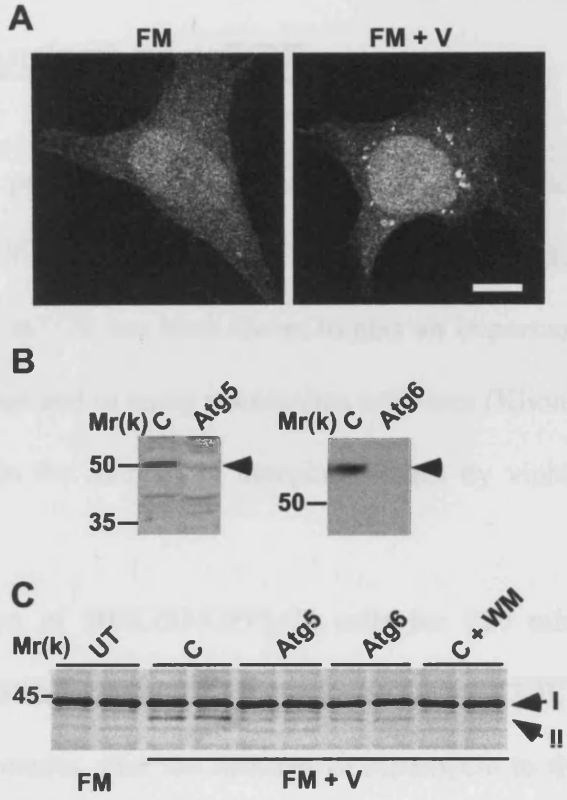

Figure 5.8: Vinblastine induces autophagy in HEK293A cells in a Atg5 and Atg6 dependent manner. A) HEK293A cells stably expressing GFP-LC3 (HEK293/GFP-LC3) were either left in FM or incubated in FM with vinblastine for 60 mins, and then visualized by confocal microscopy. B) HEK293/GFP-LC3 cells were transfected with control siRNA (C) or siRNA for Atg5 or Atg6, lysed 72 hrs later, and then analysed by immunoblotting with antibodies for Atg5 or Atg6. The positions of the Atg5-Atg12 conjugate or Atg6 are indicated by arrowheads. C) HEK293/GFP-LC3 cells were transfected with siRNA's as above and incubated in FM for 2 hrs without or with 50 μM vinblastine or 100nM wortmannin (WM). Data in C is representative of 3 independent experiments. Bar in A is 10 μm. These experiments were carried out by Edmond Chan.

5.6 Vinblastine stimulated autophagy is independent of mTOR

The data presented above suggests that vinblastine activates a signalling pathway, that ultimately leads to an increase in autophagosome formation. Since the kinase mTOR has been shown to play an important role in regulating autophagy in yeast and in many mammalian cell-lines (Klionsky, 2005), I asked if the increase in the number of autophagosomes by vinblastine depends on mTOR.

Incubation of HEK293/GFPLC3 cells for 120 minutes in FM with rapamycin led to an increase in the amount of GFP-LC3-II, which was visible as soon as 15 minutes after the addition of rapamycin to the medium (Figure 5.9A). This was likely through inactivation of mTOR by rapamycin as a corresponding decrease in the phosphorylation of threonine 389 of p70S6K was detected in the same lysates (Figure 5.9B). In accordance with the results obtained in Figure 5.8 vinblastine treatment over 120 minutes induced autophagy when added to FM. However, vinblastine treatment did not result in an inactivation of mTOR (Figure 5.9B), despite the rapamycin-sensitivity of the HEK293/GFP-LC3 cells. As a control, we confirmed that starvation of HEK293/GFP-LC3 cells in ES resulted in mTOR inactivation and GFP-LC3 conversion. These results show that the vinblastine stimulated increase in GFP-LC3-II in HEK293/GFP-LC3 cells, is independent of mTOR.

In contrast to HEK293A cells, autophagy in hepatocytes is rapamycin-insensitive (see also Chapter 4). Although rapamycin inactivated mTOR, it did

not increase the number of autophagosomes (Figure 4.1 and Figure 4.2). To investigate what effect vinblastine has on p70S6K phosphorylation in rat hepatocytes, I pre-incubated cells in FM with vinblastine followed by 120 minutes incubation in FM or ES in the presence of vinblastine. As a control I used hepatocytes cultured in FM. Interestingly, I could detect no p70S6K phosphorylation (Figure 5.9C) after 120 minutes.

To further investigate if the inhibition of p70S6 kinase by vinblastine could induce autophagy, I analysed the time at which vinblastine causes mTOR inactivation. I therefore performed a time course and compared p70S6K phosphorylation in cells incubated in FM plus vinblastine, or ES plus vinblastine, to untreated cells in ES (Fig. 9I).

Vinblastine clearly inactivated mTOR in FM after a 45 minutes incubation in FM (30 minutes pre-treatment followed by an additional 15 minutes incubation). In ES, vinblastine clearly enhanced the starvation-induced inactivation of mTOR. It is, however, unlikely that the inactivation of mTOR by vinblastine is the reason for the induction of autophagy in hepatocytes, because the time course of mTOR inactivation by vinblastine in FM does not parallel the rapid induction of autophagy. While autophagy was induced immediately after the addition of vinblastine and there was a high number of vesicles present after 30 minutes, mTOR was only inactivated after about 45 minutes in FM.

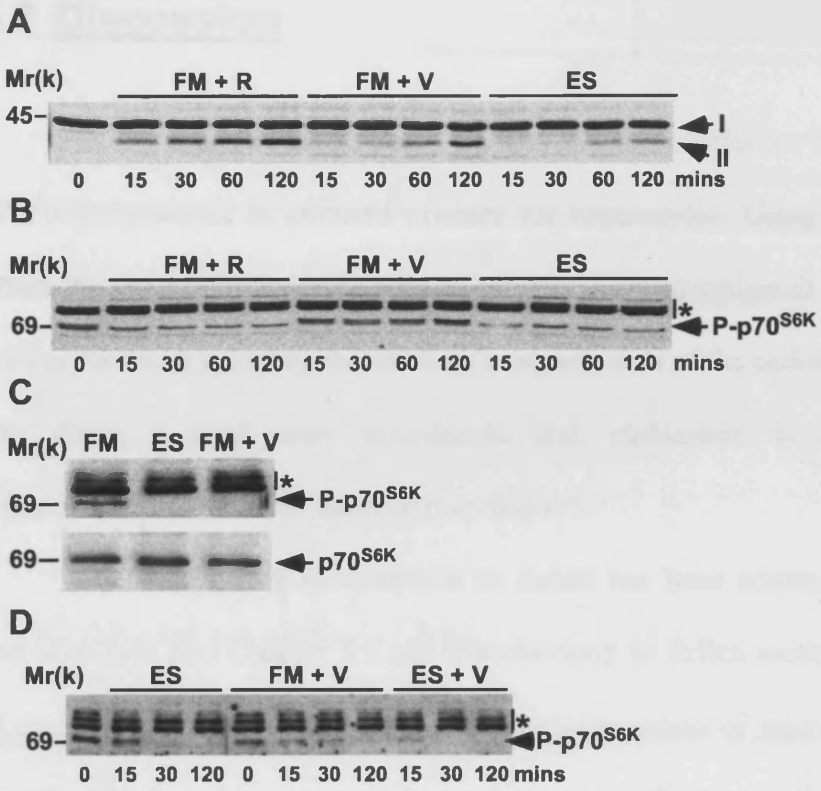

Figure 5.9: Vinblastine inhibits mTOR in hepatocytes but not in HEK293A cells A and B) Immunoblot analysis of HEK293/GFP-LC3 cells incubated for 0, 15, 30, 60 and 120 minutes in FM with 55 μM rapamycin or 50 μM vinblastine or in ES alone, with either an A) anti-GFP antibody or B) threonine389 phospho-p70S6K antibody. In HEK293/GFP-LC3 cells, a non-specific rapamycin-insensitive band is detected migrating slightly faster than p70S6K. (*) indicate positions of higher molecular weight rapamycin-insensitive bands, which are non-specifically detected by the phospho-antibody. C) Hepatocytes were incubated either in FM or in ES or FM plus vinblastine for 2 hours. The vinblastine samples were pre-treated with vinblastine for 30 minutes in FM. Samples were then solubilized and immunoblotted with the phospho-specific p70S6K antibody (upper blot). The position of p70S6K was confirmed with pan p70S6K antibody (lower blot). D) Hepatocytes grown in FM were either starved in ES for 0, 15, 30, 120 mins or pre-treated with 50 μM vinblastine in FM and then incubated for 0, 15, 30, 120 mins in FM or ES plus 50 μM vinblastine, solubilized and subjected to immunoblotting with phospho-p70S6K antibody.

5.7 Discussion

In this chapter I investigated the role of microtubules for the maturation of autophagosomes in cultured primary rat hepatocytes. Using drugs which affect the stability of microtubules, I independently investigated formation, as well as fusion of autophagosomes with compartments of the endosomal system. The drugs I used were nocodazole and vinblastine to depolymerise microtubules and taxol to stabilize microtubules.

The function of microtubules in fusion has been controversial in the literature (see also Chapter 5.1 and Introduction); in Erlich ascites tumor cells (Reunanen et al., 1988), for example, depolymerisation of microtubules with nocodazole has been reported to have no effect on the fusion of autophagosomes and lysosomes, while in NRK cells nocodazole treatment caused an accumulation of autophagosomes, which did not contain acidic hydrolases (Aplin et al., 1992b). More recently Webb et al. (Webb et al., 2004) showed that nocodazole treatment impaired the clearance of A53T α-synuclein, a protein that is normally cleared by autophagy (Webb et al., 2003). Similar conflicting results have been published with vinblastine (Fengsrud et al., 1995; Punnonen et al., 1993).

One of the reasons for the discrepancies between the different reports in the literature may be that they use different cell types. Another potential problem is that the microtubule depolymerising drugs were added at the time of starvation in most of the previous studies. It is conceivable that there is a lag period between the addition of the drug and the complete depolymerisation of

the microtubule network, depending on the concentration of the drug and the cell line used. Since I know that autophagosomes from rapidly after cells are transferred to starvation medium (see also Chapter 3.7) it is conceivable that autophagosomes form and fuse during this initial lag period.

I therefore decided to first investigate the time required to completely depolymerise the microtubule network. Nocodazole treatment of hepatocytes completely depolymerised the microtubule network within 45 minutes. Vinblastine treatment, on the other hand, led to the formation of tubulin aggregates, which became visible after 45 minutes treatment. These aggregates, however, did not co-localize with GFP-LC3-spots (data not shown).

For the following experiments I therefore decided to pre-treat the cells for 30 minutes with the respective drug. Intriguingly, in nocodazole or vinblastine treated cells, the number of autophagosomes did not increase when the samples were treated in parallel with lysosomal protease inhibitors, suggesting a block in fusion. Taxol treated cells, on the other hand behaved similarly to untreated cells, indicating that microtubules, but not dynamic microtubules, are required for the formation and fusion of autophagosomes with late endosomes.

The lack of effect of protease inhibitors could possibly be attributed to several other reasons. Both, nocodazole and vinblastine could affect the integrity of the endosomal system, thereby indirectly affecting the ability of late autophagosomes to mature to autolysosomes or alternatively, the transport of hydrolytic enzymes to late endosomes and lysosomes could be disturbed. This would then prevent the degradation of an autolysosome, and the addition of protease inhibitors would have no effect. To address these problems I stained

acidic compartments in GFP-LC3 expressing hepatocytes with LysoTracker Red and investigated the number and distribution of LysoTracker Red-positive organelles and the amount of overlap between LysoTracker and GFP-LC3. Neither, nocodazole nor vinblastine treatment had a statistically significant effect on the number and distribution of late endosomes and lysosomes, suggesting that those organelles are not affected by the short term incubation (up to 150 minutes total) with the microtubule disrupting drugs. In addition, the percent area overlap between LysoTracker Red and GFP-LC3 was clearly reduced in the drug-treated samples, showing that fusion was largely inhibited.

Interestingly, the total number of GFP-LC3-positive vesicles in nocodazole and vinblastine treated samples was different from untreated cells starved in ES for 120 minutes in the presence of protease inhibitors. One would think that in the drug treated samples, if the drugs inhibited fusion only, the total number of accumulated vesicles would be equal to that in untreated cells incubated in ES with protease inhibitors. This was clearly not the case; nocodazole-treated cells had about the same number or even slightly less GFP-LC3-positive vesicles than untreated cells in ES without protease inhibitors while vinblastine-treated cells had clearly more autophagosomes than control cells, regardless of the treatment. This suggested that formation of autophagosomes was affected as well, although apparently through different mechanisms.

Using the quantitative counting assay and time-lapse microscopy,, I could show that the rate of formation is reduced in nocodazole treated cells. This data disagrees with the findings of Aplin et al. (Aplin et al., 1992a) in NRK cells where the number of AVis was not affected by nocodazole

treatment. A possible reason for this apparent discrepancy may be the time point of nocodazole addition as discussed above. It is likely that autophagosome formation is faster than the depolymerisation of the microtubule network, necessitating pre-treatment.

My data suggest that microtubules facilitate formation, but are not absolutely required for it. It is currently unclear why microtubules are needed for efficient formation. Hamasaki et al. (Hamasaki et al., 2003) showed that components of the COPII coat and a functioning early secretory pathway are necessary for autophagosome formation in yeast. This was further confirmed by Reggiori et al. (Reggiori et al., 2004b), who hypothesised that both, ER and Golgi, could be the membrane source for forming autophagosomes. In addition, Reggiori ruled out that endosomes are involved in autophagosome formation in yeast. In mammalian cells, the ER has also been implicated in autophagosome formation (Dunn, 1990a). Vesicular transport from the ER to the Golgi complex via COPII coats is microtubule dependent. Disruption of microtubules with nocodazole has been shown to disturb the structure of the Golgi and transitional ER (tER), leading to a clustering of normally relatively immobile tER sites adjacent to immediate-sized Golgi structures (Hammond and Glick, 2000). It is possible that under starvation conditions, when the rate of autophagy is stimulated, a perturbation in the trafficking between the tER and Golgi could lead to a reduction in the rate of autophagosome formation by disturbing membrane trafficking to the PAS; while in full medium, the supply of membranes to the PAS might be sufficient to meet the demand for autophagosome formation. My data with nocodazole supports the proposal that

the autophagosome is derived from a membrane source that requires transport from the ER to the Golgi (Reggiori et al., 2004b).

Vinblastine treatment of hepatocytes, on the other hand, had a completely different effect on the number of autophagosomes. After 120 minutes in ES or FM with vinblastine, hepatocytes had approximately two times more autophagosomes than untreated cells starved in ES and at least 5 times more autophagosomes than untreated cells in FM. Cells starved in ES had approximately 3 times more vesicles than cells in FM. These changes are similar to those seen by Seglen et al. (Kovacs et al., 1982) of 6.4-fold and 2.5-fold, in FM with vinblastine and in ES, respectively. Similar increases in the number of autophagosomes after vinblastine treatment have also been seen in CHO cells (Munafo and Colombo, 2001) and in murine exocrine pancreatic cells (Rez et al., 1991).

The high number of autophagosomes in cells pre-treated with vinblastine suggests that vinblastine can induce autophagy even in full medium. The number of autophagosomes doubled within 15 minutes after the addition of vinblastine, indicating that the inducing effect of vinblastine is independent of microtubules as the stimulation occurred before all the microtubules were depolymerised. Interestingly, addition of vinblastine to ES accelerated the rate of formation at early time points. This could either mean that vinblastine-induced autophagy utilizes a pathway that is independent from starvation-induced autophagy, and both pathways have a cumulative effect on the formation rate, or alternatively that vinblastine increases the signalling through the starvation-induced pathway.

To address the question if vinblastine-stimulated autophagosome formation requires Atg proteins, we used siRNA knockdown to deplete Atg5 and Atg6 in HEK293A cells, both of which have been shown to be required for autophagy (Kuma et al., 2004; Liang et al., 1999; Qu et al., 2003; Yue et al., 2003). Both siRNA Smartpools inhibited vinblastine-induced autophagy, showing that the normal autophagy machinery is required. Interestingly wortmannin completely blocked vinblastine induced autophagy, suggesting that vinblastine acts upstream of PI3 kinases.

I then asked if vinblastine can affect mTOR activity. mTOR has been shown to be essential for autophagy in yeast and in several cell lines (Gutierrez et al., 2004a; Ravikumar et al., 2004), but not in hepatocytes (Kanazawa et al., 2004)(see also Chapter 4). Intriguingly, vinblastine treatment resulted in the inactivation of mTOR, however, with kinetics that were different to the vinblastine-induced stimulation. After 30 minutes pre-treatment cells had already a large number of autophagosomes, although mTOR was still active at that time point.

In HEK293A cells, which are rapamycin-sensitive in comparison to hepatocytes, vinblastine had no affect on mTOR activity. Thus, in both a rapamycin-insensitive and rapamycin-sensitive cell, vinblastine stimulated formation by a mTOR independent mechanism. This suggests that vinblastine stimulates autophagy either downstream of mTOR or via a novel yet to be identified signalling pathway. Further work will be required to identify the target and signalling pathway of vinblastine.

As an aside it is interesting to note that in HEK293A cells, where starvation-induced autophagy is seemingly mTOR-dependent, autophagy can

also occur in the presence of active mTOR. One explanation, as mentioned above, for this could be that vinblastine acts either downstream or on a parallel pathway and therefore inhibition of mTOR and the modulation of the signalling pathway downstream of mTOR is not required to induce autophagy. Alternatively, however, it is also possible that rapamycin-treatment of HEK293A cells, at least at high concentrations, has in addition to its specific effects on mTOR other unspecific effects on other signalling pathways, which could then increase the rate of autophagosome formation.

6 IN VITRO RECONSTITUTION OF AUTOPHAGOSOME FUSION

6.1 Aim

In yeast autophagosomes fuse directly with the vacuole. In mammalian cells on the other hand, autophagosomes fuse with compartments of the endocytic system, thereby acquiring lysosomal membrane proteins and proton pumps needed for the acidification, as well as degradative enzymes. However, it is not clear what the preferred endosomal compartment for fusion is. Depending on the cell type there is evidence supporting both a fusion event with early endosomes (Berg et al., 1998) and late endosomes (Berg et al., 1998; Punnonen et al., 1993; Tooze et al., 1990) as well as with lysosomes (Lawrence and Brown, 1992). In addition, there is also data that suggests that autophagosomes first acquire proton pumps and membrane proteins by fusing with small endosome derived vesicles before fusing with late endosomes (Dunn, 1990b; Punnonen et al., 1993).

I therefore decided to develop an *in vitro* fusion assay to firstly identify the fusion partner(s) of autophagosomes and secondly to investigate which proteins are involved in the fusion reaction, with special regards to the SNARE and Rab proteins involved in the homotypic and heterotypic fusion events of late endocytic compartments. In the following chapter I will discuss the underlying principle of the fusion assay and the progress I made to date in setting up the assay.

6.2 Underlying principle of the *in vitro* fusion assay

My *in vitro* fusion assay is based on the widely used approach of content mixing between purified autophagosomes and purified compartments of the endo-lysosomal system (see Figure 6.1). The method I developed is based on published *in vitro* fusion assays, which were used for investigating endosome – lysosome fusion and endosome – endosome fusion (Bright et al., 1997; Clague et al., 1994; Colombo et al., 1991; Colombo et al., 1992; Diaz et al., 1988; Ellis et al., 1992; Mills et al., 1998; Mullock et al., 1998).

In order to measure the extent of fusion, I internalized specific markers into endosomes, as well as lysosomes. Since the organelles I want to load are acidic, the markers had to be resistant to degradation by lysosomal hydrolases. Initially, I therefore decided to use a system based on biotin-HRP and avidin. In order to label endosomes I internalized biotin-HRP as a fluid phase marker into hepatocytes (see Chapter 0). To label autophagosomes I over-expressed avidin in my hepatocytes, using an adenoviral expression system (see also Chapter 6.3). I then induced autophagy by starving the cultured hepatocytes in ES, to allow the sequestration of the cytosolic avidin into forming autophagosomes. However, it became quickly apparent that the over-expressed avidin did not bind biotin and was toxic for the hepatocytes (data not shown). Since avidin is a tetramer and the monomers bind biotin with a lower affinity, I decided to modify the system and use streptavidin instead. To facilitate targeting to autophagosomes I tagged streptavidin with LC3 at the C-terminus. In addition, I added the sequence for the HA epitope at the N-terminus (HA-SV-LC3).

I then purified different endosomal populations (Chapter 0) and autophagosomes (Chapter 6.3), containing their respective markers and attempted to reconstitute fusion *in vitro*, by adding cytosol and ATP-regenerating system to the purified vesicles. As an alternative to biotin-HRP internalization I used anti-HA antibodies.

To assess the extent of fusion I then measured the meeting of the two internalized markers. In case of the biotin-HRP internalization I immunoprecipitated HA-SV-LC3 using an anti-HA antibody and measured HRP activity. In the case of the anti-HA antibody internalization I added protein G-sepharose beads to the lysed fusion reactions and then immunoblotted for LC3. The following sections summarize my progress to date.

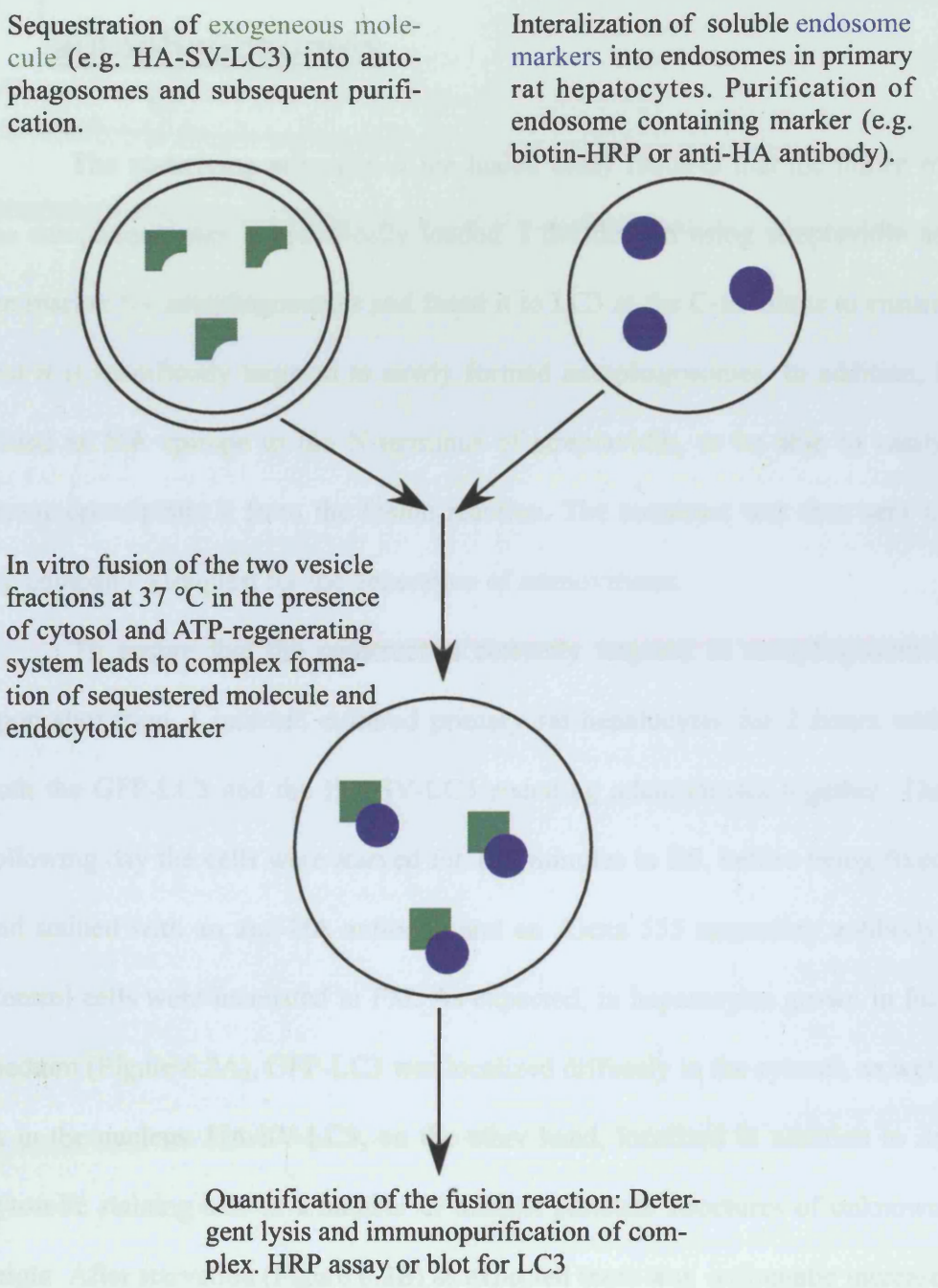

Figure 6.1: In vitro fusion assay scheme:

6.3 HA-SV-LC3 localizes to purified autophagosomes

The underlying principle of the fusion assay requires that the lumen of the autophagosomes is specifically loaded. I decided on using streptavidin as the marker for autophagosomes and fused it to LC3 at the C-terminus to ensure that it is specifically targeted to newly formed autophagosomes. In addition, I added an HA epitope to the N-terminus of streptavidin, to be able to easily immunoprecipitate it from the fusion reaction. The construct was then sent to the company Viraquest for the generation of adenoviruses.

To ensure that the construct is correctly targeted to autophagosomes upon starvation, I infected cultured primary rat hepatocytes for 2 hours with both the GFP-LC3 and the HA-SV-LC3 encoding adenoviruses together. The following day the cells were starved for 120 minutes in ES, before being fixed and stained with an anti-HA antibody and an Alexa 555 secondary antibody. Control cells were incubated in FM. As expected, in hepatocytes grown in full medium (Figure 6.2A), GFP-LC3 was localized diffusely in the cytosol, as well as in the nucleus. HA-SV-LC3, on the other hand, localized in addition to its cytosolic staining also to a number of distinct punctate structures of unknown origin. After starvation (Figure 6.2B) as expected there was a dramatic increase in autophagosomes labelled with GFP-LC3. Most of the bigger structures perfectly co-localized with HA-SV-LC3, however, there were also some smaller GFP-positive structures which did not co-localize with HA-SV-LC3 (Figure 6.2B). One possible explanation for this could be that these GFP-LC3-

positive vesicles represent amphisomes or AVds and that GFP is more stable than the HA tag.

To further confirm that HA-SV-LC3 localizes correctly and to generate material for the fusion assay, I purified autophagosomes from cultured primary rat hepatocytes, expressing HA-SV-LC3, using a method established by Stromhaug et al. (Stromhaug et al., 1998). As a control I used hepatocytes expressing GFP-LC3. To get enough material for the purification, I seeded the cells from half a liver on five 625 cm^2 tissue culture plates. This equals approximately 2.5 x 10^8 cells in total. The following day the cells were shifted to ES containing vinblastine for 120 minutes to induce autophagosome formation. I subsequently generated a PNS and enriched the autophagosomes on a nycodenz step gradient as described in Chapter 2.2.8.4. The addition of vinblastine should ensure that, firstly, autophagosome formation is highly induced and secondly, that most autophagosomes are AVis (see Chapter 5.3).

To verify that I had obtained autophagosomes and that HA-SV-LC3 localizes to the purified autophagosomes, I collected samples at each step of the purification and blotted them against GFP or HA, respectively (Figure 6.3). In the PNS I found both GFP-LC3 forms, GFP-LC-I and GFP-LC3-II, showing that autophagy was strongly induced. After the gradient, on the other hand, the cytosol fraction (top of gradient) only contained the soluble GFP-LC-I, but no membrane bound GFP-LC3-II, while the putative autophagosome fraction contained only the GFP-LC3-II form, showing that it is highly enriched in autophagosomes. HA-SV-LC3 behaved similarly to GFP-LC3. In the cytosolic fraction I could only find the HA-SV-LC3-I form while the autophagosome fraction contained both LC3 forms.

The fact that HA-SV-LC3-II localized to the same region of the gradient as GFP-LC3-II, shows that HA-SV-LC3 can bind to autophagosomes. In addition, the autophagosome fractions also contained high amounts of HA-SV-LC-I. This might be sequestered cytosolic HA-SV-LC3-I, which can be seen on the blots, perhaps due to a higher HA-SV-LC3 than GFP-LC3 expression. In addition, HA-SV-LC3-I can also be found in the mitochondrial fraction. It is possible that some streptavidin binds to mitochondrial proteins, such as monocarboxylate transporter 1 (MCT1), which is responsible for biotin uptake into mitochondria (Daberkow et al., 2003). In the mitochondria biotin binds as a co-factor to mitochondrial enzymes, such as pyruvate-carboxylase.

In summary these data suggest that HA-SV-LC3 is targeted correctly to newly formed autophagosomes and that I can obtain highly enriched autophagosomes from cultured primary rat hepatocytes in order to use them for the *in vitro* fusion assays.

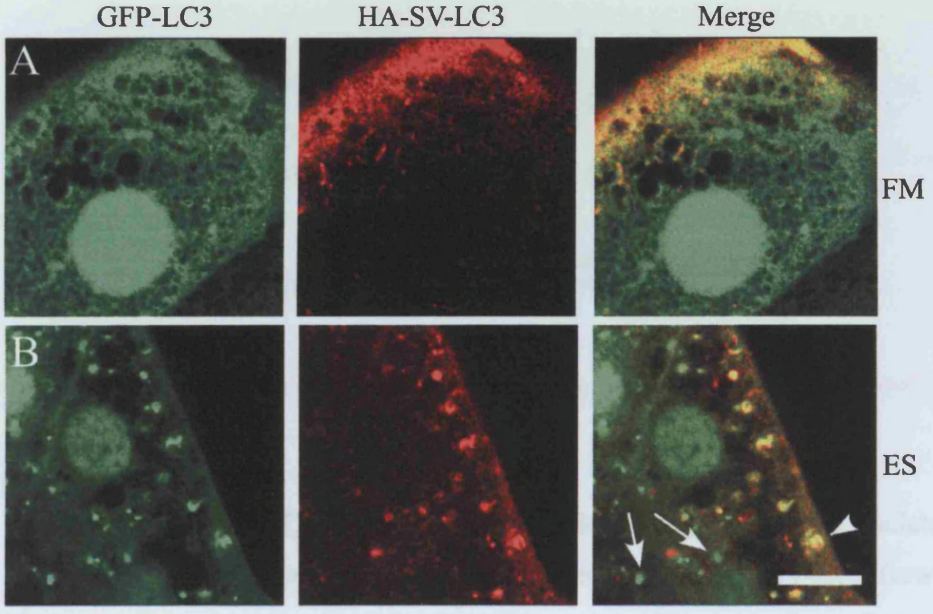

Figure 6.2: HA-SV-LC3 localizes to autophagosomes. Hepatocytes were infected with adenoviruses encoding GFP-LC3 and HA-SV-LC3 and cultured overnight. The following day cells were either incubated in FM (A) or ES (B) for 120 minutes, before being fixed. HA-SV-LC3 was stained using an anti-HA antibody and Alexa555 secondary antibodies. Arrowhead indicates an autophagosome that is GFP-LC3 and HA-SV-LC3-positive. Arrows indicate autophagosomes that contain no detectable HA-SV-LC3. Bar equals 10 μm.

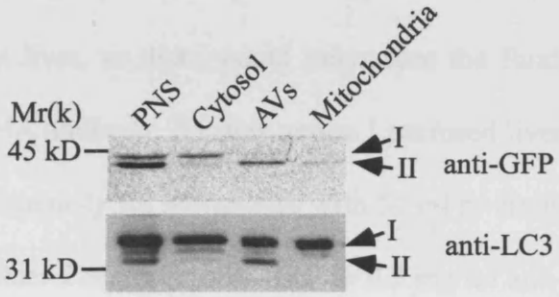

Figure 6.3: HA-SV-LC3-II localizes to purified autophagosomes. Isolated hepatocytes were infected with GFP-LC3 (upper blot) or HA-SV-LC3 (lower blot) encoding adenoviruses and cultured overnight. The next day cells were starved for 120 minutes in the presence of 50 μM vinblastine and autophagosomes were purified as described in Materials and Methods. 1/700th or 1/400th, of each fraction was loaded on a SDS-PAGE gel and analysed by blotting with either an anti-GFP antibody or an anti-LC3 antibody, respectively.

6.4 Endosome Purification

Having established that HA-SV-LC3 localizes to autophagomes and that I can obtain those autophagosomes from cultured primary rat hepatocytes, I decided to develop a method to generate highly enriched endosome fractions.

I chose to modify a published protocol by Ellis et al. (Ellis et al., 1992) for homogenized rat liver, so that I could internalize the fluid phase markers biotin-HRP or anti-HA antibody. For this reason I perfused livers of ad-libidum fed Wistar rats, continuously for 30 minutes with 50 ml re-circulating perfusion buffer, containing either 2 mg/ml biotin-HRP or 0.2 mg/ml anti-HA antibody. I then homogenized the liver and separated the endosomes on a continuous 1 % - 22% Ficoll gradient as described in Chapter 2.2.8.3.

To identify the different endosomal population I compared the localization of different markers, as well as the internalized anti-HA antibody, across the gradient (Figure 6.4 : Endosome purification). Early endosomes were identified by the presence of EEA1 and could be found in fractions 27 – 32. Late Endosomes were identified by the presence of the cation-independent Mannose-6-phosphate receptor (CI-MPR) and Rab7 in the fractions 19 – 26, while lysosomes, identified by Lamp2, were in fraction 4 – 9, just above the nycodenz cushion. The anti-HA antibody was found in all endosomal population after the 30 minute pulse, peaking in fractions 25 – 26. The above described fractions were then collected and the endosomes were further concentrated by centrifugation, before being snap-frozen in liquid nitrogen.

Since the peaks of CI-MPR and Rab7, which should represent late endosomes, were slightly shifted I collected the fractions 25 – 26 and 19 – 24 separately.

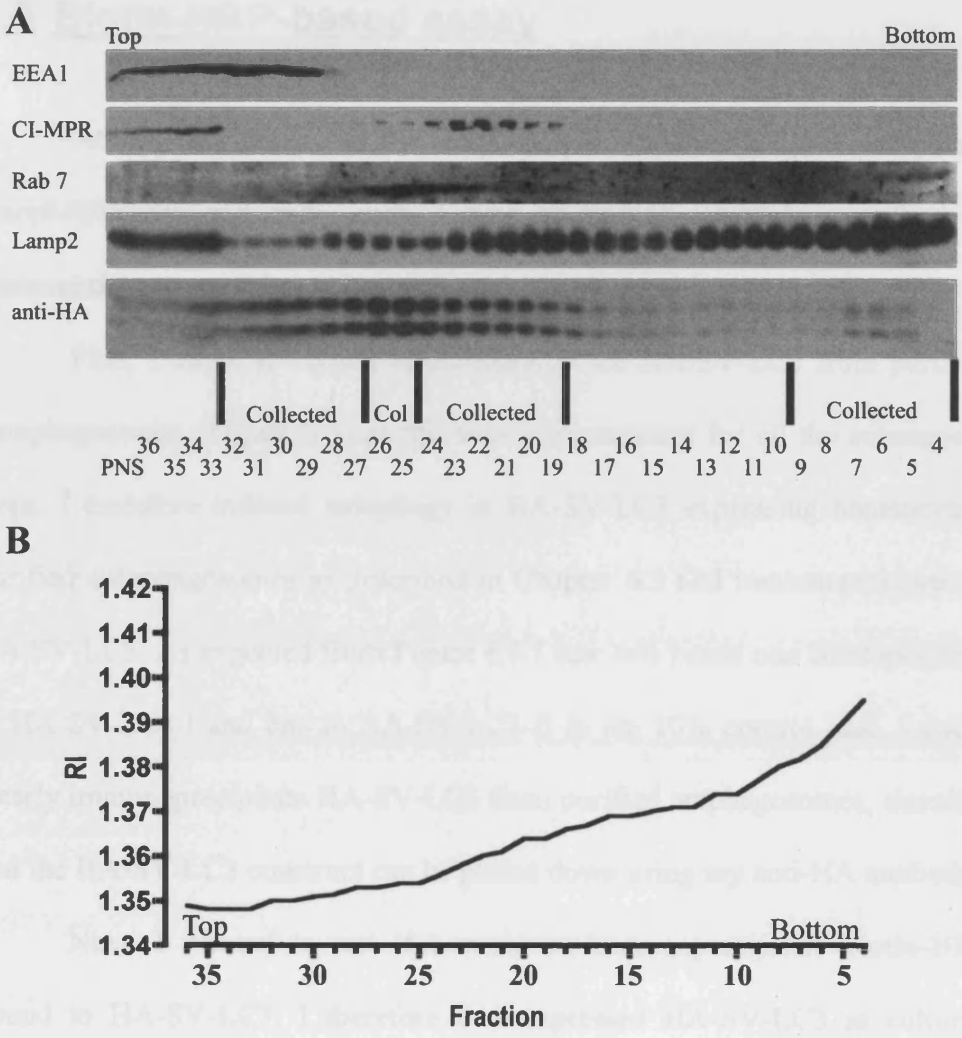

Figure 6.4: Endosome purification (A) anti-HA antibody (0.2 mg/ml) was internalized for 30 minutes into perfused liver rat liver. Endosomes were purified on a 1%-22% Ficoll gradient as described in Materials and Methods. 36 fractions were collected from each gradient and fractions 4-36 were blotted with the following antibodies: EEA1 (early endosomes), CI-MPR (TGN and late endosomes), Rab 7 (late endosomes), Lamp2 (lysosomes) and an HRP-conjugated anti-mouse antibody to detect internalized anti-HA. Fractions collected for use in the *in vitro* fusion assay are indicated. (B) Refractive Index of fractions from endosome preparation gradient.

6.5 Biotin-HRP-based assay

After I had developed the techniques to specifically label and purify autophagosomes and endosomes, I next wanted to establish a method to measure the extent of fusion between those compartments.

First, I tested if I could immunoprecipitate HA-SV-LC3 from purified autophagosomes (Figure 6.5) as this was a requirement for all the subsequent steps. I therefore induced autophagy in HA-SV-LC3 expressing hepatocytes, purified autophagosomes as described in Chapter 6.3 and immunoprecipitated HA-SV-LC3. As expected from Figure 6.3 I saw two bands one corresponding to HA-SV-LC3-I and one to HA-SV-LC3-II in the 10% control lane. I could clearly immunoprecipitate HA-SV-LC3 from purified autphagosomes, showing that the HA-SV-LC3 construct can be pulled down using my anti-HA antibody.

Next, I wanted to test if I could co-immunoprecipitate biotin-HRP bound to HA-SV-LC3. I therefore over-expressed HA-SV-LC3 in cultured primary rat hepatocytes and generated a PNS. In parallel, I internalized 2 mg/ml biotin-HRP into cultured hepatocytes for 30 minutes, washed the cells and generated a second PNS. The two lysates were mixed and solubilized with 5x TNTE to allow internalized biotin to bind to the over-expressed HA-SV-LC3. HA-SV-LC3 was then immunoprecipitated with an anti-HA antibody and the HRP activity was measured in a spectrophotometer using a colorimetric assay (Figure 6.6). As a control I used either lysates from non-infected cells or from cells which had not been incubated with biotin-HRP in the medium. I could clearly measure HRP activity in the complete reaction mix after the

immunoprecipitation. The controls had no HRP activity or a reduced amount of HRP activity, indicating that biotin-HRP specifically binds the HA-SV-LC3 construct and retains its activity during the time course of the experiment. Additionally, the presence of some background HRP activity in the controls suggest that biotin-HRP either sticks to the beads or the Eppendorf tube.

Since I used detergent-solubilized lysates for the experiments above, I next wanted to test if I can co-immunoprecipitate biotin-HRP in a mock fusion assay scenario (Figure 6.7). Over-expressed HA-SV-LC3 is largely cytosolic and only a comparatively small fraction binds to autophagosomes (see lower blot in Figure 6.3). I anticipated that using purified autophagosomes in contrast to lysates, therefore might potentially result in less biotin-HRP pulled down. Thus, I purified endosomes and autophagosomes, containing biotin-HRP and HA-SV-LC3, respectively. I then mixed 100 µl autophagosomes with 100 µl late endosomes or lysosomes with or without cytosol, and added anti-HA antibody to pull down biotin-HRP via HA-SV-LC3. To lyse the membranes I added 5x TNTE. Streptavidin-agarose was used to directly pull down biotin-HRP. As a control I used 10 µl and 50 µl late endosomes and lysosomes. However, I could not measure any HRP activity when I immunoprecipitated HA-SV-LC3 with an anti-HA antibody in the presence of cytosol. In the samples were I used streptavidin-agarose a low amount of HRP-activity was detected, approximately a quarter of the activity in 50 µl late endosomes or lysosomes. The HRP activity, pulled down with the streptavidin-agarose from the fusion mixture containing late endosomes and autophagosomes, was higher when I omitted cytosol, however, this was not the case when the lysosome fraction was used.

These results indicate that under fusion assay conditions, I can not co-immunoprecipitate HRP activity. It is possible that endogenous biotin binds HA-SV-LC3 and thereby at least partially prevents biotin-HRP binding. Using streptavidin-agarose instead, I could pull down some internalized HRP activity in the presence of cytosol, but even then it was only about 12% of the activity present in the total, suggesting that most internalized biotin-HRP does either not bind the added streptavidin, possibly due to endogenous biotin, or because HRP loses its enzymatic activity during the pull down, which, however, seems unlikely. Together these results suggest that the biotin-HRP/HA-SV-LC3 system may not suitable for an autophagosome – endosome fusion assay.

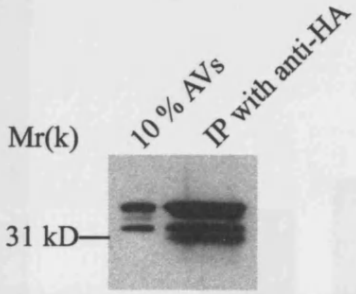

Figure 6.5: HA-SV-LC3 can be immunoprecipitated. Hepatocytes were infected for 2 hours with adenoviruses encoding HA-SV-LC3 and cultured over night. The following day autophagosomes were isolated and HA-SV-LC3 was immunoprecipitated from 300 µl autophagosomes with anti-HA antibodies, bound to protein-G, and blotted for LC3.

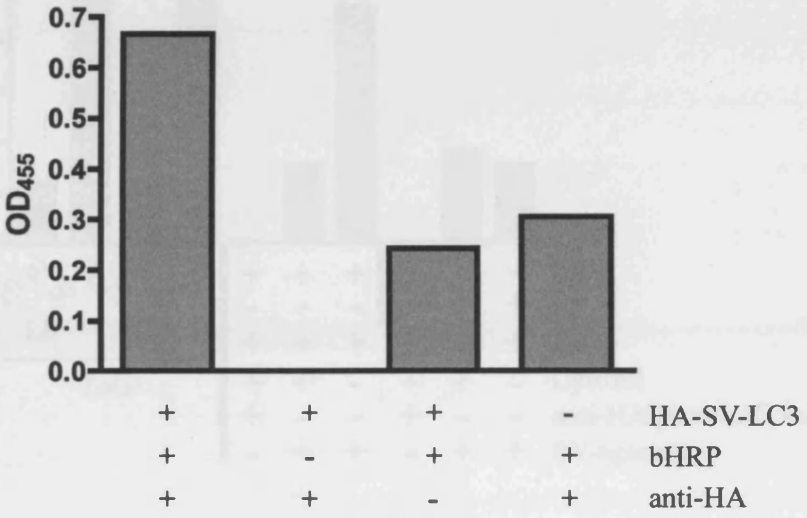

Figure 6.6: HA-SV-LC3 pulls down biotin-HRP from lysates. Hepatocytes expressing HA-SV-LC3 were used to prepare a PNS. In addition, 2 mg /ml biotin-HRP were internalized into a second culture of hepatocytes for 30 minutes before the cells were used to generate a PNS. Equal volumes of both lysates were mixed in the presence of anti-HA, protein-G beads and 5x TNTE and incubated for 2 hours at 4° C on a rotator. Beads were washed 3 x in PBS and HRP activity was measured in as described in Materials and Methods. As controls either the HA-SV-LC3 lysate or the biotin-HRP lysate were replaced with lysates from uninfected hepatocytes or the anti-HA antibody was omitted. Data is the average of two replicates.

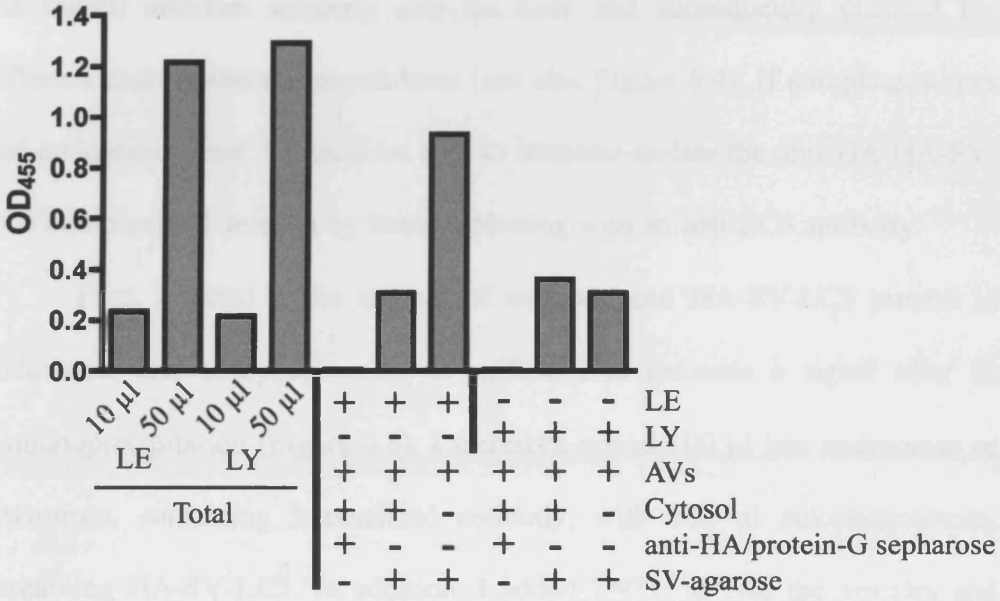

Figure 6.7: HRP activity can not be pulled down in a mock fusion assay. biotin-HRP was internalized into rat liver and late endosomes (LE) and lysosomes (LY) were isolated as described in Materials and Methods. In parallel autophagosomes (AVs) were purified from HA-SV-LC3 expressing hepatocytes. 100 µl of the different endosomal populations were mixed with 100 µl autophagosomes in the presence or absence of 100 µl rat liver cytosol (20 mg/ml) and 5x TNTE to lyse all membranes. The mixture was then incubated for 2 hours at 4° C on an end over end rotator with either anti-HA antibody and protein-G sepharose or SV-agarose beads. The beads were washed 3x with PBS and HRP activity was measured. As a control we measured the total HRP activity from 10 µl and 50 µl late endosomes or lysosomes. Data is the mean of two replicates.

6.6 HA-antibody based assay

Since the biotin-HRP based assay turned out to be problematic I decided to try an alternative approach. Instead of internalizing biotin-HRP I internalized 0.2 mg/ml anti-HA antibody into rat liver and subsequently purified the different endo-lysosomal populations (see also Figure 6.4). If autophagosomes and endosomes fuse, I should be able to immuno-isolate the anti-HA-HA-SV-LC3 complex and detect it by immunoblotting with an anti-LC3 antibody.

First, I tested if the amount of antibody and HA-SV-LC3 present in endosomes and autophagosomes is sufficient to generate a signal after an immunoprecipitation (Figure 6.8). I therefore mixed 100 µl late endosomes or lysosomes, containing internalized antibody, with 100 µl autophagosomes, containing HA-SV-LC3. In addition, I added TNTE to lyse the vesicles and allow content mixing. This mixture was incubated at 4 °C for 2 hours in the presence of protein-G sepharose beads, before the beads were washed 3x with PBS and bound protein was eluted by boiling in sample buffer and analysed by immunoblotting with an anti-LC3 antibody. The amount of antibody present in late endosomes and lysosomes was clearly high enough to immunoprecipitate HA-SV-LC3 from autophagosomes. However, the HA-SV-LC3 signal obtained from the lysosomes was much lower than in the late endosomes. This was also apparent in the controls that were not immunoprecipitated, however, the difference between the late endosome and lysosome sample was less pronounced (lanes 2 and 3 vs. 5 and 6, Figure 6.8). It is possible that HA-SV-LC3, as well as the anti-HA antibody, are being partially degraded by

lysosomal enzymes after the addition of TNTE, which then results in a loss of signal. This is a potential problem for the *in vitro* fusion assay as it can make the assessment of the fusion efficiency difficult. For this reason I decided to add lysosomal protease inhibitors to the next experiment.

With my preliminary data suggesting that the read out of the assay is working, I then carried out an *in vitro* fusion assay. I therefore isolated autophagosomes from HA-SV-LC3 expressing hepatocytes and purified late endosomes, containing internalized anti-HA antibody. The two vesicle populations were mixed in the presence of cytosol, ATP-regenerating system and HA peptide, in order to block the antibodies released from broken endosomes (Figure 6.9).

The reaction was subsequently incubated at 37 °C or 4 °C for 45 minutes, followed by the addition of TNTE and protein-G beads to pull down HA-SV-LC3. Fusion was analysed by immunoblotting the immunoprecipitate with an anti-LC3 antibody. Fusion was sensitive to temperature; no LC3 was detected when samples where incubated at 4 °C, suggesting that fusion did not occur. In addition, effective fusion was dependent on cytosol. However, fusion occurred efficiently in the absence of an ATP-regenerating system. This was unexpected since fusion between late endosomes and lysosomes, for instance, requires ATP (Mullock et al., 1994). It is however conceivable that the desalted cytosol still contained trace-amounts of ATP, sufficient to drive fusion. If this is the case, addition of apyrase, an ATP diphosphohydrolase, could be used to efficiently deplete ATP.

As a additional control I omitted the HA peptide in the reaction mix. This should give the strongest possible signal after the detergent lysis and the

immunoprecipitation and should therefore constitute "100 % fusion". Unexpectedly, this did not lead to an increase in the amount of immunoprecipitated HA-SV-LC3, suggesting that the amount of anti-HA loaded endosomes was limiting.

In summary, these results suggest that in vitro reconstitution of fusion between autophagosomes and endosomes may be possible. Using internalized anti-HA antibody and HA-SV-LC3 as markers for endosomes and autophagosomes, respectively, I could immunoprecipitate HA-SV-LC3 when the two vesicle populations were incubated at 37 °C in the presence of cytosol and ATP regenerating system. Cytosol was required for the effective meeting of the two markers. Omitting the ATP regenerating system unexpectedly had no influence on the meeting of the markers. Together these data suggests that I have developed an *in vitro* fusion assay which is suitable, once optimized, to analyse autophagosome fusion and to first, identify the fusion partner(s) of autophagosomes and second, identify the proteins regulating fusion.

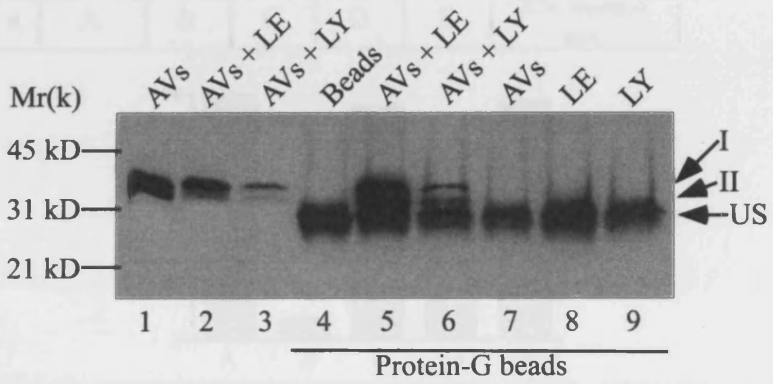

Figure 6.8: Anti-HA antibody internalized into endosomes can immunoprecipitate HA-SV-LC3 from purified autophagosomes. Autophagosomes (AVs) were purified from HA-SV-LC3 expressing hepatocytes and 100 µl were mixed with either 100 µl late endosomes (LE) or 100 µl lysosomes (LY), containing internalized anti-HA antibody and protein-G sepharose beads (lanes 5 and 6). Membranes were lysed by the addition of 5 x TNTE. Samples were incubated for 2 hours at 4° C on a rotator and the immunoprecipitate was washed 3 x with PBS and analysed by immunoblotting with an anti-LC3 antibody. As a control 50 µl AVs (lane 1) or 50 µl of mixed AVs + late endosomes (lane 2) or lysosomes (lane 3) were loaded. Additional controls included protein-G sepharose beads alone (lane 4) and immunoprecipitations from 100 µl AVs or LE or LY with protein-G sepharose beads (lanes 7-9). (I) HA-SV-LC3-I, (II) HA-SV-LC3-II, (US) indicates unspecific band, which most likely is protein-G eluted from the sepharose beads.

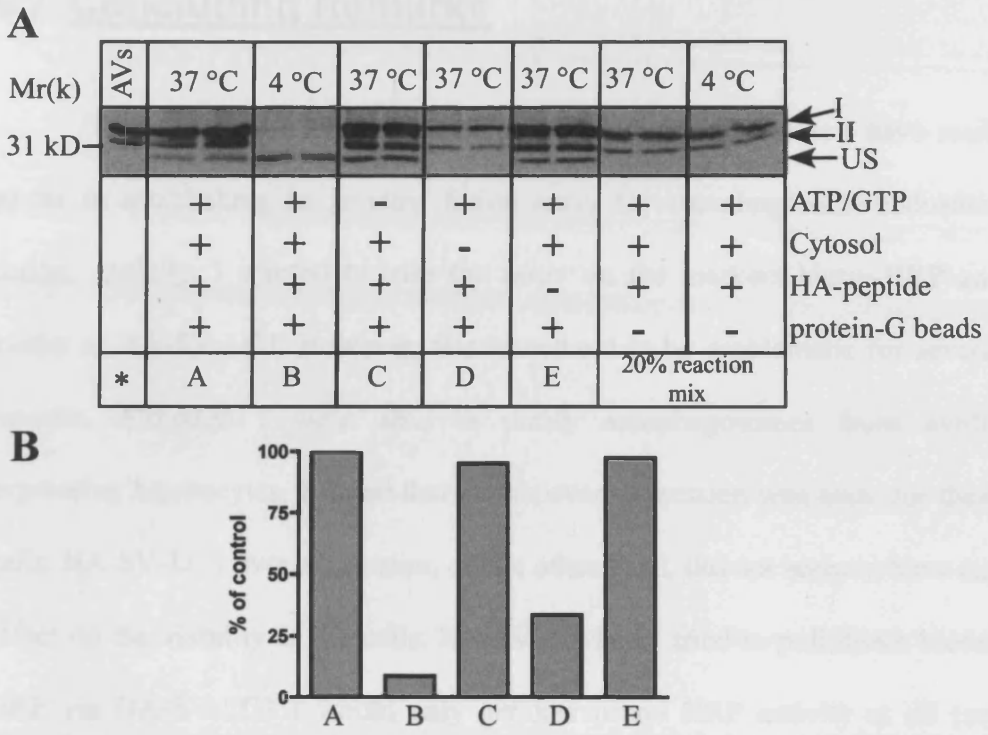

Figure 6.9: Late endosomes and autophagosomes fuse in a temperature and cytosol dependent manner. A) *In vitro* fusion assay between purified late endosomes, containing anti-HA antibody and autophagosomes purified from HA-SV-LC3 expressing hepatocytes. Endosomes were pelleted and either resuspended in rat liver cytosol or in STM buffer. 100 µl endosomes were mixed with 100 µl autophagosomes, 25 µl HA-peptide (1 mg/ml) and 10 µl ATP regenerating system, containing GTP (lane A and B). In control samples either the ATP regenerating system, the cytosol or the HA-peptide was replaced with STM buffer or water (lane B to E). The reactions were incubated either at 37 °C or 4 °C for 45 minutes before the addition of protein-G sepharose. The samples were analysed by immunoblotting with an anti-LC3 antibody. (*) 30% autophagosomes. As a control, parallel complete samples, incubated at 37 °C or 4 °C, were loaded directly without prior immuno-precipitation (20% of total reaction) (lane F and G). B) Densitometric quantification of both immunoprecipitated HA-SV-LC3 (I and II) bands from (A) with ImageJ software. Bars are the average of 2 replicates. (I) HA-SV-LC-I, (II) HA-SV-LC3-II, (US) non-specific band.

6.7 Concluding Remarks

There are several important points regarding the progress I have made so far in establishing an *in vitro* fusion assay for autophagosome-endosome fusion. Initially, I wanted to base the assay on the markers biotin-HRP and avidin or HA-SV-LC3. However, this turned out to be problematic for several reasons. Although I were able to purify autophagosomes from avidin expressing hepatocytes, I found that avidin over expression was toxic for these cells. HA-SV-LC3 over expression, on the other hand, did not seem to have any effect on the viability of the cells. However, when I tried to pull down biotin-HRP via HA-SV-LC3 I would only get low or no HRP activity at all (see Figure 6.7). To ensure that the low signal was not due to a loss of HRP activity during the time course of the experiment, I measured the HRP activity in endosomes directly (Figure 6.7). The results clearly showed that although there was strong HRP activity present in the endosomes, I was not able to pull down a significant amount of this activity, suggesting that the binding of biotin-HRP to HA-SV-LC3 is impaired. Several reasons are feasible for this. Liver is a tissue with high biotin levels. It is therefore possible that endogenous biotin binds to most of the newly synthesized HA-SV-LC3, thereby making it unavailable for binding biotin-HRP. I thus tried to grow the hepatocytes in biotin-free growth medium, however, this did not improve the binding between biotin-HRP and HA-SV-LC3 (data not shown). Alternatively, it is possible that streptavidin can not bind biotin so well because it is tagged on both sides with HA and LC3, or that the amount of HA-SV-LC3, present in autophagosomes, is too little to pull down significant amounts of biotin-HRP. The latter is unlikely,

however, because using streptavidin-agarose beads and unlabeled autophagosomes, instead of HA-SV-LC3 containing autophagosomes, only approximately $1/8^{th}$ of the total HRP activity present in endosomes was bound (Figure 6.7). The binding capacity of the streptavidin-agarose beads for biotin, should have been large enough to pull down all of the biotin-HRP present in the endosomes, assuming that there is no endogenous biotin present.

Having been unable to establish a read-out using biotin-HRP and HA-SV-LC3 for my proposed fusion assay, I decided to try an alternative approach. Instead of biotin-HRP I internalized anti-HA antibody into endosomes. This approach proved to be more promising because I could immunoprecipitate enough HA-SV-LC3 with the anti-HA antibody to detect the LC3 by immunoblotting the precipitates with an LC3 antibody (Figure 6.8). After those initial and encouraging results, I performed a fusion assay between autophagosomes purified from HA-SV-LC3 expressing hepatocytes, which have been starved in ES in the presence of vinblastine, and purified late endosomes, containing internalized anti-HA antibody. I could show that the two markers for endosomes and autophagosomes met in a temperature and cytosol dependent manner, suggesting that I was observing vesicle fusion in this assay. Unexpectedly, however, omitting the ATP-regenerating system had no effect on the meeting of the markers. This could either mean that the *in vitro* fusion is independent of ATP or alternatively, that some ATP remained in the cytosol despite it being desalted on PD-10 columns prior to the assay. A possible way to overcome this problem would be to add apyrase to the fusion assay to completely deplete any ATP left in the cytosol

In summary these preliminary results suggest that I have established an *in vitro* fusion assay. The development of this assay is still at an early phase and the assay is not optimized. In particular, the lack of effect after omission of the HA-peptide suggests that the amounts of autophagosomes, endosomes and buffer used, have to be titrated. In addition controls such as electron microscopy to assess the fusion will be necessary. It is feasible that once all the controls have been carried out, it will be possible to use this assay to identify the fusion partner(s) of autophagosomes and to determine which proteins are required for autophagosome fusion, such as SNAREs and Rab proteins and other proteins potentially regulating the fusion between autophagosomes and endosomes.

7 CONCLUDING REMARKS

Although autophagy was observed the first time at least 45 years ago, there is still much to be discovered about the molecular details of autophagosome formation and fusion. Details about the signalling pathways leading to autophagosome formation have only recently begun to be uncovered. On a molecular basis, some of the unanswered questions asked in the field are, where autophagosomes originate from, which signalling pathways are involved in the formation, and how autophagosomes interact with the endosomal system.

In this thesis I have tried to address some of these questions using an experimental system based on cultured primary rat hepatocytes. Here I show that hepatocytes are amenable to genetic manipulation using adenovirus-based transduction methods. To accurately measure autophagosome formation and fusion in fixed and live cells I have developed a light-microscopy based quantification system.

I could show that autophagosome formation in primary hepatocytes is independent of mTOR and can be efficiently inhibited by leucine alone, possibly through a novel plasma-membrane receptor. This might indicate that several signalling pathways are triggered simultaneously to induce autophagy. mTOR is undoubtedly involved in autophagy in many cell types, but the relative importance in relation to other signalling pathways might be different in different cell types and depend on cell and tissue specific protein expression patterns.

Additionally, I investigated the role of microtubules for autophagosome formation and fusion, a topic which has been discussed controversially in the literature. I found that microtubules facilitate autophagosome formation and that they are absolutely required for fusion.

Finally, I developed an *in vitro* fusion assay, with the aim to understand autophagosome maturation and in particular to identify and characterize the protein-machinery required for the fusion of autophagosomes with endosomes. The development of the assay has reached the stage, where I can reconstitute fusion in a cytosol and temperature dependent manner. Once it has been optimized, the assay will undoubtedly be useful to study autophagosome maturation *in vitro*.

8 REFERENCES

Abeliovich, H., W.A. Dunn, Jr., J. Kim, and D.J. Klionsky. 2000. Dissection of autophagosome biogenesis into distinct nucleation and expansion steps. *J Cell Biol.* 151:1025-34.

Amenta, J.S., M.J. Sargus, and F.M. Baccino. 1977. Effect of microtubular or translational inhibitors on general cell protein degradation. Evidence for a dual catabolic pathway. *Biochem J.* 168:223-7.

Amer, A.O., and M.S. Swanson. 2005. Autophagy is an immediate macrophage response to Legionella pneumophila. *Cell Microbiol.* 7:765-78.

Antonin, W., C. Holroyd, R. Tikkanen, S. Honing, and R. Jahn. 2000. The R-SNARE endobrevin/VAMP-8 mediates homotypic fusion of early endosomes and late endosomes. *Mol Biol Cell.* 11:3289-98.

Aplin, A., T. Jasionowski, D.L. Tuttle, S.E. Lenk, and W.A. Dunn, Jr. 1992a. Cytoskeletal elements are required for the formation and maturation of autophagic vacuoles. *J Cell Physiol.* 152:458-66.

Aplin, A., T. Jasionowski, D.L. Tuttle, S.E. Lenk, and W.A.J. Dunn. 1992b. Cytoskeletal elements are required for the formation and maturation of autophagic vacuoles. *J Cell Physiol.* 152:458-466.

Arstila, A.U., I.J. Nuuja, and B.F. Trump. 1974. Studies on cellular autophagocytosis. Vinblastine-induced autophagy in the rat liver. *Exp Cell Res.* 87:249-52.

Atlashkin, V., V. Kreykenbohm, E.L. Eskelinen, D. Wenzel, A. Fayyazi, and G. Fischer von Mollard. 2003. Deletion of the SNARE vti1b in mice results in the loss of a single SNARE partner, syntaxin 8. *Mol Cell Biol.* 23:5198-207.

Bennett, M.K., N. Calakos, and R.H. Scheller. 1992. Syntaxin: A synaptic protein implicated in docking of synaptic vesices at presynaptic active zones. *Science.* 257:255-259.

Berg, T.O., M. Fengsrud, P.E. Stromhaug, T. Berg, and P.O. Seglen. 1998. Isolation and characterization of rat liver amphisomes. Evidence for fusion of autophagosomes with both early and late endosomes. *J Biol Chem.* 273:21883-92.

Beugnet, A., A.R. Tee, P.M. Taylor, and C.G. Proud. 2003. Regulation of targets of mTOR (mammalian target of rapamycin) signalling by intracellular amino acid availability. *Biochem J.* 372:555-66.

Blommaart, E.F., J.J. Luiken, P.J. Blommaart, G.M. van Woerkom, and A.J. Meijer. 1995a. Phosphorylation of ribosomal protein S6 is inhibitory for autophagy in isolated rat hepatocytes. *J Biol Chem.* 270:2320-6.

Blommaart, E.F.C., J.J.F.P. Luiken, P.J.E. Blommaart, G.M. van Woerkom, and A.J. Meijer. 1995b. Phosphorylation of Ribosomal Protein S6 Is Inhibitory for Autophagy in Isolated Rat Hepatocytes. *J. Biol. Chem.* 270:2320-2326.

Bock, J.B., H.T. Matern, A.A. Peden, and R.H. Scheller. 2001. A genomic perspective on membrane compartment organization. *Nature.* 409:839-41.

Bottger, G., B. Nagelkerken, and P. van der Sluijs. 1996. Rab4 and Rab7 define distinct nonoverlapping endosomal compartments. *J Biol Chem.* 271:29191-7.

Bright, N.A., M.J. Gratian, and J.P. Luzio. 2005. Endocytic delivery to lysosomes mediated by concurrent fusion and kissing events in living cells. *Curr Biol.* 15:360-5.

Bright, N.A., B.J. Reaves, B.M. Mullock, and J.P. Luzio. 1997. Dense core lysosomes can fuse with late endosomes and are re-formed from the resultant hybrid organelles. *J Cell Sci.* 110 (Pt 17):2027-40.

Byfield, M.P., J.T. Murray, and J.M. Backer. 2005. hVps34 is a nutrient-regulated lipid kinase required for activation of p70 S6 kinase. *J Biol Chem.* 280:33076-82.

Chen, Y.A., and R.H. Scheller. 2001. SNARE-mediated membrane fusion. *Nat Rev Mol Cell Biol.* 2:98-106.

Christoforidis, S., H.M. McBride, R.D. Burgoyne, and M. Zerial. 1999. The Rab5 effector EEA1 is a core component of endosome docking. *Nature.* 397:621-625.

Clague, M.J., S. Urbe, F. Aniento, and J. Gruenberg. 1994. Vacuolar ATPase activity is required for endosomal carrier vesicle formation. *J Biol Chem.* 269:21-4.

Clark, S.L., Jr. 1957. Cellular Differentiation in the kidneys of newborn mice studied with the electron microscope. *J. Cell Biol.* 3:349-362.

Codogno, P., and A.J. Meijer. 2004. Signaling Pathways in mammalian autophagy. *In* Autophagy. D.J. Klionsky, editor. Landes Bioscience/Eurekah.com, Georgetown, Texas. 26-47.

Colombo, M.I., S. Gonzalo, P. Weidman, and P. Stahl. 1991. Characterisation of trypsin sensitive factor(s) required for endosome-endosome fusion. *J. Biol. Chem.* 266:23438-23445.

Colombo, M.I., J.M. Lenhard, L.S. Mayorga, and P.S. Stahl. 1992. Reconstitution of endosome fusion - identification of factors necessary for fusion competence. *Meth. Enz.* 219:32-44.

Contento, A.L., Y. Xiong, and D.C. Bassham. 2005. Visualization of autophagy in Arabidopsis using the fluorescent dye monodansylcadaverine and a GFP-AtATG8e fusion protein. *Plant J.* 42:598-608.

Daberkow, R.L., B.R. White, R.A. Cederberg, J.B. Griffin, and J. Zempleni. 2003. Monocarboxylate transporter 1 mediates biotin uptake in human peripheral blood mononuclear cells. *J Nutr.* 133:2703-6.

Darsow, T., S.E. Rieder, and S.D. Emr. 1997. A multispecificity syntaxin homologue, Vam3p, essential for autophagic and biosynthetic protein transport to the vacuole. *J Cell Biol.* 138:517-29.

Deretic, V. 2005. Autophagy in innate and adaptive immunity. *Trends Immunol.* 26:523-8.

Diaz, R., L. Mayorga, and P. Stahl. 1988. In vitro fusion of endosomes following receptor-mediated endocytosis. *Journal of Biological Chemistry.* 263:6093-100.

Dunn, W.A., Jr. 1990a. Studies on the mechanisms of autophagy: formation of the autophagic vacuole. *J Cell Biol.* 110:1923-33.

Dunn, W.A., Jr. 1990b. Studies on the mechanisms of autophagy: maturation of the autophagic vacuole. *J Cell Biol.* 110:1935-45.

Dunn, W.A., Jr. 1994. Autophagy and related mechanisms of lysosome-mediated protein degradation. *Trends in Cell Biol.* 4:139-143.

Ellis, J., M. Jackman, J. Perez, B. Mullock, and J. Luzio. 1992. Membrane traffic pathways in polarised epithelial cells. *In* Protein Targeting: A practical approach. A.a.W. Magee, T, editor. IRL press, Oxford. UK, Washington. 25-57.

Eskelinen, E.-L. 2005. Maturation of Autophagic Vacuoles in Mammalian Cells. *Autophagy.* 1:1-10.

Eskelinen, E.L. 2004. Macroautophagy in mammalian cells. *In* Lysosomes. S. P, editor. Landes Bioscience/Eurekah.com.

Eskelinen, E.L., A.R. Prescott, J. Cooper, S.M. Brachmann, L. Wang, X. Tang, J.M. Backer, and J.M. Lucocq. 2002. Inhibition of Autophagy in Mitotic Animal Cells. *Traffic.* 3:878-893.

Fasshauer, D., H. Otto, W.K. Eliason, R. Jahn, and A.T. Brunger. 1997. Structural Changes Are Associated with Soluble N-Ethylmaleimide-sensitive Fusion Protein Attachment Protein Receptor Complex Formation. *J. Biol. Chem.* 272:28036-28041.

Feng, Z., H. Zhang, A.J. Levine, and S. Jin. 2005. The coordinate regulation of the p53 and mTOR pathways in cells. *Proc Natl Acad Sci U S A.* 102:8204-9.

Fengsrud, M., E.S. Erichsen, T.O. Berg, C. Raiborg, and P.O. Seglen. 2000. Ultrastructural characterization of the delimiting membranes of isolated autophagosomes and amphisomes by freeze-fracture electron microscopy. *Eur J Cell Biol.* 79:871-82.

Fengsrud, M., N. Roos, T. Berg, W. Liou, J.W. Slot, and P.O. Seglen. 1995. Ultrastructural and immunocytochemical characterization of autophagic vacuoles in isolated hepatocytes: effects of vinblastine and asparagine on vacuole distributions. *Exp Cell Res.* 221:504-19.

Fengsrud, M., M.L. Sneve, A. Overbye, and P.O. Seglen. 2004. Structural aspects of mammalian autophagy. *In* Autophagy. D.J. Klionsky, editor. Landes Biosciences, Georgetown. 11-25.

Frank, A.L., and A.K. Christensen. 1968. LOCALIZATION OF ACID PHOSPHATASE IN LIPOFUSCIN GRANULES AND POSSIBLE AUTOPHAGIC VACUOLES IN INTERSTITIAL CELLS OF THE GUINEA PIG TESTIS. *J. Cell Biol.* 36:1-13.

Gao, X., Y. Zhang, P. Arrazola, O. Hino, T. Kobayashi, R.S. Yeung, B. Ru, and D. Pan. 2002. Tsc tumour suppressor proteins antagonize amino-acid-TOR signalling. *Nat Cell Biol.* 4:699-704.

Garami, A., F.J. Zwartkruis, T. Nobukuni, M. Joaquin, M. Roccio, H. Stocker, S.C. Kozma, E. Hafen, J.L. Bos, and G. Thomas. 2003. Insulin activation of Rheb, a mediator of mTOR/S6K/4E-BP signaling, is inhibited by TSC1 and 2. *Mol Cell.* 11:1457-66.

Gordon, P.B., H. Hoyvik, and P.O. Seglen. 1992. Prelysosomal and lysosomal connections between autophagy and endocytosis. *Biochem J.* 283 (Pt 2):361-9.

Gordon, P.B., G.O. Kisen, A.L. Kovacs, and P.O. Seglen. 1989. Experimental characterization of the autophagic-lysosomal pathway in isolated rat hepatocytes. *Biochem Soc Symp.* 55:129-43.

Gronostajski, R.M., and A.B. Pardee. 1984. Protein degradation in 3T3 cells and tumorigenic transformed 3T3 cells. *J Cell Physiol.* 119:127-32.

Gruenberg, J., G. Griffiths, and K.E. Howell. 1989a. Characterisation of the early endosome and putative endocytic carrier vesicles in vivo and with an assay of vesicle fusion in vitro. *J. Cell Biol.* 108:1301-1316.

Guan, J., P.E. Stromhaug, M.D. George, P. Habibzadegah-Tari, A. Bevan, W.A. Dunn, Jr., and D.J. Klionsky. 2001. Cvt18/Gsa12 Is Required for Cytoplasm-to-Vacuole Transport, Pexophagy, and Autophagy in Saccharomyces cerevisiae and Pichia pastoris. *Mol. Biol. Cell.* 12:3821-3838.

Gutierrez, M.G., S.S. Master, S.B. Singh, G.A. Taylor, M.I. Colombo, and V. Deretic. 2004a. Autophagy is a defense mechanism inhibiting BCG and Mycobacterium tuberculosis survival in infected macrophages. *Cell.* 119:753-66.

Gutierrez, M.G., D.B. Munafo, W. Beron, and M.I. Colombo. 2004b. Rab7 is required for the normal progression of the autophagic pathway in mammalian cells. *J Cell Sci.* 117:2687-97.

Hamasaki, M., T. Noda, and Y. Ohsumi. 2003. The early secretory pathway contributes to autophagy in yeast. *Cell Struct Funct.* 28:49-54.

Hammond, A.T., and B.S. Glick. 2000. Dynamics of transitional endoplasmic reticulum sites in vertebrate cells. *Mol Biol Cell.* 11:3013-30.

Hara, K., Y. Maruki, X. Long, K. Yoshino, N. Oshiro, S. Hidayat, C. Tokunaga, J. Avruch, and K. Yonezawa. 2002. Raptor, a binding partner of target of rapamycin (TOR), mediates TOR action. *Cell.* 110:177-89.

Hara, K., K. Yonezawa, Q.-P. Weng, M.T. Kozlowski, C. Belham, and J. Avruch. 1998. Amino Acid Sufficiency and mTOR Regulate p70 S6 Kinase and eIF-4E BP1 through a Common Effector Mechanism. *J. Biol. Chem.* 273:14484-14494.

Harding, T.M., K.A. Morano, S.V. Scott, and D.J. Klionsky. 1995. Isolation and characterization of yeast mutants in the cytoplasm to vacuole protein targeting pathway. *J Cell Biol.* 131:591-602.

Hayashi, T., H. McMahon, B. Yamasaki, T. Binz, Y. Hata, T.C. Sudhof, and H. Niemann. 1994. Synaptic vesicle membrane fusion complex: action of clostridial neurotoxins on assembly. *EMBO J.* 13:5051-5061.

He, H., Y. Dang, F. Dai, Z. Guo, J. Wu, X. She, Y. Pei, Y. Chen, W. Ling, C. Wu, S. Zhao, J.O. Liu, and L. Yu. 2003. Post-translational modifications of three members of the human MAP1LC3 family and identification of a novel type of modification Of MAP1LC3B. *J Biol Chem.*

Hemelaar, J., V.S. Lelyveld, B.M. Kessler, and H.L. Ploegh. 2003. A single protease, Apg4B, is specific for the autophagy-related ubiquitin-like proteins GATE-16, MAP1-LC3, GABARAP and Apg8L. *J Biol Chem.*

Hirsimaki, P., and L. Pilstrom. 1982. Studies on vinblastine-induced autophagocytosis in mouse liver. III. A quantitative study. *Virchows Arch B Cell Pathol Incl Mol Pathol.* 41:51-66.

Hirsimaki, P., and H. Reunanen. 1980. Studies on vinblastine-induced autophagocytosis in mouse liver. II. Origin of membranes and acquisition of acid phosphatase. *Histochemistry.* 67:139-53.

Hirsimaki, Y., and P. Hirsimaki. 1984. Vinblastine-induced autophagocytosis: the effect of disorganization of microfilaments by cytochalasin B. *Exp Mol Pathol.* 40:61-9.

Hoyvik, H., P.B. Gordon, and P.O. Seglen. 1986. Use of a hydrolysable probe, [14C]lactose, to distinguish between pre- lysosomal and lysosomal steps in the autophagic pathway. *Exp Cell Res.* 166:1-14.

Ichimura, Y., Y. Imamura, K. Emoto, M. Umeda, T. Noda, and Y. Ohsumi. 2004. In Vivo and in Vitro Reconstitution of Atg8 Conjugation Essential for Autophagy. *J. Biol. Chem.* 279:40584-40592.

Ishihara, N., M. Hamasaki, S. Yokota, K. Suzuki, Y. Kamada, A. Kihara, T. Yoshimori, T. Noda, and Y. Ohsumi. 2001. Autophagosome requires specific early Sec proteins for its formation and NSF/SNARE for vacuolar fusion. *Mol Biol Cell.* 12:3690-702.

Iwata, A., B.E. Riley, J.A. Johnston, and R.R. Kopito. 2005. HDAC6 and microtubules are required for autophagic degradation of aggregated huntingtin. *J Biol Chem.* 280:40282-92.

Jacinto, E., R. Loewith, A. Schmidt, S. Lin, M.A. Ruegg, A. Hall, and M.N. Hall. 2004. Mammalian TOR complex 2 controls the actin cytoskeleton and is rapamycin insensitive. *Nat Cell Biol.*

Jager, S., C. Bucci, I. Tanida, T. Ueno, E. Kominami, P. Saftig, and E.L. Eskelinen. 2004. Role for Rab7 in maturation of late autophagic vacuoles. *J Cell Sci.* 117:4837-48.

Jahn, R., and T.C. Sudhof. 1999. Membrane fusion and exocytosis. *Annu. Rev. Biochem.* 68:863-911.

Juhasz, G., and T.P. Neufeld. 2006. Autophagy: a forty-year search for a missing membrane source. *PLoS Biol.* 4:e36.

Kabeya, Y., Y. Kamada, M. Baba, H. Takikawa, M. Sasaki, and Y. Ohsumi. 2005. Atg17 Functions in Cooperation with Atg1 and Atg13 in Yeast Autophagy. *Mol Biol Cell.*

Kabeya, Y., N. Mizushima, T. Ueno, A. Yamamoto, T. Kirisako, T. Noda, E. Kominami, Y. Ohsumi, and T. Yoshimori. 2000. LC3, a mammalian homologue of yeast Apg8p, is localized in autophagosome membranes after processing. *Embo J.* 19:5720-8.

Kabeya, Y., N. Mizushima, A. Yamamoto, S. Oshitani-Okamoto, Y. Ohsumi, and T. Yoshimori. 2004. LC3, GABARAP and GATE16 localize to autophagosomal membrane depending on form-II formation. *J Cell Sci.* 117:2805-12.

Kamada, Y., T. Funakoshi, T. Shintani, K. Nagano, M. Ohsumi, and Y. Ohsumi. 2000. Tor-mediated Induction of Autophagy Via an Apg1 Protein Kinase Complex. *J. Cell Biol.* 150:1507-1513.

Kanazawa, T., I. Taneike, R. Akaishi, F. Yoshizawa, N. Furuya, S. Fujimura, and M. Kadowaki. 2004. Amino acids and insulin control autophagic proteolysis through different signaling pathways in relation to mTOR in isolated rat hepatocytes. *J Biol Chem.* 279:8452-9.

Khairallah, E.A., and G.E. Mortimore. 1976. Assessment of protein turnover in perfused rat liver. Evidence for amino acid compartmentation from differential labeling of free and tRNA-gound valine. *J Biol Chem.* 251:1375-84.

Kihara, A., T. Noda, N. Ishihara, and Y. Ohsumi. 2001. Two Distinct Vps34 Phosphatidylinositol 3-Kinase Complexes Function in Autophagy and Carboxypeptidase Y Sorting in Saccharomyces cerevisiae. *J Cell Biol.* 152:519-530.

Kim, J., W.P. Huang, P.E. Stromhaug, and D.J. Klionsky. 2002. Convergence of multiple autophagy and cytoplasm to vacuole targeting components to a perivacuolar membrane compartment prior to de novo vesicle formation. *J Biol Chem.* 277:763-73.

Kirisako, T., Y. Ichimura, H. Okada, Y. Kabeya, N. Mizushima, T. Yoshimori, M. Ohsumi, T. Takao, T. Noda, and Y. Ohsumi. 2000. The reversible modification regulates the membrane-binding state of Apg8/Aut7 essential for autophagy and the cytoplasm to vacuole targeting pathway [In Process Citation]. *J Cell Biol.* 151:263-76.

Klionsky, D.J. 2005. The molecular machinery of autophagy: unanswered questions. *J Cell Sci.* 118:7-18.

Klionsky, D.J., J.M. Cregg, W.A. Dunn, S.D. Emr, Y. Sakai, I.V. Sandoval, A. Sibirny, S. Subramani, M. Thumm, M. Veenhuis, and Y. Ohsumi. 2003. A unified nomenclature for yeast autophagy-related genes. *Dev Cell.* 5:539-45.

Kochl, R., X.W. Hu, E.Y. Chan, and S.A. Tooze. 2006. Microtubules facilitate autophagosome formation and fusion of autophagosomes with endosomes. *Traffic.* 7:129-45.

Koike, M., M. Shibata, S. Waguri, K. Yoshimura, I. Tanida, E. Kominami, T. Gotow, C. Peters, K. von Figura, N. Mizushima, P. Saftig, and Y. Uchiyama. 2005. Participation of autophagy in storage of lysosomes in neurons from mouse models of neuronal ceroid-lipofuscinoses (Batten disease). *Am J Pathol.* 167:1713-28.

Kondomerkos, D.J., S.A. Kalamidas, O.B. Kotoulas, and A.C. Hann. 2005. Glycogen autophagy in the liver and heart of newborn rats. The effects of glucagon, adrenalin or rapamycin. *Histol Histopathol.* 20:689-96.

Kopitz, J., G.O. Kisen, P.B. Gordon, P. Bohley, and P.O. Seglen. 1990. Nonselective autophagy of cytosolic enzymes by isolated rat hepatocytes. *J Cell Biol.* 111:941-53.

Kovacs, A.L., A. Reith, and P.O. Seglen. 1982. Accumulation of autophagosomes after inhibition of hepatocytic protein degradation by vinblastine, leupeptin or a lysosomotropic amine. *Exp Cell Res.* 137:191-201.

Kuma, A., M. Hatano, M. Matsui, A. Yamamoto, H. Nakaya, T. Yoshimori, Y. Ohsumi, T. Tokuhisa, and N. Mizushima. 2004. The role of autophagy during the early neonatal starvation period. *Nature.* 432:1032-6.

Kuma, A., N. Mizushima, N. Ishihara, and Y. Ohsumi. 2002. Formation of the approximately 350-kDa Apg12-Apg5.Apg16 multimeric complex, mediated by Apg16 oligomerization, is essential for autophagy in yeast. *J Biol Chem.* 277:18619-25.

Lawrence, B.P., and W.J. Brown. 1992. Autophagic vacuoles rapidly fuse with pre-existing lysosomes in cultured hepatocytes. *J Cell Sci.* 102 (Pt 3):515-26.

Liang, X.H., S. Jackson, M. Seaman, K. Brown, B. Kempkes, H. Hibshoosh, and B. Levine. 1999. Induction of autophagy and inhibition of tumorigenesis by beclin 1. *Nature.* 402:672-6.

Lin, Y., L.A. Kimpler, T.V. Naismith, J.M. Lauer, and P.I. Hanson. 2005. Interaction of the mammalian endosomal sorting complex required for transport (ESCRT) III protein hSnf7-1 with itself, membranes, and the AAA+ ATPase SKD1. *J Biol Chem.* 280:12799-809.

Locke, M., and A.K. Sykes. 1975. The role of the Golgi complex in the isolation and digestion of organelles. *Tissue Cell.* 7:143-58.

Long, X., S. Ortiz-Vega, Y. Lin, and J. Avruch. 2005. Rheb binding to mammalian target of rapamycin (mTOR) is regulated by amino acid sufficiency. *J Biol Chem.* 280:23433-6.

Mann, S.S., and J.A. Hammarback. 1994. Molecular characterization of light chain 3. A microtubule binding subunit of MAP1A and MAP1B. *J Biol Chem.* 269:11492-7.

McBride, H.M., V. Rybin, C. Murphy, A. Giner, R. Teasdale, and M. Zerial. 1999. Oligomeric complexes link Rab5 effectors with NSF and drive membrane fusion via interactions between EEA1 and syntaxin 13. *Cell.* 98:377-86.

Meijer, A.J., and P.F. Dubbelhuis. 2004. Amino acid signalling and the integration of metabolism. *Biochem Biophys Res Commun.* 313:397-403.

Melendez, A., Z. Talloczy, M. Seaman, E.-L. Eskelinen, D.H. Hall, and B. Levine. 2003. Autophagy Genes Are Essential for Dauer Development and Life-Span Extension in C. elegans. *Science.* 301:1387-1391.

Mills, I., A. Jones, and M.J. Clague. 1998. Involvement of the endosomal autoantigen EEA1 in homotypic fusion of early endosomes. *Curr. Biol.* 16:881 - 884.

Mitchener, J.S., J.D. Shelburne, W.D. Bradford, and H.K. Hawkins. 1976. Cellular autophagocytosis induced by deprivation of serum and amino acids in HeLa cells. *Am J Pathol.* 83:485-91.

Mizushima, N. 2004. Methods for monitoring autophagy. *Internat J Biochem Cell Biol.* 36:2491-2502.

Mizushima, N., T. Noda, T. Yoshimori, Y. Tanaka, T. Ishii, M.D. George, D.J. Klionsky, M. Ohsumi, and Y. Ohsumi. 1998. A protein conjugation system essential for autophagy. *Nature.* 395:395-8.

Mizushima, N., A. Yamamoto, M. Hatano, Y. Kobayashi, Y. Kabeya, K. Suzuki, T. Tokuhisa, Y. Ohsumi, and T. Yoshimori. 2001. Dissection of autophagosome formation using Apg5-deficient mouse embryonic stem cells. *J Cell Biol.* 152:657-68.

Mizushima, N., A. Yamamoto, M. Matsui, T. Yoshimori, and Y. Ohsumi. 2004. In vivo analysis of autophagy in response to nutrient starvation using transgenic mice expressing a fluorescent autophagosome marker. *Mol Biol Cell.* 15:1101-11.

Moller, M.T., H.R. Samari, and P.O. Seglen. 2004. Toxin-induced tail phosphorylation of hepatocellular S6 kinase: evidence for a dual involvement of the AMP-activated protein kinase in S6 kinase regulation. *Toxicol Sci.* 82:628-37.

Mordier, S., C. Deval, D. Bechet, A. Tassa, and M. Ferrara. 2000. Leucine limitation induces autophagy and activation of lysosome-dependent proteolysis in C2C12 myotubes through a mammalian target of rapamycin-independent signaling pathway. *J Biol Chem.* 275:29900-6.

Mortimore, G.E., A.R. Pösö, M. Kadowaki, and J.J.J. Wert. 1987. Multiphasic control of hepatic protein degradation by regulatory amino acids. General features and hormonal modulation. *J. Biol. Chem.* 262:16322-16327.

Mortimore, G.E., J.J.J. Wert, G. Miotto, R. Venerando, and M. Kadowaki. 1994. Leucine-specific binding of photoreactive Leu7-MAP to a high molecular weight protein on the plasma membrane of the isolated rat hepatocyte. *Biochem Biophys Res Commun.* 203:200 - 208.

Muller, J.M., J. Shorter, R. Newman, K. Deinhardt, Y. Sagiv, Z. Elazar, G. Warren, and D.T. Shima. 2002. Sequential SNARE disassembly and GATE-16-GOS-28 complex assembly mediated by distinct NSF activities drives Golgi membrane fusion. *J Cell Biol.* 157:1161-73.

Mullins, C., and J.S. Bonifacino. 2001. The molecular machinery for lysosome biogenesis. *Bioessays.* 23:333-43.

Mullock, B.M., N.A. Bright, C.W. Fearon, S.R. Gray, and J.P. Luzio. 1998. Fusion of lysosomes with late endosomes produces a hybrid organelle of intermediate density and is NSF dependent. *J Cell Biol.* 140:591-601.

Mullock, B.M., J.H. Perez, T. Kuwana, S.R. Gray, and J.P. Luzio. 1994. Lysosomes can fuse with a late endosomal compartment in a cell-free system from rat liver. *J Cell Biol.* 126:1173-82.

Munafo, D.B., and M.I. Colombo. 2001. A novel assay to study autophagy: regulation of autophagosome vacuole size by amino acid deprivation. *J Cell Sci.* 114:3619-29.

Munafo, D.B., and M.I. Colombo. 2002. Induction of Autophagy Causes Dramatic Changes in the Subcellular Distribution of GFP-Rab24. *Traffic.* 3:472-82.

Nara, A., N. Mizushima, A. Yamamoto, Y. Kabeya, Y. Ohsumi, and T. Yoshimori. 2002. SKD1 AAA ATPase-Dependent Endosomal Transport is Involved in Autolysosome Formation. *Cell Struct Funct.* 27:29-37.

Naslavsky, N., R. Roberto Weigert, and J.G. Donaldson. 2003. Convergence of Non-clathrin- and Clathrin-derived Endosomes Involves Arf6 Inactivation and Changes in Phosphoinositides. *Mol. Biol. Cell.* 15:417-431.

Nobukuni, T., M. Joaquin, M. Roccio, S.G. Dann, S.Y. Kim, P. Gulati, M.P. Byfield, J.M. Backer, F. Natt, J.L. Bos, F.J. Zwartkruis, and G. Thomas. 2005. Amino acids mediate mTOR/raptor signaling through activation of class 3 phosphatidylinositol 3OH-kinase. *Proc Natl Acad Sci U S A.* 102:14238-43.

Noda, T., and Y. Ohsumi. 1998. Tor, a Phosphatidylinositol Kinase Homologue, Controls Autophagy in Yeast. *J. Biol. Chem.* 273:3963-3966.

Noda, T., K. Suzuki, and Y. Ohsumi. 2002. Yeast autophagosomes: de novo formation of a membrane structure. *Trends Cell Biol.* 12:231-5.

Ogier-Denis, E., S. Pattingre, J. El Benna, and P. Codogno. 2000. Erk1/2-dependent phosphorylation of Galpha-interacting protein stimulates its GTPase accelerating activity and autophagy in human colon cancer cells. *J Biol Chem.* 275:39090-5.

Otto, G.P., M.Y. Wu, N. Kazgan, O.R. Anderson, and R.H. Kessin. 2004. Dictyostelium macroautophagy mutants vary in the severity of their developmental defects. *J Biol Chem.* 279:15621-9.

Oyler, G.A., G.A. Higgins, R.A. Hart, E. Battenberg, M. Billingley, F.E. Bloom, and M.C. Wilson. 1989. The identification of a novel synaptosomal-associated protein SNAP-25, differentially expressed by neuronal subpopulations. *J. Cell Biol.* 109:3039-3052.

Panda, D., M.A. Jordan, K.C. Chu, and L. Wilson. 1996. Differential effects of vinblastine on polymerization and dynamics at opposite microtubule ends. *J Biol Chem.* 271:29807-12.

Pattingre, S., A. Tassa, X. Qu, R. Garuti, X.H. Liang, N. Mizushima, M. Packer, M.D. Schneider, and B. Levine. 2005. Bcl-2 antiapoptotic proteins inhibit Beclin 1-dependent autophagy. *Cell.* 122:927-39.

Pfeffer, S.R. 1994. Rab GTPases: master regulators of membrane trafficking. *Curr. Opin. Cell Biol.* 6:522-6.

Pfeifer, U. 1978. Inhibition by insulin of the formation of autophagic vacuoles in rat liver. A morphometric approach to the kinetics of intracellular degradation by autophagy. *J Cell Biol.* 78:152-67.

Poli, A., P.B. Gordon, P.E. Schwarze, B. Grinde, and P.O. Seglen. 1981. Effects of insulin and anchorage on hepatocytic protein metabolism and amino acid transport. *J Cell Sci.* 48:1-18.

Poso, A., J. Wert, Jr, and G. Mortimore. 1982. Multifunctional control of amino acids of deprivation-induced proteolysis in liver. Role of leucine. *J. Biol. Chem.* 257:12114-12120.

Price, D.J., R.A. Nemenoff, and J. Avruch. 1989. Purification of a hepatic S6 kinase from cycloheximide-treated Rats. *J Biol Chem.* 264:13825-33.

Pryor PR, M.B., ...Luzio JP. 2004. Combinatorial SNARE complexes with VAMP7 or VAMP8 define different late endocytic fusion events. *EMBO Reports.* Vol 5:1-6.

Punnonen, E.L., S. Autio, H. Kaija, and H. Reunanen. 1993. Autophagic vacuoles fuse with the prelysosomal compartment in cultured rat fibroblasts. *Eur J Cell Biol.* 61:54-66.

Punnonen, E.L., and H. Reunanen. 1990. Effects of vinblastine, leucine, and histidine, and 3-methyladenine on autophagy in Ehrlich ascites cells. *Exp Mol Pathol.* 52:87-97.

Qu, X., J. Yu, G. Bhagat, N. Furuya, H. Hibshoosh, A. Troxel, J. Rosen, E.-L. Eskelinen, N. Mizushima, Y. Ohsumi, G. Cattoretti, and B. Levine. 2003. Promotion of tumorigenesis by heterozygous disruption of the beclin 1 autophagy gene. *J. Clin. Invest.* 112:1809-1820.

Raiborg, C., T.E. Rusten, and H. Stenmark. 2003. Protein sorting into multivesicular endosomes. *Curr Opin Cell Biol.* 15:446-55.

Rak, A., O. Pylypenko, T. Durek, A. Watzke, S. Kushnir, L. Brunsveld, H. Waldmann, R.S. Goody, and K. Alexandrov. 2003. Structure of Rab GDP-dissociation inhibitor in complex with prenylated YPT1 GTPase. *Science.* 302:646-50.

Ravikumar, B., C. Vacher, Z. Berger, J.E. Davies, S. Luo, L.G. Oroz, F. Scaravilli, D.F. Easton, R. Duden, C.J. O'Kane, and D.C. Rubinsztein. 2004. Inhibition of mTOR induces autophagy and reduces toxicity of polyglutamine expansions in fly and mouse models of Huntington disease. *Nat Genet.* 36:585-95.

Reggiori, F., I. Monastyrska, T. Shintani, and D.J. Klionsky. 2005a. The actin cytoskeleton is required for selective types of autophagy, but not nonspecific autophagy, in the yeast Saccharomyces cerevisiae. *Mol Biol Cell.* 16:5843-56.

Reggiori, F., T. Shintani, U. Nair, and D.J. Klionsky. 2005b. Atg9 cycles between mitochondria and the pre-autophagosomal structure in yeasts. *Autophagy.* 1:101-109.

Reggiori, F., K.A. Tucker, P.E. Stromhaug, and D.J. Klionsky. 2004a. The atg1-atg13 complex regulates atg9 and atg23 retrieval transport from the pre-autophagosomal structure. *Dev Cell.* 6:79-90.

Reggiori, F., C.W. Wang, U. Nair, T. Shintani, H. Abeliovich, and D.J. Klionsky. 2004b. Early stages of the secretory pathway, but not endosomes, are required for Cvt vesicle and autophagosome assembly in Saccharomyces cerevisiae. *Mol Biol Cell.*

Reggiori, F., C.W. Wang, P.E. Stromhaug, T. Shintani, and D.J. Klionsky. 2003. Vps51 is part of the yeast Vps fifty-three tethering complex essential for retrograde traffic from the early endosome and Cvt vesicle completion. *J Biol Chem.* 278:5009-20.

Reunanen, H., M. Marttinen, and P. Hirsimaki. 1988. Effects of griseofulvin and nocodazole on the accumulation of autophagic vacuoles in Ehrlich ascites tumor cells. *Exp Mol Pathol.* 48:97-102.

Rez, G., E. Fellinger, O. Oliva, Z. Palfia, J. Csak, L. Laszlo, A.L. Kovacs, J. Kovacs, and A.P. Karpati. 1991. Mechanism and dynamics of macroautophagy in murine exocrine pancreatic cells. A review of vinblastine-induced changes. *Acta Biol Hung.* 42:57-86.

Rink, J., E. Ghigo, Y. Kalaidzidis, and M. Zerial. 2005. Rab conversion as a mechanism of progression from early to late endosomes. *Cell.* 122:735-49.

Roccio, M., J.L. Bos, and F.J. Zwartkruis. 2006. Regulation of the small GTPase Rheb by amino acids. *Oncogene.* 25:657-64.

Rusten, T.E., K. Lindmo, G. Juhasz, M. Sass, P.O. Seglen, A. Brech, and H. Stenmark. 2004. Programmed autophagy in the Drosophila fat body is induced by ecdysone through regulation of the PI3K pathway. *Dev Cell.* 7:179-92.

Samson, F., J.A. Donoso, I. Heller-Bettinger, D. Watson, and R.H. Himes. 1979. Nocodazole action on tubulin assembly, axonal ultrastructure and fast axoplasmic transport. *J Pharmacol Exp Ther.* 208:411-7.

Sarbassov dos, D., S.M. Ali, and D.M. Sabatini. 2005. Growing roles for the mTOR pathway. *Curr Opin Cell Biol.* 17:596-603.

Schiff, P.B., and S.B. Horwitz. 1980. Taxol stabilizes microtubules in mouse fibroblast cells. *Proc Natl Acad Sci U S A.* 77:1561-5.

Scott, R.C., O. Schuldiner, and T.P. Neufeld. 2004. Role and regulation of starvation-induced autophagy in the Drosophila fat body. *Dev Cell.* 7:167-78.

Scott, S.V., D.C. Nice, 3rd, J.J. Nau, L.S. Weisman, Y. Kamada, I. Keizer-Gunnink, T. Funakoshi, M. Veenhuis, Y. Ohsumi, and D.J. Klionsky. 2000. Apg13p and Vac8p are part of a complex of phosphoproteins that are required for cytoplasm to vacuole targeting. *J Biol Chem.* 275:25840-9.

Seabra, M.C., and C. Wasmeier. 2004. Controlling the location and activation of Rab GTPases. *Curr Opin Cell Biol.* 16:451-7.

Seglen, P.O. 1993. Isolation of hepatocytes by collagenase perfusion. *In* Methods in Toxicology. Academic Press. 231-243.

Shigemitsu, K., Y. Tsujishita, K. Hara, M. Nanahoshi, J. Avruch, and K. Yonezawa. 1999. Regulation of Translational Effectors by Amino Acid and Mammalian Target of Rapamycin Signaling Pathways. Possible involvement of autophagy in cultured hepatoma cells. *J. Biol. Chem.* 274:1058-1065.

Smith, E.M., S.G. Finn, A.R. Tee, G.J. Browne, and C.G. Proud. 2005. The tuberous sclerosis protein TSC2 is not required for the regulation of the mammalian target of rapamycin by amino acids and certain cellular stresses. *J Biol Chem.* 280:18717-27.

Sollner, T., M.K. Bennet, S.W. Whiteheart, R.H. Scheller, and J.E. Rothman. 1993. A protein assembly-disassembly pathway in vitro that may correspond to sequential steps of synaptic vesicle docking, activation, and fusion. *Cell.* 75:409-418.

Stoorvogel, W., G.J. Strous, H.J. Geuze, V. Oorschot, and A.L. Schwartz. 1991. Late endosomes derive from early endosomes by maturation. *Cell.* 65:417-27.

Stromhaug, P.E., T.O. Berg, M. Fengsrud, and P.O. Seglen. 1998. Purification and characterization of autophagosomes from rat hepatocytes. *Biochem J.* 335 (Pt 2):217-24.

Surpin, M., H. Zheng, M.T. Morita, C. Saito, E. Avila, J.J. Blakeslee, A. Bandyopadhyay, V. Kovaleva, D. Carter, A. Murphy, M. Tasaka, and N. Raikhel. 2003. The VTI family of SNARE proteins is necessary for plant viability and mediates different protein transport pathways. *Plant Cell.* 15:2885-99.

Sutton, R.B., D. Fasshauer, R. Jahn, and A.T. Brunger. 1998. Crystal structure of a SNARE complex involved in synaptic exocytosis at 2.4 A resolution. *Nature.* 395:347 - 353.

Suzuki, K., T. Kirisako, Y. Kamada, N. Mizushima, T. Noda, and Y. Ohsumi. 2001. The pre-autophagosomal structure organized by concerted functions of APG genes is essential for autophagosome formation. *Embo J.* 20:5971-81.

Talloczy, Z., W. Jiang, H.W. Virgin, IV, D.A. Leib, D. Scheuner, R.J. Kaufman, E.-L. Eskelinen, and B. Levine. 2002. Regulation of starvation- and virus-induced autophagy by the eIF2alpha kinase signaling pathway. *PNAS.* 99:190-195.

Tanaka, Y., G. Guhde, A. Suter, E.L. Eskelinen, D. Hartmann, R. Lullmann-Rauch, P.M. Janssen, J. Blanz, K. von Figura, and P. Saftig. 2000. Accumulation of autophagic vacuoles and cardiomyopathy in LAMP-2-deficient mice. *Nature.* 406:902-6.

Tanida, I., M. Komatsu, T. Ueno, and E. Kominami. 2003. GATE-16 and GABARAP are authentic modifiers mediated by Apg7 and Apg3. *Biochem Biophys Res Commun.* 300:637-44.

Tanida, I., Y.S. Sou, J. Ezaki, N. Minematsu-Ikeguchi, T. Ueno, and E. Kominami. 2004a. HsAtg4B/HsApg4B/autophagin-1 cleaves the carboxyl termini of three human Atg8 homologues and delipidates microtubule-associated protein light chain 3- and GABAA receptor-associated protein-phospholipid conjugates. *J Biol Chem.* 279:36268-76.

Tanida, I., T. Ueno, and E. Kominami. 2004b. LC3 conjugation system in mammalian autophagy. *Int J Biochem Cell Biol.* 36:2503-18.

Tassa, A., M.P. Roux, D. Attaix, and D.M. Bechet. 2003. Class III phosphoinositide 3-kinase-beclin1 complex mediates the amino acid-dependent regulation of autophagy in C2C12 myotubes. *Biochem J.* Pt.

Thumm, M., R. Egner, M. Kock, M. Schlumpberger, M. Straub, M. Veenhuis, and D.H. Wolf. 1994. Isolation of autophagocytosis mutants of Saccharomyces cerevisiae *FEBS Lett.* 349:275-280.

Tokunaga, C., K. Yoshino, and K. Yonezawa. 2004. mTOR integrates amino acid- and energy-sensing pathways. *Biochem Biophys Res Commun.* 313:443-6.

Tokuyasu, K. 1973. A technique for ultra-microtomy of cells and tissues. *J Cell Biol.* 57:551-565.

Tolkovsky, A.M., L. Xue, G.C. Fletcher, and V. Borutaite. 2002. Mitochondrial disappearance from cells: a clue to the role of autophagy in programmed cell death and disease? *Biochimie.* 84:233-40.

Tooze, J., M. Hollinshead, T. Ludwig, K. Howell, B. Hoflack, and H. Kern. 1990. In exocrine pancreas, the basolateral endocytic pathway converges with the autophagic pathway immediately after the early endosome. *J Cell Biol.* 111:329-45.

Tooze, S.A., G.J.M. Martens, and W.B. Huttner. 2001. Secretory granule biogenesis: rafting to the SNARE. *Trends in Cell Biol.* 11:116-122.

Trimble, W.S., J.A. Ostrom, and S. Kornfeld. 1988. VAMP-1: A synaptic vesicle-associated integral membrane protein. *Proc. Natl. Acad. Sci.* 85:4538-4542.

Tsukada, M., and Y. Ohsumi. 1993. Isolation and characterization of autophagy-defective mutants of Saccharomyces cerevisiae. *FEBS Lett.* 333:169-74.

Tsutsui, T., H. Koide, H. Fukahori, K. Isoda, S. Higashiyama, I. Maeda, F. Tashiro, E. Yamato, J. Miyazaki, J. Yodoi, M. Kawase, and K. Yagi. 2003. Adenoviral transfection of hepatocytes with the thioredoxin gene confers protection against apoptosis and necrosis. *Biochem Biophys Res Commun.* 307:765-70.

Tzatsos, A., and K.V. Kandror. 2006. Nutrients suppress phosphatidylinositol 3-kinase/Akt signaling via raptor-dependent mTOR-mediated insulin receptor substrate 1 phosphorylation. *Mol Cell Biol.* 26:63-76.

Wang, L., E.S. Seeley, W. Wickner, and A.J. Merz. 2002. Vacuole Fusion at a Ring of Vertex Docking Sites Leaves Membrane Fragments within the Organelle. *Cell.* 108:357-69.

Webb, J.L., B. Ravikumar, J. Atkins, J.N. Skepper, and D.C. Rubinsztein. 2003. Alpha-Synuclein is degraded by both autophagy and the proteasome. *J Biol Chem.* 278:25009-13.

Webb, J.L., B. Ravikumar, and D.C. Rubinsztein. 2004. Microtubule disruption inhibits autophagosome-lysosome fusion: implications for studying the roles of aggresomes in polyglutamine diseases. *Int J Biochem Cell Biol.* 36:2541-50.

Woodside, K.H., and G.E. Mortimore. 1972. Suppression of protein turnover by amino acids in the perfused rat liver. *J Biol Chem.* 247:6474-81.

Yamamoto, A., R. Masaki, Y. Fukui, and Y. Tashiro. 1990. Absence of cytochrome P-450 and presence of autolysosomal membrane antigens on the isolation membranes and autophagosomal membranes in rat hepatocytes. *J Histochem Cytochem.* 38:1571-81.

Yorimitsu, T., and D.J. Klionsky. 2005. Autophagy: molecular machinery for self-eating. *Cell Death Differ.* 12 Suppl 2:1542-52.

Yue, Z., S. Jin, C. Yang, A.J. Levine, and N. Heintz. 2003. Beclin 1, an autophagy gene essential for early embryonic development, is a haploinsufficient tumor suppressor. *Proc Natl Acad Sci U S A.* 100:15077-82.

Zerial, M., and H. McBride. 2001. Rab proteins as membrane organizers. *Nat Rev Mol Cell Biol.* 2:107-17.